# Regulation of the Eukaryotic Redox-State through Metabolic Reconfiguration

Dissertation

zur Erlangung des akademischen Grades des
Doktors der Naturwissenschaften (Dr. rer. nat.)

eingereicht im Fachbereich Biologie, Chemie, Pharmazie
der Freien Universität Berlin


vorgelegt von

Nana-Maria Grüning

aus Grevesmühlen

Berlin 2012

Das Dissertationsprojekt wurde am Max Planck Institut für Molekulare Genetik in der Arbeitsgruppe Molekularbiologie des Metabolismus (Markus Ralser) durchgeführt.

Beginn der Bearbeitungszeit: 01. Februar 2009

1. Gutachter: Prof. Constance Scharff
   Institut für Biologie, Freie Universität Berlin
   Takustraße 6, D-14195 Berlin

2. Gutachter: Prof. Michael Breitenbach
   Fachbereich Zellbiologie, Universität Salzburg
   Hellbrunnerstraße 34, A-5020 Salzburg

Disputation am 13. Januar 2012

## Acknowledgements

This PhD thesis would not have been possible without the help of many wonderful people.

First of all, I would like to thank Dr. Markus Ralser for all his invaluable great ideas, discussions, the encouragement and support, the guidance through my beginner's time in a yeast lab, for his patience, his positive and motivating attitude, and for broadening my view on the fascination of science.

Furthermore, I am very grateful to Prof. Michael Breitenbach for his generous help in scientific discussions, providing experimental equipment, his time spent to be second reviewer of this thesis and for the warm welcome in Salzburg.

My thanks goes also to Prof. Constance Scharff for supervising the final part of becoming PhD, to Prof. Hans Lehrach for giving me the opportunity to use the research facilities at his department and the Max Planck Society for funding.

I am especially indebted to my colleagues Dr. Katharina Blümlein, Steve Michel, Antje Krüger, Michael Mülleder, Beata Lukaszewska-McGreal and Klaus-Dieter Klöppel who gave support in many ways: scientific know-how, experimental help, proofreading of this thesis, comforting in stressful times, celebrating little and bigger achievements, simply being there in case of need and spirit-lifting coffee breaks and after-work beers. This work would not have been possible without them!

Also, I would like to thank Dr. Mark Rinnerthaler for experimental help and giving advice in scientific questions. I am grateful to Dr. Mirjam Wamelink, Erwin Jansen, Prof. Cornelis Jakobs, Dr. Phillip Grote, René Feichtinger and Prof. Barbara Kofler for supporting me with technological expertise and scientific knowledge during my PhD projects.

I am deeply grateful to my "inner circle" at the MPI: Dr. Hans-Jörg Warnatz, Dr. Robert Querfurth, Dr. Bernd Timmermann, Dr. Martin Kerick, Dr. Andreas Dahl, the members of AG Schweiger, AG Krobitsch and AG Lange. These people provided so much help in questions concerning almost everything and contributed to make me feel at home at the MPI-MG.

It is also a pleasure to thank Laura just for being a special person, for her sensitivity when I needed a friend to talk to, for answering the phone at any time, and for telling me about the job offer for this PhD project three years ago. Clara, for her understanding of daily and not so daily problems, and her cheerful way of giving continuous support. Andrea, Heidi and Moni, for becoming close friends in a short time and for making my time in Salzburg unforgettable.

I would like to thank my brother Benjamin who took care of me by cooking, cooling some beer and giving a shoulder to lean on when I worked long hours. Also, I am grateful to my brother Tobias for his smart help in analyzing data and his calm and supportive way in discussions.

Finally, I would like to express my gratitude to my parents, Karin and Uwe. Their encouragement and endless love have always given me strength to go my way and also to finish this thesis.

# Table of Contents

# Introduction

The origin of life is thought to be based on the formation of compartmentalized autocatalytic chemical cycles. Over time and with the appearance of catalytical biopolymers (ribonucleic acid- or protein-based enzymes), these chemical cycles gained complexity resulting in the evolution of modern metabolic pathways [1, 2]. Metabolic pathways are sequences of enzymatic reactions that can be dynamically adjusted in turnover, and their topology within the cell forms the metabolic network [2]. The large set of biochemical reactions within the metabolic network produces chemical energy and biomolecules as building blocks for cellular components. Beyond this, the metabolic network is tightly connected to regulatory macromolecules (e.g. the transcriptional machinery) which monitor the cell's homeostasis and is therefore fundamental part of the cellular regulome [2]. Constant input of energy from the environment and their assimilation by the metabolic network is required to maintain biochemical reactions working against entropy, and thus keeping an organism alive [3, 4]. Central for the maintenance of living systems is the energy coupling agent adenosine triphosphate (ATP). ATP is regarded as the "energy currency" of the cell. Hydrolysis of ATP to ADP (adenosine diphosphate) and AMP (adenosine monophosphate) releases energy that is essential for manifold energy-consuming cellular processes, such as motility, active molecular transport, signaling events or biosyntheses of macromolecules [5]. Reversely, ATP is generated from ADP and $P_i$ (phosphate) when phototrophic organisms capture the energy of light or when organic nutrients are oxidized in chemotrophic organisms. Hence, the ATP-ADP-turnover is the fundamental mechanism of energy transfer in biological systems [5]. Moreover, metabolism must be rapidly and adequately reconfigured in order to produce or degrade compounds to maintain the cellular homeostasis and facilitate the cell's survival when conditions change [6]. In the light of cellular self-regulation, metabolic pathways exhibit fundamental importance because their turnover can be fast and dynamically adapted to the cell's current requirements.

### *Pathways in Central Carbohydrate Catabolism*

Pathways in carbohydrate metabolism take center stage in the cell's metabolic network because they provide energy (e.g. in form of ATP) and metabolites for synthetic processes, intermediary metabolism and secondary metabolic reactions. Carbohydrates such as glucose contain chemical energy stored in molecular bonds to hydrogen, which

can be released in enzymatic reactions. The main energy-releasing catabolic pathways in carbohydrate metabolism are glycolysis and fermentation or respiration.

Glycolysis (Greek: *glykos* = sweet, *lysis* = degradation, Fig. 1) is an ancient catabolic pathway that derives from a time when there was less oxygen in the atmosphere than nowadays. It is conserved in almost all organisms – aerobe or anaerobe living [7]. In ten cytosolic enzymatic steps, one molecule of glucose is converted into two molecules of pyruvate. This reaction sequence yields two molecules of ATP and one molecule of the high- energy compound NADH (reduced nicotinamide adenine dinucleotide).

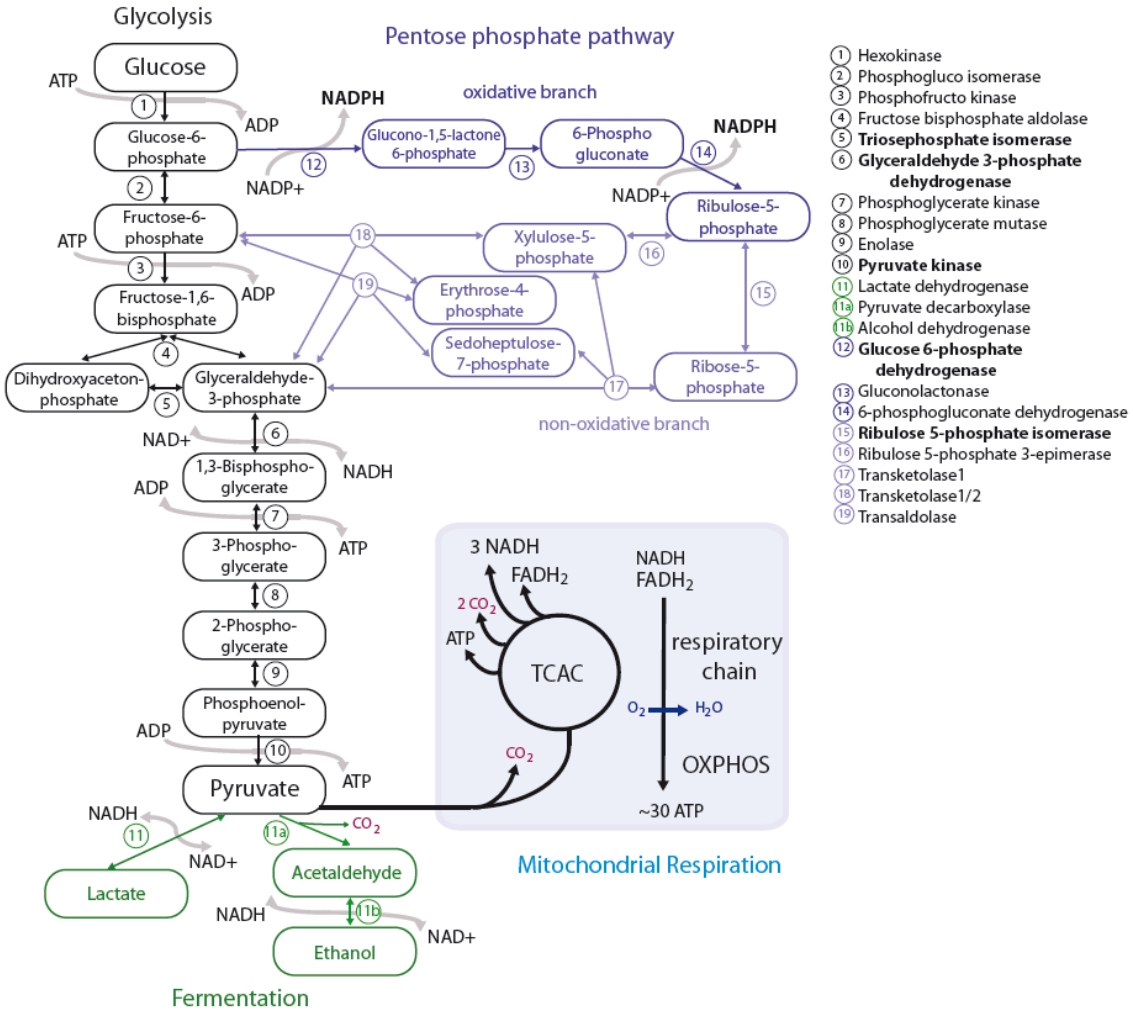


**Figure 1: Pathways in central carbohydrate metabolism.** Enzymes explicitly mentioned in the text are highlighted in bold. TCAC, tricarboxylic acid cycle, OXPHOS, oxidative phosphorylation

Under anaerobe as well as aerobe conditions, pyruvate can be processed through fermentation (Fig. 1). The last enzymatic reactions in fermentation restore $NAD^+$ (oxidized nicotinamide adenine dinucleotide) which is required for upstream reactions in

glycolysis and, thus, maintain the redox balance of the pathway. In yeast and some other microorganisms (e.g. the thermophilic bacteria *Clostridium thermohydrosulfuricum* [8]), pyruvate is converted to acetaldehyde and carbon dioxide, and in the final step to ethanol. Higher eukaryotes and lactic acid bacteria directly reduce pyruvate to lactate. The end products of fermentation (ethanol or lactate) are two carbon bodies which still contain chemical energy. Hence, fermentation only leads to partial energy release from glucose [5].

The entire oxidation and energy recovery from glucose can be facilitated when glycolysis is followed by mitochondrial respiration, which is strictly dependent on the availability of oxygen. Firstly, pyruvate is decarboxylated to carbon dioxide and acetyl-coenzyme A (acetyl-CoA). The acetyl-group of acetyl-CoA is transmitted to the tricarboxylic acid cycle (TCAC) located in the mitochondrial matrix. The TCAC reaction sequence provides intermediates for biosynthetic processes (e.g. the production of certain amino acids such as glutamic acid or fatty acids [5]) and leads to further energy releasing oxidation of the acetyl-group. One molecule of ATP is produced from one molecule acetyl-CoA, but the major part of the energy released from TCAC compounds is bound in NADH and $FADH_2$ (reduced flavin adenine dinucleotide). NADH and $FADH_2$ transmit their electrons to enzymatic complexes of the mitochondrial respiratory chain (electron transport chain), located in the inner mitochondrial membrane. A series of redox reactions *via* molecules with increasing reduction potential passes electrons to their final acceptor: molecular oxygen. Step by step, enzymatic complexes of the electron transport chain use this energy to pump protons across the inner mitochondrial membrane and thereby build up a proton gradient – a process called “chemiosmosis” [9]. At last, four electrons are transferred to their final acceptor molecular oxygen, which is thereby reduced to form water. In higher eukaryotes, the respiratory chain is composed of four enzymatic complexes (I-IV), cytochrome *c* and the lipid ubiquinone (Q) (Fig.2). However, the molecular composition of the respiratory chain might vary between different kingdoms or species. For instance, the yeast *Saccharomyces cerevisiae* lacks complex I (Fig. 2). Instead, different oxidoreductases (Nde1, Nde2, Ndi1 and Gut2) feed the respiratory chain with electrons, but without proton pumping (Fig. 2) [10].

The proton gradient is the driving force for oxidative phosphorylation (OXPHOS). Protons flow back down the gradient through the enzymatic complex ATP synthase. In this way, the transmitted energy is used in a phosphorylation reaction to form ATP from ADP and $P_i$ [11].

Whereas the ATP yield from glycolysis or the TCAC are definite numbers because they depend on the stoichiometries of chemical reactions, the number of ATP molecules attained from OXPHOS is less exactly determinable. Stoichiometries of proton pumping, ATP-synthesis and transport processes of metabolites are no integer numbers and do not have fixed values. Thus, recent estimations state a total ATP yield of ~30 molecules from the complete oxidation of one molecule glucose to $CO_2$ in higher eukaryotes [5]. However, these calculations are overestimates, as they do not take into account the energy needed to synthesize involved proteins, and for balancing the redox state. Nevertheless, glycolysis followed by mitochondrial respiration has a much higher energy yield than fermentation.

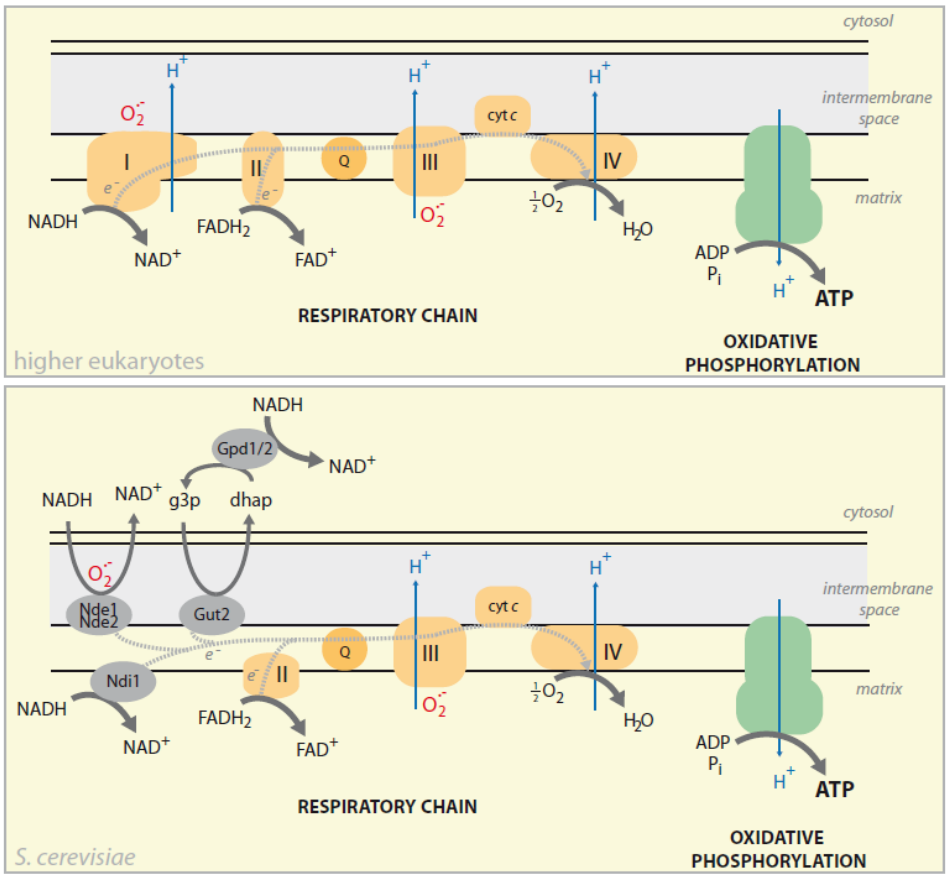


**Figure 2: Schematic overview of the respiratory chain and oxidative phoshorylation of higher eukaryotes (upper panel) and *S. cerevisiae* (lower panel).** I, II, III, IV, enzymatic complexes; Q, ubiquinon (coenzyme Q), cyt *c*, cytochrome *c*; Ndi1, internal NADH dehydrogenase; Nde1/2, external NADH dehydrogenases; Gut2, glycerol 3-phosphate:ubiquinone oxidoreductase; Gpd1/2, glycerol 3-phosphate dehydrogenases; dhap; dihydroxyaceton phosphate; g3p, glyceraldehyde 3-phosphate; $O_2^{\cdot-}$, superoxide, $e^-$, electron, $H^+$, proton

***The Pentose Phosphate Pathway (PPP)***

The Pentose Phosphate Pathway (PPP) is a carbohydrate metabolizing pathway closely connected to glycolysis (Fig. 1). The PPP can be subdivided into two independently operating metabolic units: the oxidative branch (OPPP) and the non-oxidative part (NOPPP). The OPPP consists of irreversible enzymatic reactions that convert glucose 6-phosphate to ribulose 5-phosphate and produce NADPH (reduced nicotinamide adenine dinucleotide phosphate). Whereas the NOPPP is formed by reversible enzymatic reactions that convert three-, four-, five-, six- or seven-carbon sugars into each other. Therefore, the PPP provides the cell with the five-carbon sugar ribose 5-phosphate for nucleotide biosynthesis and for production of ATP, NADH, FAD and coenzyme A, and reduces the redox-cofactor $NADP^+$ to NADPH.

***Reactive Oxygen Species and Anti-Oxidative Systems***

Cells which use aerobic metabolism gain more ATP per mole glucose, but also have to face the toxic side effects of oxygen. The mitochondrial electron transport chain is always somewhat "leaky", leading to direct one-electron transfer to molecular oxygen and to the formation of the superoxide anion radical ($O_2^{\cdot -}$, Fig. 2) [12, 13]. In higher eukaryotes, superoxide production takes place at complex I and III; in *S. cerevisiae* at Nde1/2 and complex III (Fig. 2) [14]. Superoxide is highly reactive itself and also precursor ion for different other reactive oxygen species (ROS; e.g. hydrogen peroxide, $H_2O_2$ and the hydroxyl radical, HO·). Mitochondrial respiration is the major internal source for ROS in eukaryotic cells [13]. The total rate of ROS production during respiration equals 1-2% of the metabolized oxygen [12]. ROS, precisely $H_2O_2$, were reported to play important roles in cellular signaling, e.g. as second messenger to transmit pro-inflammatory and growth-stimulatory signals [15, 16]. However, an excess of ROS can also damage macromolecules such as nucleic acids, proteins and fatty acids by oxidation, and has influence on many biochemical reactions whose function is impaired upon an redox-imbalance [17]. A shift of the redox-balance toward oxidizing molecules, also termed oxidative stress, is therefore a dangerous and deleterious situation for the cell and implicated in a number of human diseases such as cancer, stroke or late-onset neurodegenerative disorders [18].

To prevent the destructive effects of high ROS levels and to repair damaged structures, various enzymatic as well as non-enzymatic defense and repair mechanisms have evolved in eukaryotic cells. Primary defense mechanisms maintain ROS at a

harmless level; secondary defense mechanisms repair or degrade the targets of oxidization [19]. Enzymatic systems comprise superoxide dismutases, catalases, peroxiredoxins (PRX), glutaredoxins (GRX) and thioredoxins (TRX). Non-enzymatic anti-oxidants include, e.g., glutathione, ascorbate, ubiquinol, tocopherols and carotenoids [14, 19, 20]. Probably, the most important redox buffer in most eukaryotic cells is the tripeptide glutathione (GSH, γ-L-glutamyl-L-cysteinylglycine). GSH functions in two ways: by being oxidized to glutathione disulfide (GS-SG) it scavenges free radicals and by forming reversible mixed disulphides with protein thiol-groups, which are prone to oxidation (*S*-glutathionylation), it protects proteins from irreversible damage through formation of sulfonic derivatives by ROS [14]. In a predominantly oxidizing extracellular environment and because of constant ROS production through normal metabolic processes, cells need to recycle oxidized components of the anti-oxidant defense and repair mechanisms in order to maintain a reducing intracellular milieu [21]. The glutathione as well as the enzymatic systems require the redox-equivalent NADPH for recovery, e.g. for reduction of GS-SG to GSH.

***NAD(H) and NADP(H) – The Universal Redox-Cofactors***

Energy transduction through catabolic pathways and also biosynthetic processes depend on the ability to carry redox equivalents. The pyridine nucleotides NAD(H) and NADP(H) play pivotal roles in metabolic redox-reactions and cellular homeostasis. They can accept electrons when present in their oxidized state ($NAD^+$ and $NADP^+$) or donate electrons from their reduced state (NADH and NADPH).

NAD(H) and NADP(H) differ only in a phosphate group at the 2'position of the ribose ring that is connected to the adenine moiety [5]. Furthermore, this moiety is connected by a phosphate bond to a nicotinamide unit, which is the redox effector. Hence, both molecules can be used in a similar fashion for redox transport, but facilitate the maintenance of two independent redox pools in parallel, as the large phosphate group allows enzyme selectivity. Indeed, enzymes which require NAD(H) or NADP(H) for catalysis are in general highly specific for their cofactors [22]. Hence, as it has to be facilitated that oxidizing as well as reductive processes can run simultaneously, independent availability of universal pools of $NAD^+$ and NADPH is crucial for cellular life.

Energy producing metabolic pathways require oxidized NAD as redox-carrier that transfers electrons from highly energetic nutrients such as carbohydrates or fatty acids to

enzymatic complexes of the respiratory chain. Beside its function as cofactor in redox-metabolism, $NAD^+$ plays also crucial roles in regulatory mechanisms and signaling events. For instance, $NAD^+$ is the substrate molecule for members of multiple protein families. In ADP-ribosyl transfer reactions, ADP-ribosyltransferases (mono(ADP-ribosyl)transferases, ARTs; poly(ADP-ribosyl)transferases, PARPs) use the ADP-ribose moiety of $NAD^+$ for posttranslational covalent protein modifications. The targets of mono/poly ADP-ribosylation are diverse: ranging from small molecules like acetate (forming *O*-acetyl ADP-ribose, [23]) to macromolecules such as proteins (e.g. mono(ADP-ribosyl)ation of $P2X_7$ purinergic membrane receptors [24] or poly(ADP-ribosyl)ation [PARsylation] of chromatin-associated macroH2A [25, 26]). Furthermore, bifunctional cyclic ADP-ribosyl cyclases/cyclic ADP-ribose hydrolases can generate cyclic ADP-ribose (cADPr) or hydrolyze cADPr into free ADP-ribose [22, 27]. cADPr, *O*-acetyl ADP-ribose and ADP-ribose are biologically active second messenger molecules and involved in calcium homeostasis [23]. Additionally, $NAD^+$ participates in transcriptional regulation: either through $NAD^+$-dependent PARsylation of transcription factors (e.g. p53, NFκB) or RNA polymerase II [22, 28], or through chromatin remodeling events. For example, $NAD^+$ dependent class III histone deacetylases (HDACs) of the Sir2 family (silent information regulator-2) transfer acetyl-groups from their substrates, histones, to the ADP-ribose moiety of $NAD^+$ and, thus, lead to the formation of heterochromatin with subsequent gene silencing [29]. Conserved from bacteria to higher eukaryotes, the Sir2 protein family has gained much attention in the last years, because increased Sir2p activity was reported to increase lifespan in various organisms [30].

NADPH functions as universal electron donor. Thus, one of its major tasks – as mentioned above - is acting as redox-equivalent in the maintenance and recovery of all known anti-oxidative defense and repair mechanisms (glutathione, catalases, TRX, PRX, superoxide dismutases and glutathione *S*-transferases), and thereby protects the crucial cellular redox-balance [31]. Another important role of NADPH is its involvement in anabolic processes, such as fatty acid synthesis. For instance, NADPH is essential for the production of phospholipids, triacylglycerols, cholesterol and steroids. Also the production of some amino acids, such as glutamic acid and proline, depend on NADPH [5]. It is required for the reduction of ribonucleotides into deoxyribonucleotides, and therefore plays a critical role in dNTP pool homeostasis and high fidelity DNA replication and repair [32]. Furthermore, NADPH plays a central role in cellular

detoxification processes. Hydroxylation of xenobiotics through microsomal cytochrome P450 (CYP) for their subsequent degradation requires continuous re-reduction of CYPs by cytochrome P450 reductases, which are NADPH-dependent. Also *S*-glutathione transferases are involved in the biotransformation and detoxification of xenobiotics, and their recovery requires NADPH as well [33]. NADPH also functions as substrate for NADPH-oxidases (NOX). Firstly discovered in neutrophils and phagocytes, NOX play a role in the unspecific host defense. They produce superoxide which is released into the extracellular space (oxidative burst) to protect the cell from bacteria and fungi. However, NOX enzymes have also been discovered to cause continuous intracellular ROS release at a lower level which was discussed to be important for cellular signaling events [34]. $NADP^+$ also fulfills messenger functions. The 2'phosphorylated form of cADPr derived from $NADP^+$ and the NADP nicotinic acid derivate, NAADP, have been reported to take part in calcium signaling events, too [31].

Involvement of NAD(H) and NADP(H) in redox-reactions - the reversible conversion of oxidized and reduced molecular forms - does not lead to net consumption of these cofactors [23]. However, their functions as substrates for protein modifications and cellular signaling processes involve intramolecular cleavage at the glycoside bond between nicotinamide and the ADP-ribose moieties. Therefore, besides the event of cell division, the need for $NAD(P)^+$ synthesis mainly results from their substrate and signaling functions. There are two principle ways of $NAD^+$ synthesis known to date. The so-called *de novo* synthesis is based on building blocks such as the amino acid tryptophan in mammals and *S. cerevisiae*. Also, more complex components that are taken up with nutrition, e.g. vitamin B3 (nicotinic acid), can be used for $NAD^+$ *de novo* synthesis. Similar components as nicotinic acid are generated when $NAD^+$ is cleaved to release the ADP-ribose moieties, and are recycled in the salvage pathway. The salvage pathway recycles the degradation products containing a nicotinamide ring (nicotinic acid and nicotinamide) in order to resynthesize $NAD^+$. Regarding the overall $NAD^+$ synthesis rate, the salvage pathway is of higher activity than *de novo* $NAD^+$ production [23].

In order to build up and maintain also cellular pools of NADP(H), some $NAD^+$ is further processed to produce $NADP^+$. NAD-kinases (NADKs) are ubiquitous enzymes that preferably use $NAD^+$ and ATP as phosphate donor to synthesize $NADP^+$. Except from the intracellular parasite *Chlamydia trachomatis*, at least one NADK gene has been identified in all sequenced organisms [31, 35]. Regarding the fact that there are transport complexes that shuttle NAD(H) across the inner mitochondrial membrane (e.g. malate-

aspartate shuttle for NADH [36], Ndt1p and Ndt2p for $NAD^+$ in *S. cerevisiae* [37]), but none for NADP(H), the requirement for the presence of cytosolic as well as mitochondrial NADK isoforms becomes obvious. For instance, in *S. cerevisiae*, there are three NADK isoforms: one isoform (Pas5p) was found in mitochondria [38, 39], whereas two isoforms (Utr1p, Yef1p) are located in the cytosol [40-42]. Surprisingly, only one NADK enzyme species has been identified in mammals to date [43].

Biosynthetic processes, continuous ROS production through the respiratory chain and through NADPH-oxidases, and the constant threat of oxidizing environmental conditions require universally available pools of cytosolic as well as mitochondrial NADPH in order to maintain the cellular redox balance. Thus, $NADP^+$-dependent dehydrogenases reduce $NADP^+$ into NADPH, and thereby maintain the physiological NADPH/ $NADP^+$ ratio. Two enzymes of the OPPP, glucose 6-phosphate dehydrogenase (G6PD) and 6-phospho gluconate dehydrogenase, are regarded to hold key positions in maintaining the cytosolic NADPH-pool, especially under oxidative stress situations. For instance, in *S. cerevisiae*, it was shown that NADPH cannot be sufficiently regenerated when G6PD is deleted and the cells are treated with $H_2O_2$ [44]. However, alternative NADPH generating systems are located in different cellular compartments. Such systems comprise $NADP^+$-dependent isoenzymes of isocitrate dehydrogenases (IDPs), malic enzymes (MEs) and acetaldehyde dehydrogenases (ALDHs), as well as mitochondrial transhydrogenases. IDPs convert isocitrate to α-ketoglutarate. In mammalian and yeast cells, IDP isoenzymes can be found in the cytosol, mitochondria and peroxisomes [22]. MEs, also located in the cytosol and mitochondria, generate pyruvate from malate by oxidative decarboxylation [5]. ALDHs contribute to oxidation of aldehydes to their corresponding carboxylic acids [5]. In mammalian cells, ALDH isoenzymes have been found in the cytosol and mitochondria [31], whereas only a cytosolic isoform was yet identified in *S. cerevisiae* [45]. Furthermore, located in the membrane of bacteria and mammals, nicotinamide nucleotide transhydrogenases (NNT) use the proton-motive force to directly generate NADPH by transferring a hydride ion from NADH to $NADP^+$ [22].

Although multiple enzymes can produce NADPH, their relative contribution to the overall NADPH production rate may vary between cell types, organisms and under different growth as well as environmental conditions. The existence of diverse NADPH-generating enzymes along with their differential localizations could be necessary to ensure reductive capacities to prevent oxidative damage [31]. In the last years, different enzymes such as IDPs and MEs were reported to play important roles under oxidizing

conditions, e.g. for self-protection of phagocytes upon oxidative-burst [46]. However, NADPH regeneration through the PPP seems to be pivotal in oxidative stress situations. The first and rate limiting enzyme of the OPPP, G6PD, is regarded to hold a key position in the oxidative stress response. In mice, G6PD knock-out was shown to be lethal during embryogenesis [47]. However, cultured mouse embryonic stem cells deleted for G6PD were viable as long as they were not exposed to oxidative stress [31, 48]. Similar observations were made in a *S. cerevisiae* G6PD knock-out: depletion of G6PD caused hypersensitivity to oxidizing substances [49]. Indeed, exposure to oxidative stress leads to up-regulation of G6PD mRNA and activity [50], and engineered cells overexpressing G6PD were shown to be more tolerant to oxidizing substances [51]. Furthermore, the human metabolic disease G6PD-deficiency causes hypersensitivity to oxidizing substances, leading to severe physiological dysfunctions, e.g. haemolytic anaemia [52]. Hence, PPP activity is crucial for immediate regeneration of NADPH under oxidative stress conditions.

***Flexibility and Non-Linearity of Metabolic Pathways***

Pathway flexibility is essential for maintaining robustness of the metabolic network, and thus to grant survival in a dynamically changing environment. To fulfill this challenge, metabolic reactions underlie tight regulation. Regulation of enzyme activities, e.g., through allosteric effectors, post-translational modifications, up- or down-regulation of enzyme abundances or expression of isoenzymes with different kinetics tunes the flux through metabolic pathways. Enzymes can interact with substrates, intermediates, products or allosteric effectors [53]. Thus, metabolic pathways are not always linear. Feedback or feedforward control is a characteristic feature of metabolic self-regulation. When a certain metabolite reaches a certain concentration, a feedback/feedforward loop is triggered in order to adjust the flux through the pathway. Feedback regulation modulates the activity of an upstream enzymatic reaction; feedforward activation targets downstream reactions (Fig. 3A). Regulatory circuits can occur in the same "substrate-enzyme-product" unit, span distant enzymatic steps or even build the bridge between metabolism and transcription regulation to adjust enzyme concentrations (e.g. the *lac* operon in *Escherichia coli*, [54]). Feedback/feedforward regulation accelerates (positive regulation, activation) or decreases (negative regulation, inhibition) the flux through enzymatic units or pathways. Modulation of enzymatic activity through binding of small molecules or changing conditions such as pH occurs rapidly. Purely happening on the

enzymatic level, feedback/feedforward control can lead to fast temporal concentration changes of metabolic intermediates or products in order to adjust the pathway turnover to acute cellular demands. Differences in metabolite concentrations in time are characteristic for cellular adaptations to changes in nutrient supply or external as well as internal perturbations.

Glycolytic and respiratory oscillations are examples for time-dependent changes in metabolite concentrations dependent on feedback control. Glycolytic oscillation is a well studied metabolic feature which was first discovered by monitoring NADH concentration changes in cultures of the yeast *S. cerevisiae* [55-57]. The amounts of glycolytic intermediates rise and fall in a periodic manner [58] – a phenomenon which has, since then, also been reported for various other organisms, e.g. in human and rat cells [59]. In glycolysis, oscillations occur with a frequency in the minute-range even at constant glucose supply, but accelerate with increasing glucose feed [60]. Glycolytic oscillations originate from the interaction of pathway components among themselves [61-63] (Fig. 3B). Various cyclic operations within single enzymatic units or over distant enzymatic steps demonstrate the non-linearity of the pathway [64]. Different models were published to elucidate the causes and mechanisms for yeast glycolytic oscillations [65-67]. Firstly, phosphofructokinase and its allosteric regulator AMP were revealed as key pacemakers for single-cell glycolytic oscillations [65]. However, recent results suggest rather a combination of various molecular mechanisms within glycolysis, involving the cofactors ATP/ADP and NAD(H), and the stoichiometry of the reaction pathway itself to be causative for the coordination of the oscillation frequency [68-71]. Furthermore, also periodic respiratory bursts can be followed by measuring dissolved oxygen in yeast cultures. They are often connected to the cell cycle and occur with a frequency of one burst in 1-40 hrs [60]. As direct function of oxygen consumption, these respiratory oscillations are tightly connected to and regulated by broad transcriptional changes [72, 73]. However, another type of respiratory oscillation is called “short period synchronized metabolic oscillation” [60]. This form of metabolic oscillation does not depend on the growth phase and is also detectable under glucose depletion. Not only the concentration of dissolved oxygen, but also the amount of carbon dioxide, pyruvate, NADH, ATP, acetate and glycogen oscillate. Possible mechanisms for this type of oscillation were presented, e.g., in a mathematical model by Wolf and coworkers [74], and might result mainly from feedback mechanisms in the comprised pathways.

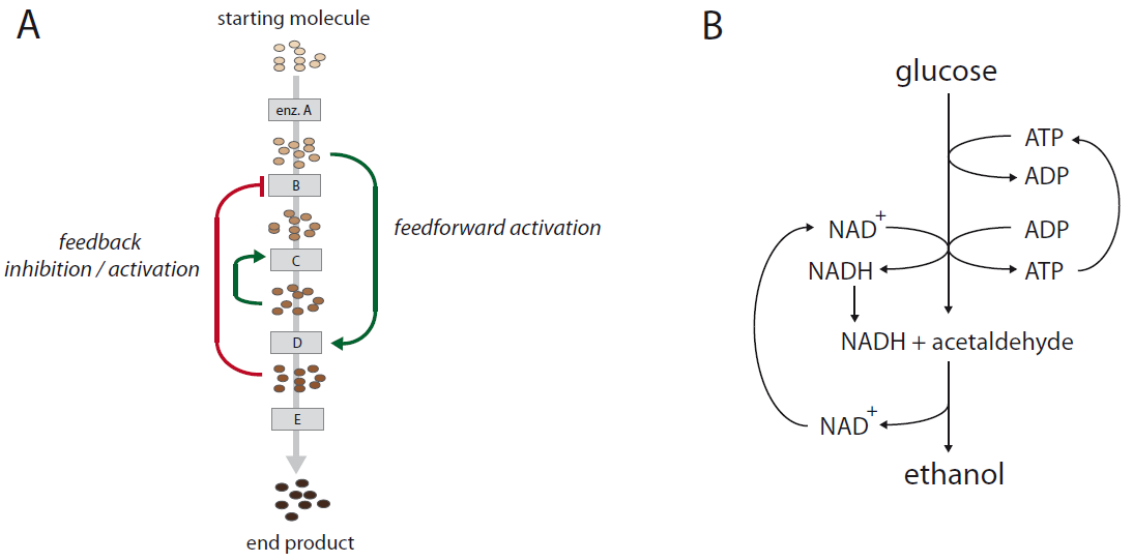


**Figure 3: A, feedback and feedforward regulation within metabolic pathways. B, schematic overview of glycolysis and the biochemical cycles involved in oscillation in *S. cerevisiae*** (modified from Bier *et al.* 2000 [66])

Although the biological reasons for the existence of these phenomena and their molecular underpinnings are not yet fully understood, it can be assumed that the temporal metabolite concentration changes play an important role in processing of frequency encoded biological information to facilitate the coordination of energy production and usage [75]. In general, multienzymatic sequences such as glycolysis do not only need the constant input of energy, they also need to operate in a coordinated manner to avoid interference of single biochemical reactions, and thereby sustain their existence far from thermodynamic equilibrium. Hence, the temporal compartmentalization of biochemical reactions is a source of supramolecular order independent of genes and a characteristic for the self-organization and functioning of biological systems [76, 77].

Most information on the behavior of oscillating biochemical pathways and systems are based on experimental data derived from chemostat cultures of yeast cells synchronized in growth phase and *in silico* models. However, establishing of sustained synchronized glycolytic oscillations can only be achieved under certain experimental conditions. Yeast cells of a culture have to be starved for hours and then exposed to a glucose pulse with subsequent addition of cyanide [60]. This fact hampers studying biochemical oscillations under diverse conditions in synchronized yeast cultures. Therefore, in-depth knowledge of the causes, pacemaker and biological reasons for biochemical oscillations is limited due to the lack of appropriate single-cell analytical methods. To take a “picture” of the momentary metabolic state of a cell, large sets of often chemically diverse metabolites have to be structurally elucidated and quantified. In

principle, NMR spectroscopy (nuclear magnetic resonance spectroscopy) and MS (mass spectrometry) are the two methods of choice for detection and identification of metabolites. Especially when combined with a chromatography device (LC, liquid chromatography or GC, gas chromatography), MS is of higher sensitivity than NMR spectroscopy. Thus, most metabolome data sets are generated on hybrid LC- or GC-MS instruments [78]. Nevertheless, because of the small volume of single cells (*S. cerevisiae* haploid 70 fl, diploid 120 fl [79]), concentrations of multiple metabolite species are often still below the MS detection limit. Further improvements of sample preparation methods and MS sensitivity are vital tasks for the research community and will, when eventually achieved, provide fundamental insights into biochemical organization, heterogeneity and processing of environmental information.

***Metabolic Transition to Counter-Act Oxidative Stress***

Not only changes in nutrient supply cause variations in metabolic fluxes, also external as well as internal disturbances influence metabolite concentrations. Perturbations somewhere in the metabolic network often result in alterations of enzymatic rates around that perturbation. These changes in metabolic turn-over are often entailed by secondary changes in enzymatic activities [80]. However, the organization of the metabolic network aims at elasticity, which means to facilitate the coordination of such parallel reaction chains in order to return to a balanced and stable state [81, 82]. Oxidative stress is a prominent example for an environmental perturbation that provokes an immediate cellular adaptation.

Although high ROS dosages can damage macromolecules through oxidation, they also cause immediate *de novo* post-translational modifications in numerous proteins - and thus affect protein functionality and localization [18]. In oxidative stress situations, a key target for ROS-induced modifications is the glycolytic enzyme glyceraldehyde 3-phosphate dehydrogenase (GAPDH). Posttranslational modifications of GAPDH such as *S*-nitrosylation, *S*-thiolation, carbonylation and ADP-ribosylation have been reported for different cell types and organisms when exposed to oxidizing substances [18, 83-88]. Upon treatment with various oxidants, GAPDH was also found to be inactivated and transported into the nucleus [88]. Remarkably, oxidative inactivation of GAPDH is responsible for increased tolerance of yeast cells to toxic oxidant doses [18]. The underlying mechanism is a redirection of the carbohydrate flux into the PPP. A reduction of GAPDH activity, while glucose transporters remain active, leads to accumulation of

glycolytic metabolites upstream the blocked reaction and also to elevation of metabolites of the glycolysis adjacent PPP [18]. Increased PPP metabolite levels under oxidative stress have also been reported for rat cardiomyocytes and human epithelial cells [89, 90]. Activation of the PPP boosts NADPH production, and NADPH is required for the anti-oxidative machinery to keep the redox-balance in check and protect cells from oxidative damage [23, 91]. Especially upon a sudden oxidative perturbation, rapid metabolic reconfiguration is essential in order to circumvent a lethal redox-imbalance. Inactivation of GAPDH within the first seconds after oxidant treatment facilitates an immediate, transcription-independent metabolic response [92].

Not only oxidative stress is a cataclysmic situation for the cell, also a shift of the delicate redox-balance toward reducing molecules would cause defects in the cellular reaction network. Constitutively high NADPH production might cause reductive stress. Reductive stress impairs biochemical reactions, protein folding, signaling events and is also involved in human diseases [93, 94]. Therefore, dynamic mechanisms to activate the PPP, such as the temporary inactivation of GAPDH, are necessary to clear ROS and also to tune the production of redox-equivalents according to cellular demands.

In the next step after PPP activation and with delay in the minute-range, changes in global gene expression are induced. Up-regulation of PPP enzymes, of proteins with reactive oxygen intermediate scavenging properties, and of proteins involved in protein degradation pathways as well as down-regulation of glycolytic enzymes and proteins involved in biosynthetic processes have been reported in yeast [95]. GAPDH activity recovers within 1-2 hours after the perturbation has ceased. Thus, the glycolytic flux is re-established when transcriptional adaptation is complete [86, 96, 97]. Therefore, dynamic PPP activation upon oxidative inactivation of the glycolytic enzyme GAPDH is necessary to ensure the cell's survival in an acute oxidative stress situation. Transcriptional changes follow the metabolic shift and are essential to balance the redox-state in the long term and compensate naturally occurring ROS level variations [95, 98-100].

### *The Warburg Effect – A Metabolic Transition from Respiration to Fermentation*

Another transition in carbohydrate metabolism is the so-called "Warburg effect". As early as in the 1920s, Otto Warburg and his co-workers observed an elevation in fermentative metabolism when cells undergo tumorigenesis [101]. The Warburg effect is characterized by an increase in glucose uptake and fermentation rate, and a reduction in mitochondrial respiration even under sufficient oxygen supply [102-104]. In healthy

differentiated tissue, pyruvate is subjected to mitochondrial respiration when oxygen levels are high. Fermentation under normoxic conditions is thus also termed “aerobic glycolysis” [105]. Recent results demonstrate that the Warburg effect is not limited to tumor tissue and rather a common feature of rapidly proliferating cells. Warburg-like effects have been reported for yeast [106], proliferating T-cells [107] and during reprogramming of fibroblasts into IPS cells [108]. The reasons why cells resign a higher ATP gain through mitochondrial respiration and switch to low energy yielding fermentation is not yet completely understood. It is broadly assumed that decreased mitochondrial respiration leads to elevated production of intermediates for synthetic processes [102, 103, 109]. This assumption is supported by studies showing that stroma cells which provide tumors with metabolites for energy production undergo the Warburg effect as well [110, 111]. Also, the mechanisms that initiate the transition from respiration toward fermentation remain elusive. However, different factors have been found to be implicated in regulation of the Warburg effect. Signaling cascades such as STAT3 and HIF1α seem to play modulating roles [112, 113], and intensive research has focused on the glycolytic enzyme pyruvate kinase (PYK) which turned out to be a crucial hub in the regulation of the Warburg effect [102, 114, 115].

PYK dephosphorylates phosphoenolpyruvate (PEP) to pyruvate, a reaction which yields one molecule ATP and is therefore responsible for net ATP production in glycolysis. The PYK product pyruvate is either converted to lactate (in mammals; to ethanol in yeast) or it is subjected to mitochondrial respiration. Humans express four different isoforms of PYK. The L and R forms are found in liver and red blood cells, and the M1 and M2 forms were originally identified in muscle [115, 116]. Earlier literature described that most differentiated tissues express PKM1, whereas proliferating cells – especially tumor cells - exclusively express the PKM2 isoform [105, 117, 118]. Studies in cell lines and mouse postulated a switch from PKM1 to PKM2 to be causative for tumor development and growth [119]. These two spliceforms of the same gene only differ in a single exon (exon 9 for PKM1, exon 10 for PKM2). PKM1 has high affinity for its substrate PEP and is of constitutive activity, whereas in PKM2, the amino acid sequence encoded by exon 10 facilitates binding of the glycolytic metabolite fructose 1,6-bisphosphate (FBP). Upon binding, PKM2 changes from its dimeric to its tetrameric state, which also increases the enzyme’s activity [120]. Furthermore, it was shown that post-translational modifications result in PYK-activity regulation. In response to growth factor signaling, phosphorylation of tyrosin residue 105 leads to release of FBP and

hampers tetramer formation in cancer cells, and thus keeps the enzyme in its lower active state [121, 122]. It can be assumed that fine-tuning of PYK-activity is necessary to meet the cell's metabolic demands under varying growth conditions and has broad impacts on the metabolic and cellular network. In support to this presumption are recent data which show that under mild hypoxia, hydroxylation of PKM2 proline 403/408 stimulates binding of HIF1α. This leads to up-regulation of metabolic enzymes in a PYK-activity dependent manner [123]. Along this line of thought, elucidating the effects of PYK-activity changes on the metabolic network and beyond remain major subjects for investigation of pathway flexibility and cellular self-adaptation.

***Crosstalk of the Metabolic Network with Regulatory Macromolecules***

Pathway transitions do not only meet changed cellular demands on the metabolome, they also have wide-ranging effects on the transcriptome and proteome. The metabolic network takes a fundamental position in the cellular regulome and often builds the interface between environmental stimuli and the macromolecular universe of the cell. Changing metabolite concentrations are sensed by enzymes, transcription factors, chromatin, RNA molecules, translational regulators and ion channels [2]. Intermediates whose concentrations are monitored by sensing structures (e.g. the chromatin), and which are surrounded by significant transcriptional changes have been termed "reporter metabolites" [2, 124, 125]. Reporter metabolites are divided into two classes: global and specialized reporter metabolites. Global reporter metabolites are pathway interconnecting factors (e.g. ATP and NAD(H)) that take part in multiple metabolic reactions and sequences. Specialized reporter metabolites are intermediates of distinct metabolic units (e.g. FBP in glycolysis of *Bacillus subtilis* [126]). Reporter metabolites function as transducers of metabolic signals to macromolecular regulatory components of the cell.

Alterations in global reporter metabolite amounts reflect the overall state of the metabolic network and point to broad perturbations or a suboptimal nutrient status. For example, a decrease of the ATP:AMP ratio indicates a severe shortage of cellular energy. Sensing of this signal and transduction to central pathways including TOR (target of rapamycin), AMPK (AMP-activated kinase) and PKA (protein kinase A), which balance energy expenditure and regeneration, leads to blocking of the cell cycle, prevention of ribosome biogenesis, activation of compensatory systems (e.g. autophagy), increased nutrient uptake and mitochondrial activity [127, 128]. Thus, by stopping growth, a collapse of the cellular energy state can be prevented [127, 128].

The regulatory response to concentration changes of specialized reporter agents results in adaptation of the respective metabolic unit; for instance, in up-regulation of pathway-specific enzymes by transcriptional feedforward activators. This can be exemplified by the release of calorie-restriction in yeast, as sudden availability and consumption of nutrients lead to rapid growth acceleration. Simultaneously, ATP turnover increases quickly [129]. However, a decrease in ATP would trigger a stress program, namely – the above mentioned - signaling pathways involving the stress sensors AMPK and TOR, that would hinder further growth [127, 128]. To prevent this problem, yeast reacts by anticipatory up-regulation of purine biosynthesis and salvage enzymes. Two metabolic intermediates of the *de novo* purine producing pathway, AICAR (5'-phosphoribosyl-5-amino-4-imidazole carboxyamide) and SAICAR (succinyl-AICAR) are of fundamental importance in this adaptational process. Binding of AICAR stimulates the formation of the transcription factor heterodimers Pho2p-Pho4p or Pho2p-Bas1p, whereas binding of AICAR and its upstream metabolite SAICAR only directs Pho2p-Bas1p formation. These transcription factor complexes cooperatively induce the expression of purine biosynthesis (*ADE*) and phosphate utilization (*PHO*) pathways [130]. The reason for the induction of different responses to AICAR and SAICAR could result from their dual function in inosine monophosphate (IMP) and AMP-biosynthesis, and the fact that purine nucleotide synthesis leads to significant phosphate consumption. Thus, the competition between Pho4p and Bas1p for the formation of the active transcription factor dimer with Pho2p could be responsible for fine tuning of the responses to changes in the *de novo* pathway, altered GMP:AMP ratios and concerted regulation of purine synthesis and phosphate utilization during growth acceleration [130-132]. Understanding connection points between the small molecular and macromolecular universe of the cell is therefore key issue for systems biology research and will provide essential knowledge of biological organization.

### *Inheritable Disorders of Carbohydrate Metabolism*

Genetic disorders which cause malfunctions of metabolic enzymes can lead to detrimental consequences for the cellular homeostasis, and are responsible for various diseases in man. Mutations often modulate enzymatic activity or lead to the production of abnormal metabolites [133]. Thus, defective biochemical reactions interfere with the normal function of the metabolic pathway and with related pathways – last but not least, can disturb the whole metabolic network.

Deficiencies of glycolytic enzymes perturb the cellular energy and redox-balance. This becomes most evident in tissues or cells that lack mitochondria, e.g. mature red blood cells (RBCs) depend on glycolysis for ATP generation [134]. Most glycolytic enzyme deficiencies, e.g. triosephosphate isomerase (TPI), pyruvate kinase, hexokinase or GAPDH deficiency, cause haemolytic anaemia [135-138]. Reduced glycolytic flux leads to abnormal breakdown of RBCs. Dependent on the degree of glycolysis impairment, the level of anaemia can range from harmless to life-threatening [136].

Disruptions of a normal flux through the oxidative branch of the PPP, as it is the case in glucose 6-phosphate dehydrogenase (G6PD) deficiency, impair the cell's NADPH production and cause increased sensitivity to oxidative stressors as infections or drugs. RBCs are especially prone to oxidative damage [139]. Due to their oxygen transport function, they are highly dependent on a constantly available cytosolic NADPH pool to recycle oxidized GS-SG [31]. Haemolytic anaemia is therefore a typical and frequent symptom of G6PD deficiency as well [52].

With ~400 million diagnosed patients worldwide, G6PD deficiency is the most common metabolic enzymopathy [52]. However, numerous deficiencies of metabolic enzymes are diagnosed far less frequently or never [140]. Mutations in the mammalian genome occur non-directed and at a frequency of ~$10^{-6}$ per locus and gamete [141]. Thus, following the laws of probability every enzymopathy has a calculable incidence. However, many enzyme deficiencies in central carbohydrate metabolism occur well below the expected rate [142]. This fact points to lethality of homozygous null alleles. A complete loss of enzyme activity would lead to total breakdown of the metabolic balance.

An example for a rare glycolytic enzymopathy is triosephosphate isomerase (TPI)-deficiency. Only ~100 patients have been diagnosed for TPI-deficiency since description of the ailment in the 1960's [137, 143, 144]. This autosomal recessive disorder becomes evident when TPI alleles are homozygous or compound heterozygous for mutations that do not inactivate the enzyme, but impair its quaternary structure and stability. Therefore, only a residual and strongly decreased enzymatic activity is maintained [145, 146]. Symptoms of TPI-deficiency are haemolytic anaemia, cardiomyopathy, severe neurological dysfunctions and susceptibility to infections – malfunctions that mostly lead to death in early childhood [144]. Except for members of a Hungarian family, all diagnosed TPI-patients were homozygous or compound heterozygous for the same amino acid exchange (Glu104Asp) [144, 147].

Alterations in protein expression level and enzyme activity can result from specific single point mutations. This fact also contributes to the rareness of inheritable metabolic disorders. Some mutations that affect only a specific base, and therefore bring up such effects as described for TPI-deficiency, are much less frequent than mutations which lead to the entire loss of an enzyme. Complete loss of protein expression or activity mostly results from frameshift mutations which can occur all along the coding sequence [142].

Fast diagnosis of inheritable syndromes is necessary in order to predict a child's prognosis and choose the right treatments, if available, to protect its health [140]. However, the individual rareness of inheritable metabolic disorders often hampers diagnosis. The determination of affected alleles by classic mapping strategies and cloning approaches is only applicable if several affected individuals of unrelated families are known. Lacking knowledge of diagnostic biomarkers and the etiologies of infrequent metabolic syndromes, often keep metabolic enzymopathies unrevealed [140]. A big step forward to fast diagnosis was made with the development of new analytical technologies (e.g. mass spectrometry), which already helped to elucidate various inborn dysfunctions of metabolic enzymes, including extremely rare diseases such as transaldolase- (8 patients diagnosed before 2008) and ribose 5-phosphate isomerase-deficiency (1 patient diagnosed before today) [148-151].

***Robustness of the Metabolic Network is Premise for Cellular Survival***

Cellular survival is under constant threat of environmental perturbations. The metabolic network is susceptible to changes in the environment and transmits those changes to regulatory components, such as the proteome or transcriptome. A characteristic for metabolic stability is functional redundancy. In *S. cerevisiae*, ~75% of enzyme deletions can be balanced and have no detectable effects on the metabolic network flux [152]. This experimental number might be biased due to multiple paralogues enzymes [152] and varying experimental conditions [153], but still underlines the enormous robustness of the entire metabolic network. Indeed, deletion of most paralogue-free enzymes causes metabolic flux disruptions [152, 154]. However, those flux changes can be detected in surprisingly narrow parts of the network [152, 155]. Thus, perturbations can often be balanced within distinct metabolic modules. Metabolic modules can comprise sets of biochemical reactions or whole biochemical pathways [2]. Since the network aims at flexibility under changing conditions, metabolic modules can be adjusted in activity to

meet the required cellular demands to keep the entire network in a stable state. Therefore, robustness depends on metabolic modularity and dynamic metabolic reconfigurations.

**Aim of this Thesis**

Dynamic adaptation of the metabolic network to environmental and biological changes is vital for cellular survival. The glycolytic enzyme pyruvate kinase (PYK) has been reported to play a paramount role in the regulation of energy metabolism in proliferating cells. In human tissue, a decrease in PYK activity was stated to be essential for promoting the Warburg effect – a shift from oxidative to fermentative metabolism during tumorigenesis. This shift from aerobic to anaerobic metabolism requires adaptation of cellular antioxidant-systems. However, it had not been understood how redox- and energy metabolism are coordinated. Therefore, main task of this thesis was to develop and exploit yeast models in order to elucidate the coordination of the activity of these fundamental metabolic processes in eukaryotic cells.

In this context, it has been postulated that the human pyruvate kinase isozymes PKM1 and PKM2 define normal versus cancer tissue, and that alternative splicing between these isoforms is responsible for the induction of the Warburg effect [119]. However, these conclusions had to be challenged, as they would imply a simultaneous shutdown of glycolytic and oxidative energy metabolism under conditions for rapid growth that has high energetic demands. Therefore, we aimed to use more advanced analytical technology to verify or disprove these assumptions.

Exposing cells to an oxidative stressor causes a fast but temporally limited redirection of the carbohydrate flux into the PPP. This metabolic reconfiguration is part of the cellular anti-oxidative system and increases the production of redox-equivalents for the anti-oxidative machinery in form of NADPH. However, there were indications that the function of the PPP could go beyond its role as NADPH donor during the stress response. As rapid metabolic changes can be sensed by macromolecules, we speculated that this transition could be part of the eukaryotic gene expression program that is induced in response to perturbations. A combination of yeast genetics and transcriptional profiling should be used to investigate this hypothesis.

Finally, the importance of the metabolic network balance in humans should be studied in the context of a concrete medical problem, the metabolic disorder ribose 5-phosphate isomerase (RPI)-deficiency. RPI-deficiency was reported as malfunction of

central carbohydrate metabolism, and with a single diagnosed case, it is currently considered as the rarest diagnosed human disease. However, the uniqueness of this case cannot be explained by the natural mutation rate, and as the molecular etiology of RPI-deficiency had been unknown, there had also been no explanation for its occurrence. Therefore, a combination of metabolic and gene expression studies in both patient cells and yeast models was exploited to shed light on the molecular disease etiology of this case.

## Manuscript 1

(pages 22-30 in print version)

# Regulatory crosstalk of the metabolic network

Nana-Maria Grüning, Hans Lehrach and Markus Ralser

Max Planck Institute for Molecular Genetics, Ihnestrasse 73, 14195 Berlin, Germany

Trends in Biochemical Sciences. 2010 Apr;35(4):220-7

journal homepage: http://www.cell.com/trends/biochemical-sciences

DOI link for original publication: http://dx.doi.org/10.1016/j.tibs.2009.12.001

***Contributions to Manuscript 1***

Writing of this review article, including figure design and generation, was part of this thesis. Markus Ralser contributed equally to writing of the manuscript. He also structured the text and gave support in finding solutions for graphical depiction of the text content. Hans Lehrach was involved in scientific discussions.

## Manuscript 2

# Pyruvate Kinase Triggers a Metabolic Feedback Loop that Controls Redox Metabolism in Respiring Cells

Cell Metabolism. 2011 Sep 7;14(3):415-27.

Nana-Maria Grüning[1], Mark Rinnerthaler[2], Katharina Bluemlein[1], Michael Muelleder[1], Mirjam MC Wamelink[3], Hans Lehrach[1], Cornelis Jakobs[3], Michael Breitenbach[2] and Markus Ralser[1,4*]

[1] Max Planck Institute for Molecular Genetics, Ihnestrasse 73, D-14195 Berlin

[2] Dept. of Cell Biology, University of Salzburg, Hellbrunnerstrasse 34, A-5020 Salzburg

[3] VU University Medical Center, Metabolic Unit, Dept. Clinical Chemistry, De Boelelaan 1117, NL- 1081 HV Amsterdam

[4] Cambridge Systems Biology Centre & Dept. of Biochemistry, University of Cambridge, Sanger Building, 50 Tennis Court Road, Cambridge CB2 1GA, UK

Cell Metabolism
Article

# Pyruvate Kinase Triggers a Metabolic Feedback Loop that Controls Redox Metabolism in Respiring Cells

Nana-Maria Grüning,[1] Mark Rinnerthaler,[2] Katharina Bluemlein,[1] Michael Mülleder,[1] Mirjam M.C. Wamelink,[3] Hans Lehrach,[1] Cornelis Jakobs,[3] Michael Breitenbach,[2] and Markus Ralser[1,4,5,*]
[1]Max Planck Institute for Molecular Genetics, Ihnestrasse 73, 14195 Berlin, Germany
[2]Department of Cell Biology, University of Salzburg, Hellbrunnerstrasse 34, 5020 Salzburg, Austria
[3]Metabolic Unit, Department of Clinical Chemistry, VU University Medical Center, De Boelelaan 1117, 1081 HV Amsterdam, The Netherlands
[4]Cambridge Systems Biology Centre
[5]Department of Biochemistry
University of Cambridge, Sanger Building, 50 Tennis Court Road, Cambridge CB2 1GA, UK
*Correspondence: mr559@cam.ac.uk
DOI 10.1016/j.cmet.2011.06.017

## SUMMARY

**In proliferating cells, a transition from aerobic to anaerobic metabolism is known as the Warburg effect, whose reversal inhibits cancer cell proliferation. Studying its regulator pyruvate kinase (PYK) in yeast, we discovered that central metabolism is self-adapting to synchronize redox metabolism when respiration is activated. Low PYK activity activated yeast respiration. However, levels of reactive oxygen species (ROS) did not increase, and cells gained resistance to oxidants. This adaptation was attributable to accumulation of the PYK substrate phosphoenolpyruvate (PEP). PEP acted as feedback inhibitor of the glycolytic enzyme triosephosphate isomerase (TPI). TPI inhibition stimulated the pentose phosphate pathway, increased antioxidative metabolism, and prevented ROS accumulation. Thus, a metabolic feedback loop, initiated by PYK, mediated by its substrate and acting on TPI, stimulates redox metabolism in respiring cells. Originating from a single catalytic step, this autonomous reconfiguration of central carbon metabolism prevents oxidative stress upon shifts between fermentation and respiration.**

## INTRODUCTION

Glycolysis and oxidative phosphorylation are primary sources of cellular energy. Pyruvate, the end product of glycolysis, is either metabolized through the citrate cycle and respiratory chain or fermented to lactate or ethanol. Eukaryotic cells depend on glycolysis but can grow without oxidative phosphorylation. In the first half of the twentieth century, Otto Warburg and his coworkers observed that cells switch from oxidative to fermentative metabolism during tumorigenesis. Despite the presence of oxygen, most cancer tissue respires with low efficiency but has increased glucose consumption and lactate secretion (Hsu and Sabatini, 2008; Levine and Puzio-Kuter, 2010; Najafov and Alessi, 2010; Warburg, 1956). Recently, it has become clear that this metabolic transition is not specific to cancer cells but rather a common metabolic feature of cells that rapidly proliferate. Warburg-like effects have been described in yeast (Ruckenstuhl et al., 2009), during T cell proliferation (Colombo et al., 2010), and upon reprogramming fibroblasts into IPS cells (Prigione et al., 2010).

The glycolytic enzyme pyruvate kinase (PYK) which catalyzes the conversion of phosphoenolpyruvate (PEP) to pyruvate has been implicated in the regulation of the Warburg effect. The low-active splice form of the PKM-type pyruvate kinase (PKM2) is present at higher concentration in cancers compared to matched control tissue (Bluemlein et al., 2011; Christofk et al., 2008). A change to expression of the higher active PKM1 using a lentiviral system slowed cancer progression in xenograft models (Christofk et al., 2008). Recent results indicate that PKM2 is regulated by phosphorylation of tyrosine residue 105. This modification inhibited the formation of the active PKM tetramer in cancer cells (Hitosugi et al., 2009). Furthermore, PKM2 hydroxylation on proline 403/408 stimulates binding and activation of hypoxia-induced factor HIF1$\alpha$, increasing the expression of metabolic enzymes under hypoxia in a PYK activity-independent manner (Luo et al., 2011).

Respiration and fermentation differ in their metabolic consequences. Although highly efficient, oxidative phosphorylation produces a significant amount of reactive oxygen species (ROS). Under physiological conditions, up to 1%–2% of metabolized oxygen is converted to superoxide (Cadenas and Davies, 2000). To avoid an excess of oxidizing compared to reducing molecules in the cell (oxidative stress), ROS are removed by a complex machinery. ROS neutralization, and maintenance of the redox balance, involves shuttling of reduction power through the pyridine nucleotide NADPH. NADPH serves as cofactor for fatty acid synthesis, and the recycling steps within the glutathione, thioredoxin, and peroxiredoxin systems, whose redox state control is crucial (Pollak et al., 2007; Ying, 2008).

Here we describe a mechanism that synchronizes redox metabolism when respiration is activated, and show that both respiration and the production of redox equivalents are

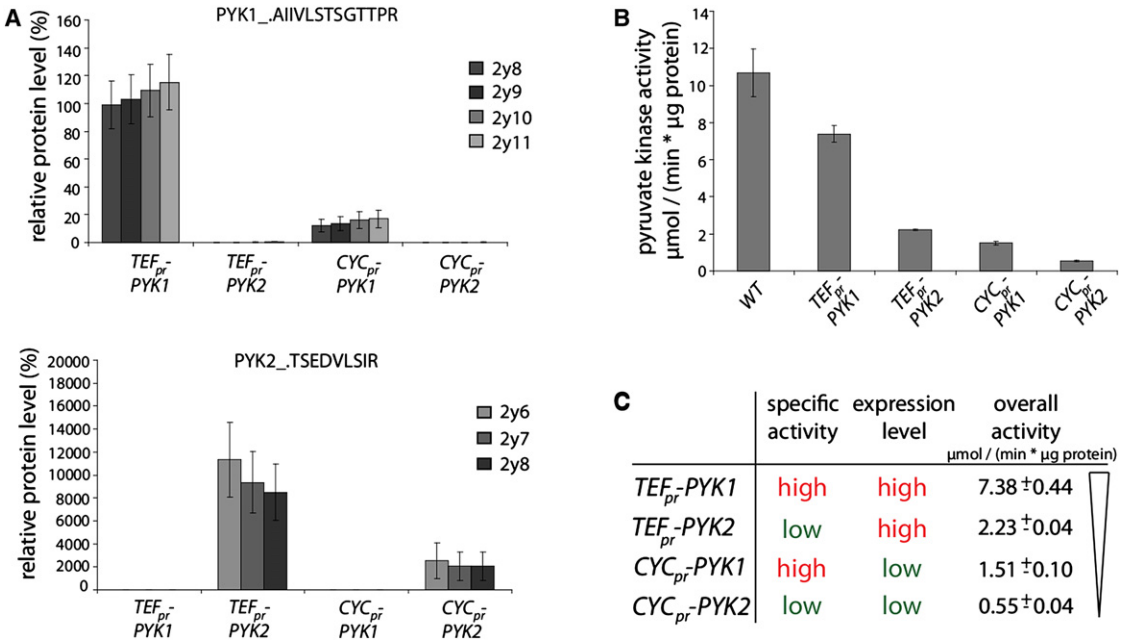


**Figure 1. A Yeast Model for Studying Pyruvate Kinase**

(A) PYK expression levels. Quantification of a Pyk1p (upper panel)- or Pyk2p (lower panel)-specific peptide in *Δpyk1Δpyk2* yeast expressing $TEF_{pr}$-*PYK1*, $TEF_{pr}$-*PYK2*, $CYC_{pr}$-*PYK1*, or $CYC_{pr}$-*PYK2*. Normalized peak intensities of >3 MRM transitions are presented as the relative expression level (%) compared to the concentrations in the wild-type strain BY4741. For both isoforms, levels from the *CYC1* promoter ($CYC_{pr}$) were around 20% of the expression levels from the *TEF1* ($TEF_{pr}$) promoter. Error bars, ±SD from normalization to three reference peptides.

(B) Pyruvate kinase activity of BY4741 (WT) and $TEF_{pr}$-*PYK1*, $TEF_{pr}$-*PYK2*, $CYC_{pr}$-*PYK1*, or $CYC_{pr}$-*PYK2* yeast. Error bars, ±SD.

(C) Overview on the yeast models with varying PYK activity.

synchronized by PYK. We engineered yeast strains with different PYK activities and discovered that yeast respiration is inversely correlated with PYK enzyme activity. However, an increase in ROS levels was not detected when respiration was activated, and in addition, resistance to oxidants increased.

We found that a metabolic feedback loop is responsible for preventing an increase in ROS upon respiration activation. Low PYK enzyme activity caused accumulation of PEP, its substrate, which in turn inhibited TPI, an enzyme of upper glycolysis. This inhibition of TPI increased metabolite content of the pentose phosphate pathway (PPP), a catabolic pathway closely connected to glycolysis. PPP is an important source of reduced NADPH (Slekar et al., 1996; Wamelink et al., 2008) and is involved in the adaptation of gene expression during stress conditions (Krüger et al., 2011). In yeast strains deficient for this process, ROS were improperly cleared, accumulated, and caused damage on macromolecules when cells started respiration. Thus, metabolic feedback activation of the PPP prevents oxidative stress upon induction of oxidative metabolism. Both processes are concordantly regulated by the same enzyme, PYK, a new hub in the regulation of these fundamental metabolic processes.

## RESULTS

### Generation of Yeast Strains with Varying PYK Activity

Yeast possesses two PYK paralogues (PYK1, PYK2) which are differentially expressed between fermentative and oxidative metabolism (Boles et al., 1997). By expressing either Pyk1p or Pyk2p under the control of either a strong (*TEF1*) or a weak (*CYC1*) constitutive promoter in yeast strains deleted for both endogenous loci, we generated four yeast strains with different PYK activities. Expression of Pyk1p and Pyk2p was quantitated using liquid chromatography/multiple reaction monitoring (LC-MRM) by four MRM (Q1/Q3) transitions as described (Bluemlein and Ralser, 2011). *PYK1* expression driven by the *TEF1* promoter was at a similar level as endogenous *PYK1* expression level in the wild-type strain ($2.9 \times 10^5$ copies per cell) (Ghaemmaghami et al., 2003) (Figure 1A). Consistent with this, *PYK2* (expressed at $2.13 \times 10^3$ copies in wild-type cells [Ghaemmaghami et al., 2003]) exceeded the concentration when expressed under the *TEF1* promoter (Figure 1A, lower panel). In both cases, the *CYC1* promoter constructs expressed at ~20% of this level.

Then we determined the enzymatic activity of PYK in these strains. $TEF1_{pr}$-*PYK1* yeast had 69% of wild-type activity, $CYC1_{pr}$-*PYK1* yeast 14%. As expected, activity in PYK2-expressing cells was lower: the $TEF1_{pr}$-*PYK2* strain had 22% and the $CYC_{pr}$-*PYK2* strain 5% activity (Figure 1B). Thus, protein quantification and enzyme activity measurements confirmed that, in wild-type yeast, *PYK2* is expressed at lower levels compared to *PYK1* and has a lower specific activity. Controlled expression of these proteins with two promoters of different strength generated four strains with gradually decreasing PYK activity (Figure 1C).

### Low Pyruvate Kinase Activity Activates Respiration

Growth of these yeast strains correlated with PYK activity. $TEF_{pr}$-*PYK2* grew slower as $TEF_{pr}$-*PYK1*, $CYC_{pr}$-*PYK1* even

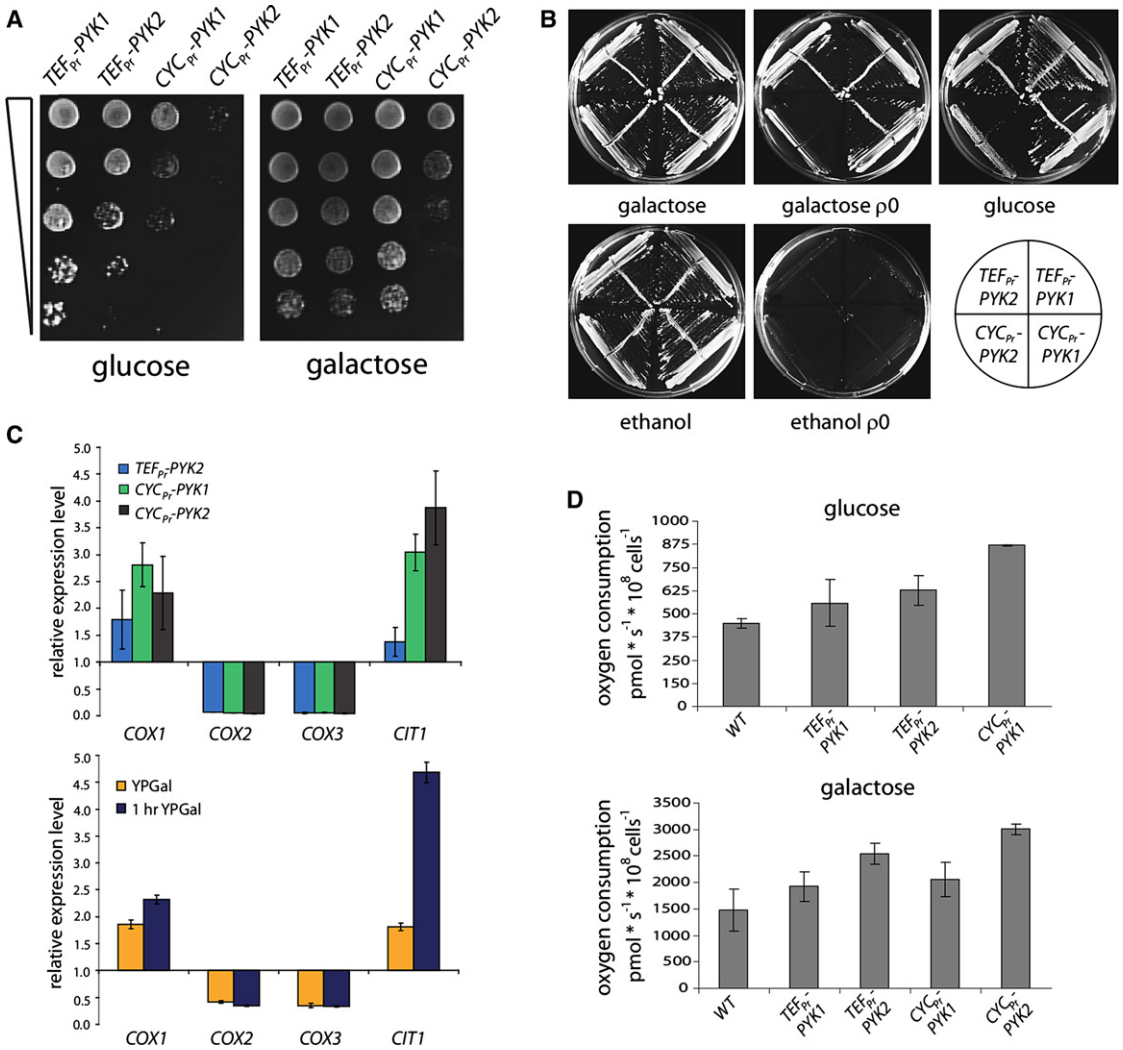


**Figure 2. PYK Activity Regulates Respiration**

(A) Growth deficits caused by low PYK activity are rescued on galactose. Strains were grown overnight, diluted to an $OD_{600}$ of 3.0, and spotted as serial dilutions (1:1, 1:5, 1:25, 1:125, and 1:625) on YPD (glucose) and YPGal (galactose).

(B) Galactose rescue of low PYK activity requires a functional respiratory chain. Yeast strains with deficient mitochondrial DNA (ρ0) were grown alongside with controls (ρ+) on YP media with the indicated carbon sources. Galactose did not compensate for the growth deficits caused by low PYK activity in ρ0 yeast.

(C) Regulation of oxidative metabolism's mRNA expression by PYK and galactose. *COX1*, *COX2*, *COX3*, and *CIT1*, implicated in oxidative energy metabolism, were analyzed by qRT-PCR. Expression values are given as fold change compared to $TEF_{pr}$-*PYK1* yeast, relative to glucose grown yeast (upper panel). Changes in mRNA expression of the same transcripts in yeast shifted to galactose for 1 hr, or permanently, activating oxidative metabolism (lower panel). Both conditions caused a similar mRNA expression fingerprint. Error bars, ±SD.

(D) Oxygen consumption increases with low PYK activity. Oxygen consumption in logarithmically growing wild-type yeast and PYK mutants was determined on glucose (upper panel) and galactose media (lower panel), and cell numbers were determined with an electric field multichannel cell counting system (CASY). Overall oxygen consumption was three times increased in galactose, low PYK activity increased oxygen uptake under both conditions. Error bars, ±SD.

more slowly, and the strain with the lowest PYK activity ($CYC1_{pr}$-*PYK2*) showed very slow growth only (illustrated by a spot test [Figure 2A, left panel]; phenotypes in liquid culture were similar [data not shown]).

Surprisingly, the differences in growth were largely rescued by a switch of the carbon source from glucose to galactose (Figure 2A, right panel). Both carbon sources are fermentable but have different effects on respiration. Glucose represses respiration, much more than galactose (Carlson, 1999; Ruckenstuhl et al., 2009). Therefore we investigated whether the galactose rescue was attributable to an increase in respiration.

First, we tested if galactose also rescued the growth defects in respiratory-deficient (ρ0) cells. Bona fide ρ0 strains were generated by the method of Goldring et al. (1970) and lost the capability to grow on nonfermentable carbon sources (ethanol, glycerol; *pet* phenotype), indicating mitochondrial deficiency (Figure 2B). Differences in growth between glucose and galactose media were abolished; i.e., ρ0-$CYC_{pr}$-*PYK2* cells were not viable on galactose media and displayed a similar growth

phenotype as their ρ+ counterparts on glucose (Figure 2B). Thus, galactose rescue of growth deficiencies caused by low PYK activity required a functional respiratory chain.

Next, we analyzed transcripts involved in oxidative energy metabolism (*COX1*, *COX2*, *COX3*, and *CIT1*) by qRT-PCR. Low PYK activity led to the upregulation of *COX1* and *CIT1* and the downregulation of *COX2* and *COX3* (Figure 2C, upper panel). Shifting cells from glucose to galactose had a similar effect (Figure 2C, lower panel). Thus, low PYK activity and a shift to respiratory-active media led to a similar regulation of these enzymes.

Finally, we measured oxygen uptake in a closed chamber oxygraph (Oroboros). There was a strong increase in oxygen uptake when PYK activity was low (Figure 2D, upper panel). On glucose, oxygen consumption doubled in $CYC_{pr}$-*PYK1* yeast compared to the wild-type strain. A similar set of experiments was conducted on galactose media, which facilitated including $CYC_{pr}$-*PYK2* yeast. Galactose increased the overall oxygen consumption ~3-fold; but also here respiration was stimulated by PYK activity (Figure 2D, lower panel). The $CYC_{pr}$-*PYK2* strain consumed 3005 pmol oxygen * $10^8$ cells$^{-1}$ * s$^{-1}$ (6-fold greater than glucose wild-type). Consequently, PYK-mediated regulation of respiration was additive to the release of glucose repression and is thus an independent process.

In summary, several experiments demonstrated an increase in oxidative metabolism when PYK activity was low. Growth differences between PYK mutants were abolished on respiratory-active galactose media, and depletion of the respiratory chain prevented this effect. Furthermore, reduced PYK activity and a release of glucose repression provoked a similar mRNA expression fingerprint on studied enzymes of oxidative metabolism. Most importantly, oxygen consumption was inversely correlated with PYK activity.

## High Respiration Rates Are Coupled to an Increased Antioxidative Capacity

Respiration is responsible for most of the macromolecule oxidation that occurs in living cells, since high amounts of ROS leak from the respiratory chain (Cadenas and Davies, 2000; Turrens, 1997). To detect overall ROS levels, we stained yeast with dihydroethidium (DHE). The DHE oxidation products 2-hydroxyethidium and ethidium are fluorescent, transferring this dye into a sensitive and reliable ROS probe, which primarily detects the superoxide anion (Benov et al., 1998). Remarkably, the 3-fold greater oxygen consumption in yeast grown on SC-galactose media (Figure 2D) did not result in an increased DHE fluorescence, which indicates that superoxide levels were unchanged (Figure 3A, upper panel). A similar result was obtained for low PYK activity: despite the strong increase in respiration, ROS levels did not increase (Figure 3A, lower panel). A staining for $H_2O_2$, the first intermediate when superoxide is neutralized through superoxide dismutase, confirmed these results (Figure 6B). Thus, respiring cells compensate for the increased ROS leakage.

We tested the influence that respiration activation had on oxidant resistance. Strains with varying PYK activity were spotted onto agar containing the oxidants $H_2O_2$, diamide, cumene hydroperoxide (CHP), tert-butyl hydroperoxide (TBH), juglone, and menadione. Growth was measured as relative spot intensities using CellProfiler (Carpenter et al., 2006) (Figure 3B). Remarkably, increased respiration of cells with low PYK activity did not sensitize them to oxidants. Indeed, resistance to diamide, CHP, and TBH was strongly increased. Similar results were obtained when respiration was activated with galactose, as tested with diamide (see Figure S1 available online). Low PYK activity also increased resistance to $H_2O_2$, juglone, and menadione, although to a lesser extend (Figure 3B). Effects of diamide, CHP, tert-butylhydroperoxide, and menadione were further tested in liquid cultures. Overnight cultures of BY4741 and the PYK mutants were diluted, supplemented with the oxidants, and their growth followed spectrophotometrically. Low PYK activity increased the resistance to these oxidants, as higher growth capacity was maintained (Figure 3C). Interestingly, also the slight difference in PYK activity between the wild-type BY4741 and the $TEF_{pr}$-PYK1 strain (Figure 1) pictured as increase in oxidant resistance (Figures 3B and 3C). Finally, we tested for maintenance in colony formation in the presence of a high oxidant dose. Liquid cultures were supplemented with 3 mM diamide and plated onto YPD agar before and 24 hr after addition of the oxidant. $CYC_{pr}$-*PYK1* yeast maintained a higher number of forming colonies, indicating increased survival under very strong redox stress (Figure 3D). Thus, low PYK activity triggered respiration but broadly increased oxidant resistances rather than ROS levels.

## Low PYK Activity Causes Accumulation of Its Substrate Phosphoenolpyruvate

To investigate whether metabolic changes were responsible for the increased oxidant resistances, we started by quantifying the PYK substrate PEP. We developed a hydrophilic interaction liquid chromatography/multiple reaction monitoring (HILIC-MRM) method suitable for quantification of this highly polar metabolite out of whole-cell extracts. PEP was extracted with methanol/water and separated on a HILIC column (1.7 μm particle size, 2.1 × 100 mm) using ultra-high-pressure binary pump (Agilent 1290) at 800–1000 bar and a flow rate of 1 ml/min. Quantification was conducted on a triple-quadrupole mass spectrometer (AB/Sciex QTRAP5500) with electrospray ionization (ESI) and achieved by standard addition, which resulted in a reliable method as solid linear correlations ($R^2$ 0.97–0.99) were achieved (Figure 4A, left panel).

PEP was determined in $TEF_{pr}$-*PYK1*, $CYC_{pr}$-*PYK1*, and $CYC_{pr}$-*PYK2* yeast that were pregrown overnight in YPD, diluted with fresh media to an $OD_{600}$ of 0.15, and cultivated in triplicates for further 5 hr. Low PYK activity resulted in strong accumulation of PEP. $CYC_{pr}$-PYK2 yeast had a 13.6 times higher PEP concentration as the $TEF_{pr}$-*PYK1* strain (Figure 4A, right panel).

## PEP Is an Inhibitor of Triosephosphate Isomerase

Searching for physiological consequences of accumulating PEP, we noticed that this molecule influenced an enzyme-coupled assay of phosphofructokinase, due to inhibition of the component TPI (Fenton and Reinhart, 2009). TPI is a glycolytic enzyme that converts the three carbon sugars glyceraldehyde 3-phosphate (gly3p) and dihydroxyacetone phosphate (dhap). We examined TPI activity and determined the kinetic parameters for yeast TPI (endogenous), human TPI (expressed in yeast), and rabbit TPI (purified from muscle). Yeast TPI had a $K_m$ of

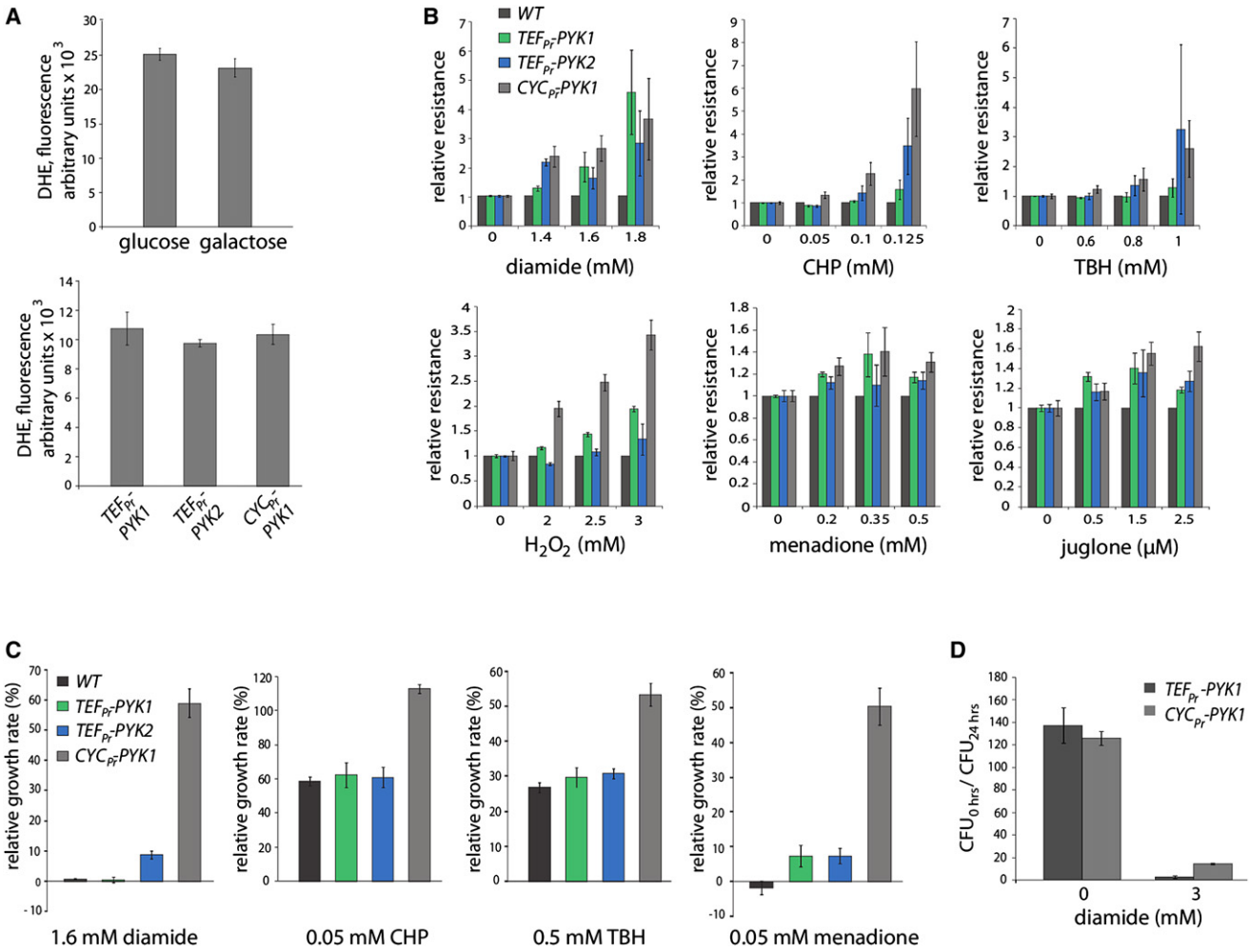


**Figure 3. Activation of Respiration Does Not Increase ROS Levels, but It Does Increase Oxidant Resistance**

(A) Superoxide levels are not increased upon the activation of oxidative metabolism. ROS levels were determined by assaying DHE fluorescence in exponentially growing yeast in SCGluc and SCGal media (upper panel) or in yeast with varying PYK activity (lower panel). Error bars, ±SD. See also Figure 6B.

(B) Oxidant resistances increase with low PYK activity. BY4741 and yeast strains with varying PYK activity were spotted in triplicates on media containing diamide, cumene hydroperoxide (CHP), tert-butyl hydroperoxide (TBH), hydrogen peroxide ($H_2O_2$), menadione, or juglone. Pictures taken from spot tests were analyzed with CellProfiler, values indicate the ratio of spot intensity of the indicated strain to the wild-type control. Error bars, ±SD. See also Figure S1.

(C) Low PYK activity increases growth capacity in the presence of oxidants. Yeast models with different PYK activity were grown with our without oxidants and analyzed spectrophotometrically. Values indicate the doubling time relative to the nontreated control culture. Error bars, ±SD.

(D) Increased survival of yeast with low PYK activity in oxidant media. *$TEF_{pr}$-PYK1* and *$CYC_{pr}$-PYK1* yeast was incubated in YPD and in YPD supplemented with 3 mM diamide for 24 hr, plated, and formed colonies counted. Error bars, ±SD.

854 μM, human TPI 710 μM, and rabbit TPI 698 μM (Figure 4B). Next, we tested whether PEP inhibits TPI (black axes). All TPI paralogues were efficiently inhibited by titrating PEP (Figure 4B). Using the Cheng-Prusoff equation (Cheng and Prusoff, 1973), we calculated a PEP inhibitory constant ($K_i$) of 392 μM for yeast TPI, 163 μM for human TPI, and 156 μM for rabbit TPI. Thus, TPI is inactivated by physiological PEP concentrations. Human and rabbit TPI were inactivated twice as efficiently compared to yeast TPI.

## TPI Inhibition Is Required for Increased Antioxidative Capacity in Respiring Yeast

We investigated whether TPI feedback inhibition is mechanistically linked to the increase in oxidant resistance of respiring cells, as we had observed earlier that low TPI activity increases oxidative stress resistance in yeast and *C. elegans* (Ralser et al., 2007, 2009).

First, PEP inhibition was tested on five human TPI alleles that have been associated with the pathogenesis of the metabolic syndrome TPI deficiency (Orosz et al., 2009). Wild-type human TPI, $TPI_{Cys41Tyr}$, $TPI_{Glu104Asp}$, $TPI_{Gly122Arg}$, and $TPI_{Phe240Leu}$ were all strongly inhibited in the presence of 900 μM PEP. However, $TPI_{Ile170Val}$, an allele with low catalytic activity (Ralser et al., 2006), was significantly less inhibited (Figure 4C).

The identification of the relative PEP resistance of $TPI_{Ile170Val}$ allowed the generation of yeast strains in which TPI activity was insensitive to PEP accumulation. Double knockout mutants (Δ*pyk1*Δ*tpi1*) that expressed either human TPI or human

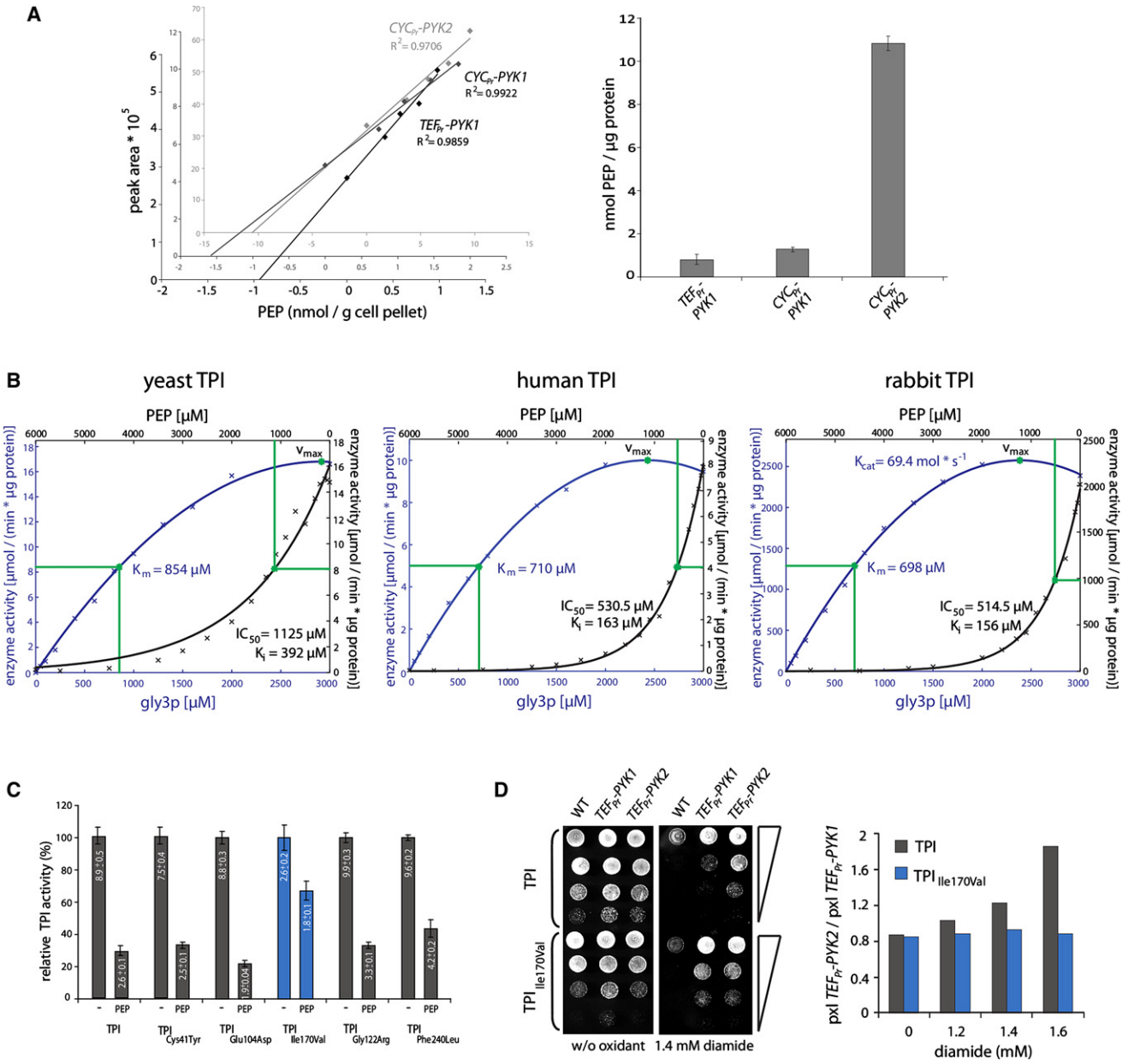


**Figure 4. Phosphoenolpyruvate Accumulates in Cells with Low PYK Activity and Inhibits Triosephosphate Isomerase**

(A) HILIC-MRM quantification of PEP (left panel) Standard addition of PEP to whole-cell methanol/water yeast extracts; and quantification of PEP separated by HILIC using multiple reaction monitoring (MRM). Quantification is demonstrated by linear regression, $R^2$ vales of >0.97 were obtained. (Right panel) HILIC-MRM quantification of PEP in *TEF$_{pr}$-PYK1*, *CYC$_{pr}$-PYK1*, and *CYC$_{pr}$-PYK2* yeast; PEP is strongly accumulated in yeast with low PYK activity. Error bars, ±SD, n = 3.

(B) PEP inactivates yeast and mammalian TPI. Michaelis-Menten kinetics were determined for yeast TPI (left panel), human TPI (middle panel), and rabbit muscle TPI (right panel). To determine $v_{max}$ and $K_m$, the TPI substrate gly3p was added in incremental doses (left y and lower x axis, blue; y values are normalized to total cellular protein [left and middle panel] or to the purified protein [right panel]). For all TPI isozymes, $v_{max}$ is highlighted with a green dot in the saturation curve; $K_m$ values are given in µM (right y and upper x axis, black). Inhibition of TPI activity demonstrated by addition of PEP in incremental concentrations; $IC_{50}$ values and the inhibitory constant $K_i$ are given in µM, the Kcat in Mol*$s^{-1}$.

(C) Inactivation of pathogenic TPI alleles by PEP. TPI activity was assayed in transgenic yeast expressing human TPI (WT) or indicated pathogenic TPI alleles without or in the presence of 900 µmol PEP. Error bars, ±SD. Values within bars indicate the absolute enzyme activity in µmol/(min*µg protein).

(D) PYK activity does not change oxidant resistance in yeast expressing TPI$_{Ile170Val}$. The wild-type control, transgenic yeast expressing either *PYK1* or *PYK2*, and either human TPI or human TPI$_{Ile170Val}$ were spotted as serial dilutions onto SC media without or with diamide (left panel). Spot growth on different concentrations was analyzed with CellProfiler and normalized to the strain with highest PYK activity (right panel). Low PYK activity increased diamide tolerance if expressed in combination with human TPI, but there were no differences in TPI$_{Ile170Val}$-expressing yeast.

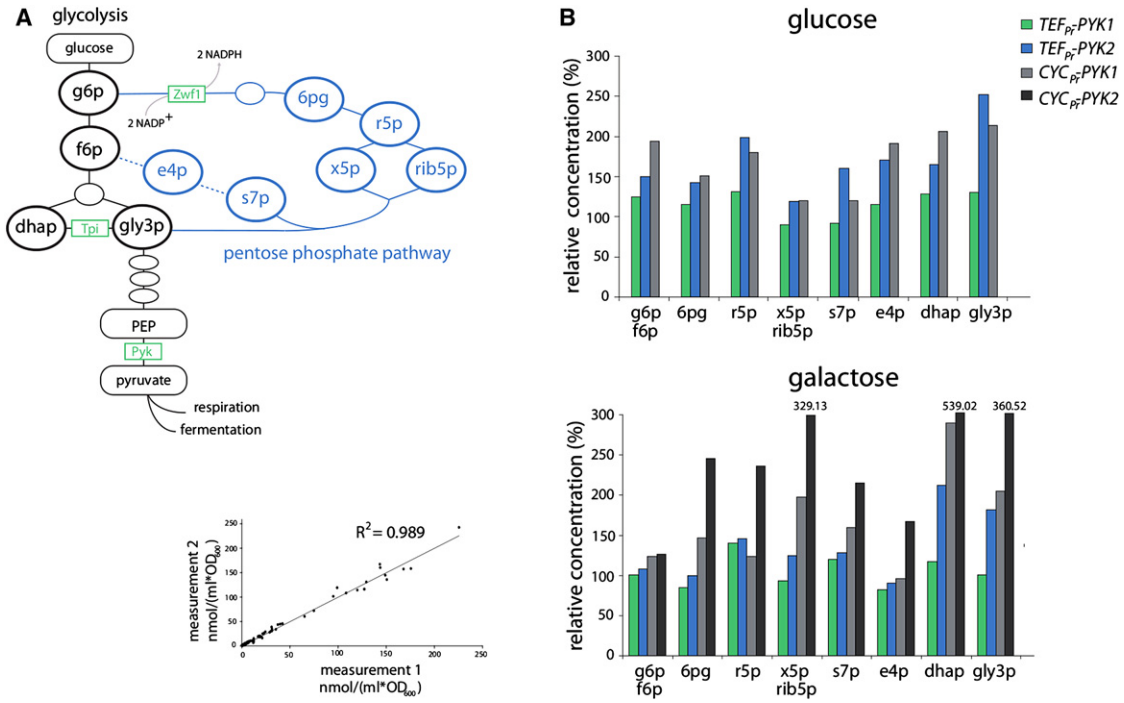


**Figure 5. The PYK-PEP-TPI Feedback Loop Stabilizes ROS Levels by Activating the Pentose Phosphate Pathway**

(A) Overview on the PPP and glycolysis.

(B) Cells with low PYK activity have increased concentrations of PPP intermediates. Sugar phosphates were extracted from exponential cultures and quantified by LC-MRM. All measured PPP intermediates—g6p (glucose 6-phosphate), f6p (fructose 6-phosphate), 6pg (6-phosphogluconate), r5p (ribose 5-phosphate), rib5p (ribulose 5-phosphate), x5p (xylulose 5-phosphate), s7p (sedoheptulose 7-phosphate), and e4p (erythrose 4-phosphate)—as well as TPI substrates dhap (dihydroxyacetone phosphate) and gly3p (glyceraldehyde 3-phosphate) were increased in yeast with low PYK activity grown in glucose (upper panel) and galactose media (lower panel). Reproducibility of sugar phosphate quantification is demonstrated by linear regression ($R^2$ 0.989) (lower panel left). See also Table S1.

$TPI_{Ile170Val}$ and either *PYK1* or *PYK2* ectopically were generated and assayed for their oxidant tolerance. The strain with low *PYK2* activity gained diamide resistance when expressed in combination with wild-type human TPI. This effect was abolished when $TPI_{Ile170Val}$ was expressed, as there were no differences in oxidant tolerance between low and high PYK activity in this strain (Figure 4D). Thus, redox-protective effects of low PYK activity were not additive to low TPI activity, and not observed in a yeast strain where TPI is insensitive to PEP inhibition.

## PPP Activation in Respiring Yeast through TPI Feedback Inhibition

Previously, it was reported that $NADP^+$ reduction, and the concentration of PPP intermediates, increases when TPI is mutant (Kleijn et al., 2007; Ralser et al., 2007). To investigate if feedback inhibition had a similar effect, we quantified PPP intermediates by LC-MRM (Wamelink et al., 2009) (Figure 5A). In cells with low PYK activity there was an increase in all PPP intermediates examined (Figure 5B, upper panel, absolute values are given as Table S1, reproducibility is demonstrated by linear regression [Figure 5B, lower left]). The TPI substrates dhap and gly3p were included in the analyses. Indicating lowered TPI activity, these two metabolites showed the strongest increase. Including the $CYC_{pr}$-*PYK2* strain, these measurements were then performed on galactose-grown cultures (Figure 5B, lower panel). Effects were similar to glucose, although there dhap and gly3p accumulation was stronger; overall the $CYC_{pr}$-*PYK2* with lowest PYK activity exhibited strongest changes.

## PPP Activation Prevents ROS Accumulation and Is Necessary for Increased Oxidant Tolerance of Respiring Cells

PPP splits into a nonoxidative and oxidative branch, of which the latter is responsible for the reduction of $NADP^+$ to NADPH, and not reversible. Therefore, deletion of its first enzyme, glucose 6-phosphate dehydrogenase (*Zwf1p*), separates the oxidative PPP from glycolysis and prevents its function as NADPH donor (Wamelink et al., 2008).

To determine if PPP activation is responsible for the increased stress resistance, we deleted *ZWF1* in respiring PYK mutants. *Δpyk1Δpyk2Δzwf1* yeast expressing $TEF_{pr}$-*PYK1* or $CYC_{pr}$-*PYK1* was tested for oxidant resistance. Low levels of *PYK1* increased diamide resistance only in *ZWF1*, but not in *Δzwf1* yeast (Figure 6A). This indicated that oxidative PPP is required in order for PYK to augment oxidative stress resistance.

Then we tested whether the *Δzwf1* deletion also affected ROS levels. ROS levels were measured in logarithmically grown yeast by DHE and DCFDA fluorescence. Similar to Figure 3A, in wild-type *ZWF1* cells, ROS levels did not increase when there was

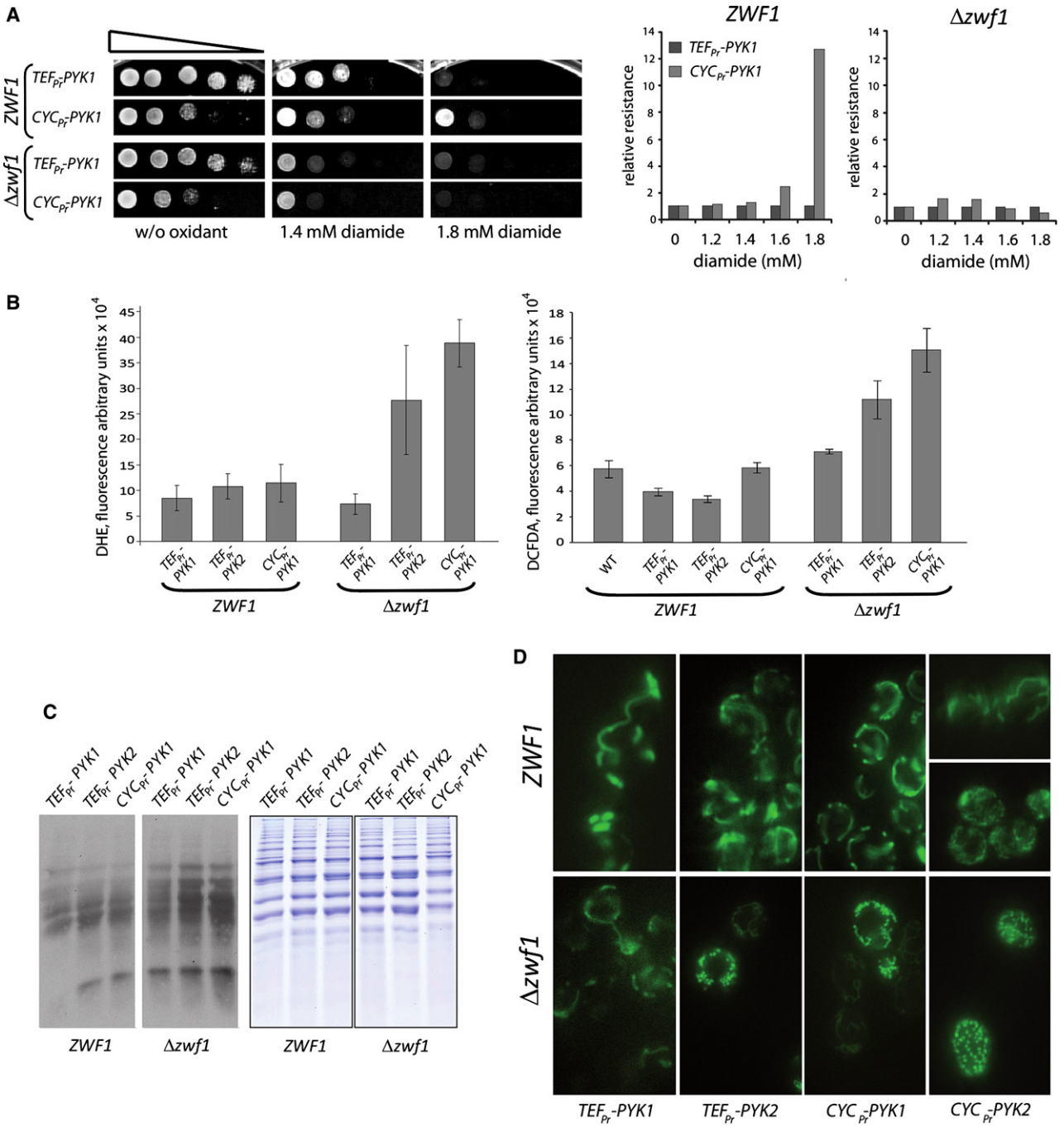


**Figure 6. The PYK-PEP-TPI Feedback Loop Protects Cells from ROS-Induced Damage during Respiration**

(A) Low PYK activity in *Δzwf1* yeast does not protect against oxidants. The first enzyme involved in the irreversible NADPH producing oxidative PPP branch (*ZWF1*) was deleted, and PYK strains were tested for diamide resistance (left panels). Densitometric processing of (A), including more oxidant concentrations (right panels). Deletion of *ZWF1* prevented the increase in redox tolerance in yeast with low PYK activity.

(B) ROS levels increase in respiring cells when the PPP is deficient. ROS levels in *ZWF1* and Δ*zwf1* yeast with varying PYK activity were determined with DHE, which preliminarily detects superoxide (left panel), and DCFDA, which detects $H_2O_2$ (right panel). Low PYK activity did not increase DHE and DCFDA oxidation in wild-type, but in Δ*zwf1* yeast. Error bars, ±SD.

(C) Low PYK activity increases protein carbonylation in Δzwf1 yeast. Protein extracts (7.5 μg) were analyzed by oxyblotting (left panel) and extracts controlled with Coomassie staining (right panel). *ZWF1* and Δ*zwf1* are juxtaposed images from the same blot/gel. Low PYK activity strongly increased carbonylation in Δ*zwf1* yeast.

(D) Mitochondrial damage in *Δzwf1* cells with low PYK activity. PYK models expressing Aco1-eGFP were analyzed for mitochondria morphology. Strains wild-type for *ZWF1* contain typical tubular mitochondria. In combination with low PYK activity, Δ*zwf1* caused mitochondrial fragmentation gradually increasing with low PYK activity; Aco1p indicated 100% mitochondrial network fragmentation in Δ*zwf1 CYC*$_{pr}$*-PYK2* yeast.

lower PYK activity. However, both stainings detected an increase with respiration when *zwf1* was deleted (Figure 6B). Thus, ROS accumulate in respiring cells only when the oxidative PPP is deficient.

To illustrate consequences on cellular macromolecules, we studied protein carbonylation and mitochondrial morphology. Although no increase in carbonyl levels was observed by oxyblotting in *ZWF1* wild-type cells, these rose upon deletion of Δ*zwf1* (Figure 6C). Thus macromolecules are sufficiently protected from oxidative carbonylation in respiring cells as long as the oxidative PPP is activable. Effects were clearly pictured on the mitochondrial shape. Aco1p tagged with eGFP was chosen as marker for mitochondrial oxidative damage, because it contains an iron-sulfur cluster that is prone for oxidation (Klinger et al., 2010). Aco1-eGFP stained a typical mitochondrial, tubular network in cells with high PYK activity, and when cells were *ZWF1* wild-type. However, depletion of *zwf1* in models with low PYK activity resulted in gradual relocalization. In *Δzwf1 CYC$_{pr}$-PYK2* yeast, the mitochondrial network fragmented to 100% into numerous small roundish mitochondria (Figure 6D). This indicates strong oxidative damage and was previously associated with loss of aconitase activity (Klinger et al., 2010).

## DISCUSSION

Cellular life depends on energy which is shuffled between biochemical reactions in the form of ATP. Its energy charge is maintained by the metabolic network and restored primarily by glycolytic fermentation and respiration (Bolanos et al., 2010; Grüning et al., 2010). Oxidative metabolism is more efficient in producing ATP but produces ROS, such as the superoxide anion in the electron transport chain (Novo and Parola, 2008). In yeast, superoxide preliminary originates from complex III, but also from oxidoreductases which feed the respiratory chain without proton pumping (Nde1, Nde2, and Ndi1) (Luttik et al., 1998). The total rate of ROS production during respiration equals 1%–2% of the metabolized oxygen (Cadenas and Davies, 2000).

Here we show that PYK regulates respiration in *S. cerevisiae.* Yeast express *PYK1* when grown in fermentable carbon sources, where *PYK2* is suppressed (Boles et al., 1997). A switch from *PYK1* to *PYK2*, or simple lowering expression of either isoform, was sufficient to shift from fermentative to oxidative metabolism. Cells with low PYK activity exhibited increased oxygen consumption and displayed growth phenotypes and mRNA expression fingerprints that indicated an increase in mitochondrial energy metabolism.

We were surprised that ROS levels did not increase upon the induction of respiration. ROS oxidize macromolecules (fatty acids, nucleic acids, and proteins). If not properly balanced, the redox state may fall out of equilibrium and cause oxidative or reductive stress. Although oxidative stress is better understood, also excess of reducing equivalents is pathogenic and leads to defects in biochemical reactions, protein folding, and signaling events (Rajasekaran et al., 2007; Tu and Weissman, 2002). As a consequence, respiratory metabolism relies on the capacity of clearing oxidizing molecules, but also on the ability to tune the production of redox equivalents.

We found that the respiring PYK mutants had increased resistance to oxidants. Since clearance of ROS occurs irrespective of the source of free radicals (Apel and Hirt, 2004), this pointed to an increased potential to neutralize superoxide released from the respiratory chain. The grade of resistance to the external stressors varied (Figure 3). Yeast reacts differentially to different oxidants, which depends on the type of free radical released, but also on the oxidant's redox (Nearnst) potential, its primary targets, and different grades of evolutionary adaptation (Thorpe et al., 2004). In this particular case, further differences originate from GAPDH, the TPI neighboring enzyme in glycolysis, which is inactivated by various oxidants to a different extend (Grant et al., 1999) and influences oxidant resistance of yeast with reduced TPI activity (Ralser et al., 2007). As only a marginal fraction of oxidant resistant yeast mutants tolerated a comparably broad spectrum of oxidants in an earlier study (Thorpe et al., 2004), it could be concluded that PYK stimulated a general component of the redox balancing machinery.

A central component of redox metabolism is the PPP. For every glucose equivalent, its oxidative branch reduces two molecules of $NADP^+$. In the glutathione system, the primary free radical scavenger, as well as in peroxiredoxin and glutaredoxin systems, NADPH is required to recycle the oxidized form, e.g., to reduce GS-SG to GSH (Grant, 2001; Holmgren et al., 2005). Most mutants of PPP enzymes are sensitive to oxidants (Juhnke et al., 1996), and the NADPH/$NADP^+$ ratio collapses when PPP-deficient cells are exposed to $H_2O_2$ (Castegna et al., 2010).

Dynamic PPP activation has been observed upon extracellular addition of oxidants and when cells shift to a nonfermentable carbon source (Cakir et al., 2004; Grant, 2008; Ralser et al., 2007; Shenton and Grant, 2003). This protected cells in two distinct (but overlapping) ways, as it augmented the NADPH/$NADP^+$ ratio (Grant, 2008; Ralser et al., 2007) and activated part of the antioxidant gene expression program (Krüger et al., 2011).

In case of exposure to a toxic oxidant dose, PPP activity is rapidly stimulated through oxidative inactivation of glycolytic enzymes (Ralser et al., 2009; Shenton and Grant, 2003). However, there was evidence that this mechanism is not induced by ROS leakage from the respiratory chain: glycolysis is not inhibited during respiration (Meredith and Romano, 1977), redox-prone GAPDH is stable to a continuous oxidant exposure (Cyrne et al., 2010), and even after strong bursts its activity is re-established after a few hours (Colussi et al., 2000). Finally, as shown in this manuscript, ROS levels are not necessarily increased in respiring cells, thus they do not possess a redox state which would trigger oxidative enzyme inactivation.

We discovered that in respiring cells the activity of the oxidative PPP is stimulated through a metabolic feedback loop. PEP accumulated in yeast with low PYK activity and acted as inhibitor of the glycolytic enzyme TPI. This appeared to be a conserved process, as yeast, rabbit, and human TPI were all efficiently inhibited by PEP. Our data do not exclude the possibility that PEP acts also as inhibitor or modulator on other enzymes, but demonstrates that TPI inhibition is sufficient to trigger ROS clearance during oxidative metabolism. We isolated one TPI allele, $TPI_{Ile170Val}$, which was inefficiently inhibited by PEP. This allele has reduced catalytic activity itself, and we have shown earlier that it increases the metabolite content in the PPP (Ralser et al., 2007). When this isoform was expressed, low PYK activity

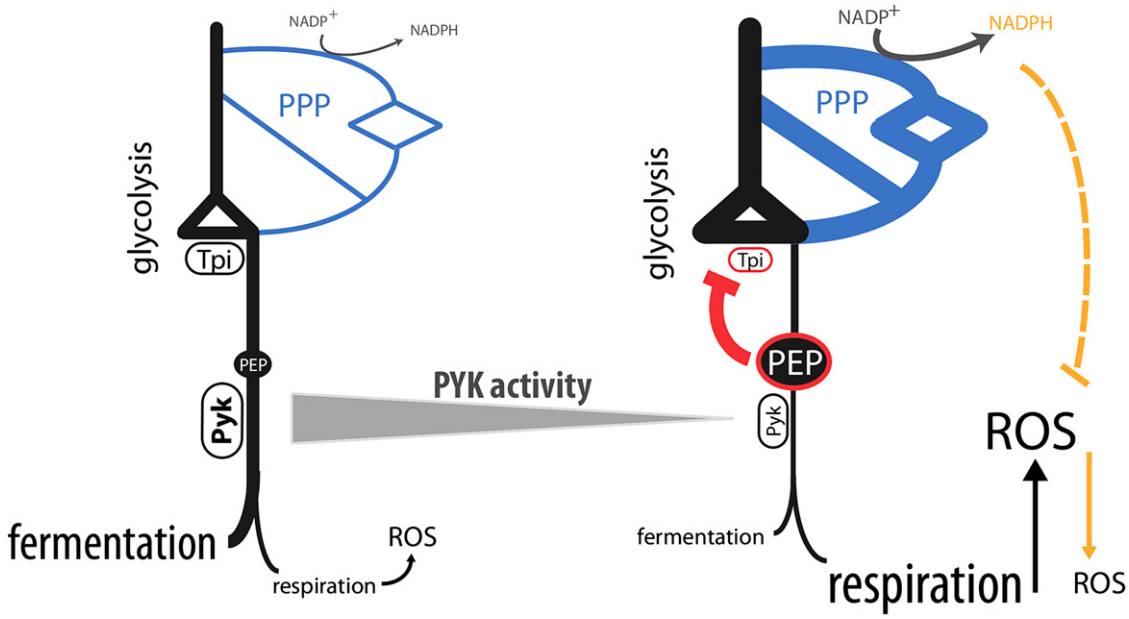


**Figure 7. Synchronization of Redox and Energy Metabolism by Pyruvate Kinase**
Low PYK activity increases respiration. At the same time, the PYK substrate PEP accumulates. This stimulates the PPP by feedback inhibition of TPI, which in turn prevents ROS accumulation during respiration.

did not further increase oxidant tolerance when PYK activity was lowered.

TPI mutations cause a rare metabolic syndrome, TPI deficiency. Most patients suffering from this rare genetic disease are homozygous, or compound heterozygous for a single TPI allele ($TPI_{Glu104Asp}$) which alters stability and dimer formation (Rodriguez-Almazan et al., 2008). However, the pathogenesis of other alleles is still unknown. The discovery that at least one mutant protein was deficient for PEP feedback inhibition opens a new aspect for research on the pathomechanism, as impaired redox metabolism has been reported as feature of TPI deficiency (Ahmed et al., 2003).

Finally, we investigated whether the PPP is required to clear free radicals upon respiration activation. We prevented the reduction of $NADP^+$ in the oxidative PPP by deleting its first enzyme (Zwf1p). Lowering PYK activity did not augment stress resistance in Δ*zwf1* cells. In addition, we used DHE and DCFDA fluorescence to determine ROS levels in respiring PYK mutants. Remarkably, they were unaffected as long as the oxidative PPP was functional, but accumulated in respiring cells upon deletion of Zwf1. Thus, the oxidative PPP is essential for both the increase in oxidant resistance and the stabilization of ROS levels upon the induction of respiration.

These results propose a mechanism for how PYK increases antioxidative capacities (Figure 7). PEP, the PYK substrate, accumulates when the activity of this enzyme is low. This inhibits the glycolytic enzyme TPI. The resulting increase in PPP activity protects cells against oxidants and prevents accumulation of ROS. Recently, it has been reported that PEP in PKM2-expressing cells converts phosphoglycerate mutase (PGM) into a lactate-producing enzyme, which alters glycolysis in proliferating mammalian cells. This may explain the requirement of this feedback loop, as a block of PYK alone would not cause accumulation of upstream metabolites, if the reaction can be surpassed by PGM (Vander Heiden et al., 2010).

PYK-mediated regulation of respiration may differ between yeast and mammalian cells. Consistent with the yeast model are recent investigations demonstrating higher concentration of PKM2 in tumors as in control tissue (Bluemlein et al., 2011), and demonstrating that PKM2 activates fermentative gene expression independent of its activity (Luo et al., 2011). Conversely, however, others have reported increased oxidative phosphorylation with reduced lactate production when PKM maintained high activity (Hitosugi et al., 2009). Further investigations are required to elaborate these yet-unsolved discrepancies in mammalian cells. In this context, both in yeast and mammalian cells, the mechanism for how PYK stimulates oxidative phosphorylation remains to be discovered. We rule out an active role of the PPP, as oxygen uptake also increased upon deletion of PPP enzymes (Supplemental Information, Figure 2). Furthermore, as oxygen uptake of the PYK models increased also on galactose media (Figure 2), a detection of energy shortage by a respective energy sensor falls short in explaining the regulatory mechanism.

However, there is evidence that the metabolic feedback loop presented here is evolutionarily conserved. First, there is evidence that metabolites upstream of PYK accumulate in mammalian cells during the Warburg effect (Vander Heiden et al., 2010) and when PYK is depleted in *B. subtilis* (Emmerling et al., 2002). Second, we have shown here that human and rabbit TPI are more effectively inhibited by PEP compared to yeast TPI (Figure 4B). This could explain our previous observation that transgenic yeast expressing human TPI are more oxidant resistant compared to those expressing yeast TPI

(Ralser et al., 2007). Finally, the effect that reduced TPI activity causes an increase in oxidant resistance is conserved, and depletion of Zwf1 (G6PDH) paralogues decreases oxidant tolerance and NADPH in mammalian models (Ho et al., 2000; Ralser et al., 2007; Zhang et al., 2010). Aside the regulation of respiratory energy metabolism, it is assumed that the Warburg effect enables rapidly proliferating tissue to synthesize essential macromolecules (nucleic acids, amino acids, and lipids) from metabolic intermediates, permitting growth and duplication of cellular components during division (Hsu and Sabatini, 2008; Najafov and Alessi, 2010; Vander Heiden et al., 2010). A major fraction of the required intermediates originate from PPP and upper glycolysis; thus metabolic feedback inhibition of TPI by PYK can assure production of these intermediates. Following this line of thought, the feedback loop may represent a therapeutic target because it opens an opportunity to deprive cancer cells from their supply of metabolic intermediates.

## EXPERIMENTAL PROCEDURES

Yeast cultivation, enzyme activity assays, plasmid and yeast strain generation, and qRT-PCR were conducted by standard methods and are available in the Supplemental Information.

### Measurement of Oxygen Consumption, ROS Levels, Carbonylation, and Aconitase 1

Oxygen consumption in exponentially growing yeast cells was determined in an Oxygraph 2k (Oroboros) following the manufacturer's instructions. DHE fluorescence was used to measure ROS (superoxide) as described in Klinger et al. (2010). DCFDA (2′,7′-dichlorofluoresceine diacetate) was used to determine $H_2O_2$ levels in cells grown to midexponential phase in YPD media. DCFDA (10 μM) was added to the cultures for 30 min at 30°C and pellets washed and measured in four replicates in a POLARstar Omega plate reader (BMG Labtech, λex = 490 nm, λem = 524 nm). Protein damage by carbonylation was determined using the OxyBlot Protein Oxidation Detection Kit (Millipore) according to the manufacturer's instructions blotting 7.5 μg protein on PVDF membrane. Aconitase was pictured in yeast cultures transformed with the plasmid pUG35-ACO1. Transformants were diluted from an overnight culture to an OD600 = 0.1 in SC medium lacking uracil and were grown till midexponential phase. Distribution of Aco1-eGFP was pictured with a 100× objective on a Zeiss Axioscope 50 fluorescence microscope.

### Oxidant Tolerance Tests

Oxidant tolerance spot tests were performed as described in (Ralser et al., 2007) and pictures taken after 2–3 days of incubation at 30°C. Quantification of spot growth was achieved via digital image processing using CellProfiler software (Carpenter et al., 2006). In the survival assays, overnight cultures were diluted to an OD600 = 0.1 in YPD and supplemented with diamide to a final concentration of 3 mM or left untreated as control. Of a 1:200 or 1:20000 dilution, 100 μl was plated in triplicates at time points 0 hr and 24 hr onto YPD agar plates. Oxidant resistance in liquid cultures was assayed in replicates of four in 96-well plates. Cells were grown from an OD600 = 0.6 (tert-butyl hydroperoxid), 0.12 (CHP, menadione), or 0.1 (diamide) for 4 hr (menadione, CHP, TBH) or 17 hr (diamide). Growth was measured photometrically in a Spectra Max 250 plate reader (Molecular Devices).

### Metabolite Quantification by MS/MS

Sugar phosphates were quantified by LC-MS/MS as described earlier (Wamelink et al., 2009). In brief, metabolites were extracted in HBSS with 2% perchloric acid, and proteins were precipitated after neutralization with a phosphate buffer. The samples were subsequently supplemented with an internal isotope labeled standard $^{13}C_6$-glucose-6P, separated on a water-acetonitrile gradient on a $C_{18}$ RP-HPLC column (LC packings), and analyzed on an API3000 triple quadrupole mass spectrometer (AB/Sciex).

For the determination of PEP, yeast was YPD grown to mid-log phase, centrifuged, washed with water, and frozen at −80°C. To the frozen yeast pellets, glass beads (425–600 μm, Sigma) and 80% methanol in water (300 μl) were added, followed by one cycle on a Fast Prep-24 (MP Biomedicals) for 20 s at 6.5 m/s. Extracts were then cleared by 2× centrifugation at 16,000 g. Quantitative PEP measurements were conducted on a QTRAP5500 hybrid ion-trap/triple quadrupole mass spectrometer (AB/Sciex), coupled online to an Agilent 1290 LC system. Separation was achieved on a HILIC column (Acquity BEH HILIC, 1.7 μm, 2.1 × 100 mm [Waters]) by a linear gradient from 100% acetonitrile/ammonium hydrogen carbonate (90/10; A) to 100% acetonitrile/ammonium hydrogen carbonate (50/50; B) between 0.5 and 1 min at a flow rate of 1 ml $min^{-1}$. The gradient was kept at 100% B for 0.5 min before returning to starting conditions. The stop time was set to 3.5 min to allow equilibration of the system prior to the following sample injection. The column temperature was set to 35°C. PEP quantification in yeast extracts was conducted by standard addition.

The MS was run in the negative mode and at a source temperature of 350°C. All other parameters, such as nebuliser and drying gas, influencing the sensitivity of the analysis were optimized prior to the measurements. Quantification of PEP was achieved by monitoring its collision induced (collision energy, −10 V) fragmentation from m/z 167 to 78.8. A detailed protocol will be published elsewhere.

## SUPPLEMENTAL INFORMATION

Supplemental Information includes two figures, one table, Supplemental Experimental Procedures, and Supplemental References and can be found with this article online at doi:10.1016/j.cmet.2011.06.017.

## ACKNOWLEDGMENTS

We thank Beata Lukaszewska-McGreal, René Buschow, and Phillip Grote (MPI-MG); Erwin E. Jansen (VUMC); and Tobias Grüning for help with experiments and data analysis. M. Ralser is a Wellcome Trust Research Career development and Wellcome Beit price fellow. We acknowledge funding of the Max Planck society and the ERC (Starting Grant StG-260809 [MetabolicRegulators]).

Received: February 17, 2011
Revised: May 23, 2011
Accepted: June 22, 2011
Published: September 6, 2011

## REFERENCES

Ahmed, N., Battah, S., Karachalias, N., Babaei-Jadidi, R., Horanyi, M., Baroti, K., Hollan, S., and Thornalley, P.J. (2003). Increased formation of methylglyoxal and protein glycation, oxidation and nitrosation in triosephosphate isomerase deficiency. Biochim. Biophys. Acta *1639*, 121–132.

Apel, K., and Hirt, H. (2004). Reactive oxygen species: metabolism, oxidative stress, and signal transduction. Annu. Rev. Plant Biol. *55*, 373–399.

Benov, L., Sztejnberg, L., and Fridovich, I. (1998). Critical evaluation of the use of hydroethidine as a measure of superoxide anion radical. Free Radic. Biol. Med. *25*, 826–831.

Bluemlein, K., and Ralser, M. (2011). Monitoring protein expression in whole-cell extracts by targeted label- and standard-free LC-MS/MS. Nat. Protoc. *6*, 859–869.

Bluemlein, K., Gruning, N.M., Feichtinger, R.G., Lehrach, H., Kofler, B., and Ralser, M. (2011). No evidence for a shift in pyruvate kinase PKM1 to PKM2 expression during tumorigenesis. Oncotarget *2*, 393–400.

Bolanos, J.P., Almeida, A., and Moncada, S. (2010). Glycolysis: a bioenergetic or a survival pathway? Trends Biochem. Sci. *35*, 145–149.

Boles, E., Schulte, F., Miosga, T., Freidel, K., Schluter, E., Zimmermann, F.K., Hollenberg, C.P., and Heinisch, J.J. (1997). Characterization of a glucose-repressed pyruvate kinase (Pyk2p) in Saccharomyces cerevisiae that is

catalytically insensitive to fructose-1,6-bisphosphate. J. Bacteriol. *179*, 2987–2993.

Cadenas, E., and Davies, K.J. (2000). Mitochondrial free radical generation, oxidative stress, and aging. Free Radic. Biol. Med. *29*, 222–230.

Cakir, T., Kirdar, B., and Ulgen, K.O. (2004). Metabolic pathway analysis of yeast strengthens the bridge between transcriptomics and metabolic networks. Biotechnol. Bioeng. *86*, 251–260.

Carlson, M. (1999). Glucose repression in yeast. Curr. Opin. Microbiol. *2*, 202–207.

Carpenter, A.E., Jones, T.R., Lamprecht, M.R., Clarke, C., Kang, I.H., Friman, O., Guertin, D.A., Chang, J.H., Lindquist, R.A., Moffat, J., et al. (2006). CellProfiler: image analysis software for identifying and quantifying cell phenotypes. Genome Biol. *7*, R100.

Castegna, A., Scarcia, P., Agrimi, G., Palmieri, L., Rottensteiner, H., Spera, I., Germinario, L., and Palmieri, F. (2010). Identification and functional characterization of a novel mitochondrial carrier for citrate and oxoglutarate in Saccharomyces cerevisiae. J. Biol. Chem. *285*, 17359–17370.

Cheng, Y., and Prusoff, W.H. (1973). Relationship between the inhibition constant (K1) and the concentration of inhibitor which causes 50 per cent inhibition (I50) of an enzymatic reaction. Biochem. Pharmacol. *22*, 3099–3108.

Christofk, H.R., Vander Heiden, M.G., Harris, M.H., Ramanathan, A., Gerszten, R.E., Wei, R., Fleming, M.D., Schreiber, S.L., and Cantley, L.C. (2008). The M2 splice isoform of pyruvate kinase is important for cancer metabolism and tumour growth. Nature *452*, 230–233.

Colombo, S.L., Palacios-Callender, M., Frakich, N., De Leon, J., Schmitt, C.A., Boorn, L., Davis, N., and Moncada, S. (2010). Anaphase-promoting complex/cyclosome-Cdh1 coordinates glycolysis and glutaminolysis with transition to S phase in human T lymphocytes. Proc. Natl. Acad. Sci. USA *107*, 18868–18873.

Colussi, C., Albertini, M.C., Coppola, S., Rovidati, S., Galli, F., and Ghibelli, L. (2000). H2O2-induced block of glycolysis as an active ADP-ribosylation reaction protecting cells from apoptosis. FASEB J. *14*, 2266–2276.

Cyrne, L., Antunes, F., Sousa-Lopes, A., Diaz-Berrio, J., and Marinho, H.S. (2010). Glyceraldehyde-3-phosphate dehydrogenase is largely unresponsive to low regulatory levels of hydrogen peroxide in Saccharomyces cerevisiae. BMC Biochem. *11*, 49.

Emmerling, M., Dauner, M., Ponti, A., Fiaux, J., Hochuli, M., Szyperski, T., Wuthrich, K., Bailey, J.E., and Sauer, U. (2002). Metabolic flux responses to pyruvate kinase knockout in Escherichia coli. J. Bacteriol. *184*, 152–164.

Fenton, A.W., and Reinhart, G.D. (2009). Disentangling the web of allosteric communication in a homotetramer: heterotropic inhibition in phosphofructokinase from Escherichia coli. Biochemistry *48*, 12323–12328.

Ghaemmaghami, S., Huh, W.K., Bower, K., Howson, R.W., Belle, A., Dephoure, N., O'Shea, E.K., and Weissman, J.S. (2003). Global analysis of protein expression in yeast. Nature *425*, 737–741.

Goldring, E.S., Grossman, L.I., Krupnick, D., Cryer, D.R., and Marmur, J. (1970). The petite mutation in yeast. Loss of mitochondrial deoxyribonucleic acid during induction of petites with ethidium bromide. J. Mol. Biol. *52*, 323–335.

Grant, C.M. (2001). Role of the glutathione/glutaredoxin and thioredoxin systems in yeast growth and response to stress conditions. Mol. Microbiol. *39*, 533–541.

Grant, C.M. (2008). Metabolic reconfiguration is a regulated response to oxidative stress. J. Biol. *7*, 1.

Grant, C.M., Quinn, K.A., and Dawes, I.W. (1999). Differential protein S-thiolation of glyceraldehyde-3-phosphate dehydrogenase isoenzymes influences sensitivity to oxidative stress. Mol. Cell. Biol. *19*, 2650–2656.

Grüning, N.M., Lehrach, H., and Ralser, M. (2010). Regulatory crosstalk of the metabolic network. Trends Biochem. Sci. *35*, 220–227.

Hitosugi, T., Kang, S., Vander Heiden, M.G., Chung, T.W., Elf, S., Lythgoe, K., Dong, S., Lonial, S., Wang, X., Chen, G.Z., et al. (2009). Tyrosine phosphorylation inhibits PKM2 to promote the Warburg effect and tumor growth. Sci. Signal. *2*, ra73.

Ho, H.Y., Cheng, M.L., Lu, F.J., Chou, Y.H., Stern, A., Liang, C.M., and Chiu, D.T. (2000). Enhanced oxidative stress and accelerated cellular senescence in glucose-6-phosphate dehydrogenase (G6PD)-deficient human fibroblasts. Free Radic. Biol. Med. *29*, 156–169.

Holmgren, A., Johansson, C., Berndt, C., Lonn, M.E., Hudemann, C., and Lillig, C.H. (2005). Thiol redox control via thioredoxin and glutaredoxin systems. Biochem. Soc. Trans. *33*, 1375–1377.

Hsu, P.P., and Sabatini, D.M. (2008). Cancer cell metabolism: Warburg and beyond. Cell *134*, 703–707.

Juhnke, H., Krems, B., Kotter, P., and Entian, K.D. (1996). Mutants that show increased sensitivity to hydrogen peroxide reveal an important role for the pentose phosphate pathway in protection of yeast against oxidative stress. Mol. Gen. Genet. *252*, 456–464.

Kleijn, R.J., Geertman, J.M., Nfor, B.K., Ras, C., Schipper, D., Pronk, J.T., Heijnen, J.J., van Maris, A.J., and van Winden, W.A. (2007). Metabolic flux analysis of a glycerol-overproducing Saccharomyces cerevisiae strain based on GC-MS, LC-MS and NMR-derived C-labelling data. FEM. Yeast Res. *7*, 216–231.

Klinger, H., Rinnerthaler, M., Lam, Y.T., Laun, P., Heeren, G., Klocker, A., Simon-Nobbe, B., Dickinson, J.R., Dawes, I.W., and Breitenbach, M. (2010). Quantitation of (a)symmetric inheritance of functional and of oxidatively damaged mitochondrial aconitase in the cell division of old yeast mother cells. Exp. Gerontol. *45*, 533–542.

Krüger, A., Grüning, N.M., Wamelink, M.M., Kerick, M., Kirpy, A., Parkhomchuk, D., Bluemlein, K., Schweiger, M.R., Soldatov, A., Lehrach, H., et al. (2011). The pentose phosphate pathway is a metabolic redox sensor and regulates transcription during the anti-oxidant response. Antioxid. Redox Signal. *15*, 311–324.

Levine, A.J., and Puzio-Kuter, A.M. (2010). The control of the metabolic switch in cancers by oncogenes and tumor suppressor genes. Science *330*, 1340–1344.

Luo, W., Hu, H., Chang, R., Zhong, J., Knabel, M., O'Meally, R., Cole, R.N., Pandey, A., and Semenza, G.L. (2011). Pyruvate kinase M2 is a PHD3-stimulated coactivator for hypoxia-inducible factor 1. Cell *145*, 732–744.

Luttik, M.A., Overkamp, K.M., Kotter, P., de Vries, S., van Dijken, J.P., and Pronk, J.T. (1998). The Saccharomyces cerevisiae NDE1 and NDE2 genes encode separate mitochondrial NADH dehydrogenases catalyzing the oxidation of cytosolic NADH. J. Biol. Chem. *273*, 24529–24534.

Meredith, S.A., and Romano, A.H. (1977). Uptake and phosphorylation of 2-deoxy-D-glucose by wild type and respiration-deficient bakers' yeast. Biochim. Biophys. Acta *497*, 745–759.

Najafov, A., and Alessi, D.R. (2010). Uncoupling the Warburg effect from cancer. Proc. Natl. Acad. Sci. USA *107*, 19135–19136.

Novo, E., and Parola, M. (2008). Redox mechanisms in hepatic chronic wound healing and fibrogenesis. Fibrogenesis Tissue Repair *1*, 5.

Orosz, F., Olah, J., and Ovadi, J. (2009). Triosephosphate isomerase deficiency: new insights into an enigmatic disease. Biochim. Biophys. Acta *1792*, 1168–1174.

Pollak, N., Dolle, C., and Ziegler, M. (2007). The power to reduce: pyridine nucleotides—small molecules with a multitude of functions. Biochem. J. *402*, 205–218.

Prigione, A., Fauler, B., Lurz, R., Lehrach, H., and Adjaye, J. (2010). The senescence-related mitochondrial/oxidative stress pathway is repressed in human induced pluripotent stem cells. Stem Cells *28*, 721–733.

Rajasekaran, N.S., Connell, P., Christians, E.S., Yan, L.J., Taylor, R.P., Orosz, A., Zhang, X.Q., Stevenson, T.J., Peshock, R.M., Leopold, J.A., et al. (2007). Human alpha B-crystallin mutation causes oxido-reductive stress and protein aggregation cardiomyopathy in mice. Cell *130*, 427–439.

Ralser, M., Heeren, G., Breitenbach, M., Lehrach, H., and Krobitsch, S. (2006). Triose phosphate isomerase deficiency is caused by altered dimerization—not catalytic inactivity—of the mutant enzymes. PLoS ONE *1*, e30. 10.1371/journal.pone.0000030.

Ralser, M., Wamelink, M.M., Kowald, A., Gerisch, B., Heeren, G., Struys, E.A., Klipp, E., Jakobs, C., Breitenbach, M., Lehrach, H., et al. (2007). Dynamic rerouting of the carbohydrate flux is key to counteracting oxidative stress. J. Biol. *6*, 10.

Ralser, M., Wamelink, M.M., Latkolik, S., Jansen, E.E., Lehrach, H., and Jakobs, C. (2009). Metabolic reconfiguration precedes transcriptional regulation in the antioxidant response. Nat. Biotechnol. *27*, 604–605.

Rodriguez-Almazan, C., Arreola, R., Rodriguez-Larrea, D., Aguirre-Lopez, B., de Gomez-Puyou, M.T., Perez-Montfort, R., Costas, M., Gomez-Puyou, A., and Torres-Larios, A. (2008). Structural basis of human triosephosphate isomerase deficiency: mutation E104D is related to alterations of a conserved water network at the dimer interface. J. Biol. Chem. *283*, 23254–23263.

Ruckenstuhl, C., Buttner, S., Carmona-Gutierrez, D., Eisenberg, T., Kroemer, G., Sigrist, S.J., Frohlich, K.U., and Madeo, F. (2009). The Warburg effect suppresses oxidative stress induced apoptosis in a yeast model for cancer. PLoS ONE *4*, e4592. 10.1371/journal.pone.0004592.

Shenton, D., and Grant, C.M. (2003). Protein S-thiolation targets glycolysis and protein synthesis in response to oxidative stress in the yeast Saccharomyces cerevisiae. Biochem. J. *374*, 513–519.

Slekar, K.H., Kosman, D.J., and Culotta, V.C. (1996). The yeast copper/zinc superoxide dismutase and the pentose phosphate pathway play overlapping roles in oxidative stress protection. J. Biol. Chem. *271*, 28831–28836.

Thorpe, G.W., Fong, C.S., Alic, N., Higgins, V.J., and Dawes, I.W. (2004). Cells have distinct mechanisms to maintain protection against different reactive oxygen species: oxidative-stress-response genes. Proc. Natl. Acad. Sci. USA *101*, 6564–6569.

Tu, B.P., and Weissman, J.S. (2002). The FAD- and O(2)-dependent reaction cycle of Ero1-mediated oxidative protein folding in the endoplasmic reticulum. Mol. Cell *10*, 983–994.

Turrens, J.F. (1997). Superoxide production by the mitochondrial respiratory chain. Biosci. Rep. *17*, 3–8.

Vander Heiden, M.G., Locasale, J.W., Swanson, K.D., Sharfi, H., Heffron, G.J., Amador-Noguez, D., Christofk, H.R., Wagner, G., Rabinowitz, J.D., Asara, J.M., et al. (2010). Evidence for an alternative glycolytic pathway in rapidly proliferating cells. Science *329*, 1492–1499.

Wamelink, M.M., Struys, E.A., and Jakobs, C. (2008). The biochemistry, metabolism and inherited defects of the pentose phosphate pathway: a review. J. Inherit. Metab. Dis. *31*, 703–717.

Wamelink, M., Jansen, E., Struys, E., Lehrach, H., Jakobs, C., and Ralser, M. (2009). Quantification of Saccharomyces cerevisiae pentose-phosphate pathway intermediates by LC-MS/MS. Nat. Protoc. 10.1038/nprot.2009.140.

Warburg, O. (1956). Origin of cancer cells. Science *123*, 309–314.

Ying, W. (2008). NAD+/NADH and NADP+/NADPH in cellular functions and cell death: regulation and biological consequences. Antioxid. Redox Signal. *10*, 179–206.

Zhang, Z., Liew, C.W., Handy, D.E., Zhang, Y., Leopold, J.A., Hu, J., Guo, L., Kulkarni, R.N., Loscalzo, J., and Stanton, R.C. (2010). High glucose inhibits glucose-6-phosphate dehydrogenase, leading to increased oxidative stress and beta-cell apoptosis. FASEB J. *24*, 1497–1505.

Cell Metabolism, Volume *14*

## Supplemental Information

# Pyruvate Kinase Triggers a Metabolic Feedback Loop that Controls Redox Metabolism in Respiring Cells

**Nana-Maria Grüning, Mark Rinnerthaler, Katharina Bluemlein, Michael Mülleder, Mirjam M.C. Wamelink, Hans Lehrach, Cornelis Jakobs, Michael Breitenbach, and Markus Ralser**

**Inventory of Supplemental Information**

Figure S1

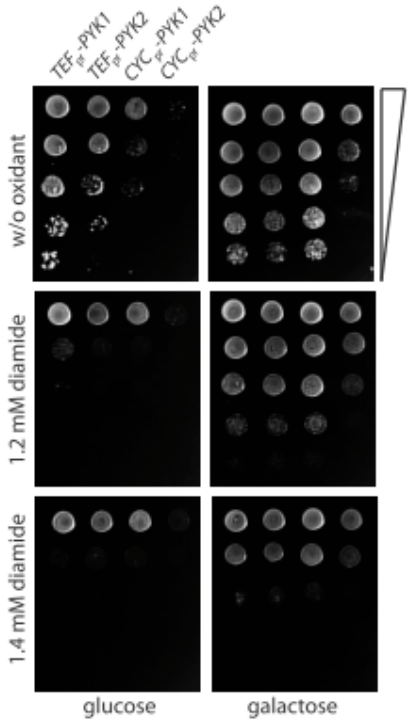


**Figure S1, related to Figure 3B: Reduced PYK activity and galactose media leads to higher resistance to oxidants.** Strains were grown over night, diluted to an $OD_{600}$ of 3.0, and spotted as 1:5 dilution series onto YPD and YPGal containing diamide at the indicated concentration.

Table S1

| | | g6p / f6p | 6pg | r5p | x5p / rib5p | s7p | e4p | dhap | gly3p | |
|---|---|---|---|---|---|---|---|---|---|---|
| glucose | BY4741 wt | 0,685 | 0,075 | 0,117 | 0,033 | 0,080 | 0,050 | 0,760 | 0,011 | mM / (ml*OD600) |
| | | 100,00 | 100,00 | 100,00 | 100,00 | 100,00 | 100,00 | 100,00 | 100,00 | relative concentration (%) |
| | *TEFpr-PYK1* | 0,854 | 0,087 | 0,154 | 0,029 | 0,073 | 0,058 | 0,979 | 0,014 | |
| | | 124,61 | 115,70 | 131,17 | 89,73 | 91,67 | 115,69 | 128,81 | 130,07 | |
| | *TEFpr-PYK2* | 1,028 | 0,107 | 0,233 | 0,039 | 0,129 | 0,085 | 1,252 | 0,027 | |
| | | 150,09 | 142,41 | 198,32 | 118,80 | 160,74 | 170,56 | 164,75 | 252,24 | |
| | *CYCpr-PYK1* | 1,329 | 0,113 | 0,211 | 0,039 | 0,096 | 0,095 | 1,567 | 0,023 | |
| | | 194,10 | 150,69 | 180,00 | 120,46 | 120,01 | 190,93 | 206,15 | 213,50 | |
| galactose | BY4741 wt | 3,949 | 0,177 | 0,161 | 0,059 | 0,118 | 0,120 | 1,081 | 0,026 | |
| | | 100,00 | 100,00 | 100,00 | 100,00 | 100,00 | 100,00 | 100,00 | 100,00 | |
| | *TEFpr-PYK1* | 3,973 | 0,149 | 0,226 | 0,055 | 0,141 | 0,098 | 1,266 | 0,026 | |
| | | 100,61 | 84,46 | 140,20 | 93,20 | 119,77 | 81,82 | 117,16 | 100,52 | |
| | *TEFpr-PYK2* | 4,280 | 0,177 | 0,234 | 0,074 | 0,151 | 0,109 | 2,296 | 0,048 | |
| | | 108,37 | 99,99 | 145,51 | 124,65 | 128,22 | 90,37 | 212,50 | 181,65 | |
| | *CYCpr-PYK1* | 4,899 | 0,259 | 0,199 | 0,117 | 0,188 | 0,115 | 3,135 | 0,054 | |
| | | 124,04 | 146,85 | 123,37 | 197,37 | 159,30 | 95,91 | 290,09 | 205,26 | |
| | *CYCpr-PYK2* | 4,988 | 0,434 | 0,381 | 0,195 | 0,253 | 0,201 | 5,825 | 0,095 | |
| | | 126,31 | 245,83 | 236,48 | 329,13 | 215,17 | 167,25 | 539,02 | 360,52 | |

**Table S1, related to Figure 5B: PPP metabolites are increased in strains with low PYK activity.** Values are given normalized to dhap concentration in a reference measurement (correction factor 36.5, black) and as ratio to metabolite concentration in the BY4741 wild-type strain (grey). g6p (glucose 6-phosphate), f6p (fructose 6-phosphate), 6pg (6-phospho gluconate), r5p (ribose 5-phosphate), x5p (xylulose 5-phosphate), rib5p (ribulose 5-phosphate), s7p (sedoheptulose 7-phosphate), e4p (erythrose 4-phosphate), dhap (dihydroxyacetone phosphate), gly3p (glyceraldehydes 3-phosphate).

Figure S2

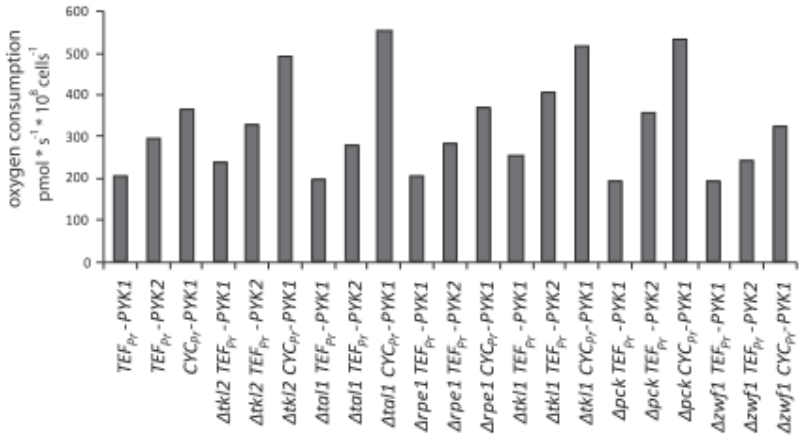


**Figure S2, related to discussion/Figure 7: Oxygen consumption increases in with low PYK activity in PPP and *PCK* mutants.** PPP enzymes or *PCK1 were deleted in ⊿pyk1⊿pyk2* yeast strains containing the different PYK constructs. Oxygen consumption was determined for logarithmically YPD -growing cultures in a closed chamber oxygraph (Oroboros). Tkl2 (encoding transketolase), Tal1 (transaldolase), Rpe1 (ribulose 5-phosphate epimerase), Tkl1 (transketolase), Pck (pyruvate carboxykinase), Zwf1 (glucose 6-phosphate dehydrogenase). Low PYK activity increased oxygen consumption in all deletion strains tested.

## Supplemental Experimental Procedures

### Yeast cultivation

Yeast were grown at 28-30°C either in yeast-extract peptone 2% dextrose (YPD), yeast-extract peptone 2% galactose (YPGal), 3% ethanol/0.1% glucose (YPEtOH) or in synthetic complete (SC) media lacking the indicated amino acids/bases.

### Plasmids

Plasmids encoding TPI were previously described (Ralser et al., 2006). PYK-encoding plasmids were generated by amplifying *PYK1* and *PYK2* from yeast genomic DNA by PCR, and ligating the products into centromeric yeast plasmids containing the *TEF1* promoter (p413TEF), the *CYC1* promoter (p413CYC), or a *GPD1* promoter (p416GPD) (Mumberg et al., 1995). All plasmids were verified by sequencing and primer sequences are given in the table below.

| | |
|---|---|
| PYK1-fw-BamH1 | 5'-GAGGATCCATGTCTAGATTAGAAAGA-3' |
| PYK1-as-Sal | 5'-GAGTCGACTTAAACGGTAGAGACTTG-3' |
| PYK2-fw-BamH1 | 5'-GAGGATCCATGCCAGAGTCCAGATTG-3' |
| PYK2-as-Sal1 | 5'-GAGTCGACCTAGAATTCTTGACCAAC-3' |
| underlined DNA sequences indicate introduced restriction sites | |

### Gene deletion

Genes were deleted in BY4741 strains by homologous recombination, by single gene replacement with the nourseothricin (natMX4), kanamycin (kanMX4), or hygromycin (hphMX4) markers. Primer pairs (which overlap with 20 bases of the marker gene and 35-45 bases with the target locus) were used to amplify the marker cassette and then transformed into yeast. Positive transformants were selected on YPD containing antibiotics, and isolated recombinants were verified by PCR. Primer sequences are given in the table below.

| | |
|---|---|
| MX4 deletion cassettes for PYK1 fwd | ATTTACAAGACACCAATCAAAACAAATAA AACATCATCACAAGCTTGCCTTGTCCCCGCCG |
| MX4 deletion cassettes for PYK1 rev | TTAAACGGTAGAGACTTGCAAAGTGTTGG AGTGACCAGCATCGACACTGGATGGCGGCGT |
| MX4 deletion cassettes for PYK2 fwd | CCTCTACGTCCATTGTAAGATTACAACAAA AGCACTATCGAGCTTGCCTTGTCCCCGCCG |
| MX4 deletion cassettes for PYK2 rev | TACTAGAATTCTTGACCAACAGTAGAAATG CGTAAGGTATTCGACACTGGATGGCGGCGT |
| underlined DNA sequences indicate introduced restriction sites | |

Isogenic PYK mutants were generated by plasmid shuffling**.** *Δpyk2* yeast was transformed with an *URA3*-plasmid encoding for PYK1 (p416GPD-PYK1). Then, endogenous *PYK1* was deleted using *natMX4*, and positive knock-outs were selected by PCR. The *Δpyk1Δpyk2* pCEN-*URA3-PYK1* strain was subsequently transformed with HIS3-marked PYK plasmids (*p413TEF-PYK1, p413CYC-PYK1, p413TEF-PYK2, p413CYC-PYK2*). Finally, the *URA3*-plasmid was counter-selected for positive transformants on $SC^{-HIS}$ containing 0.15% 5'FOA. *Δpyk1Δpyk2Δzwf1* and *Δpyk1Δtpi1* yeast expressing *PYK1*, *PKY2*, and/or TPI from centromeric plasmids were generated in a similar fashion.

*Bona fide* ρ0 strains were generated through repeated treatment with 50 µg/ml ethidium bromide as previously described (Goldring et al., 1970).

Quantitative RT-PCR

qRT-PCR was performed as previously described in (Wamelink et al., 2010). Yeast were cultivated overnight in YPD, washed once in water, and grown to log phase ($OD_{600}$ ~ 0.8) in YPD or YPGal. For boost experiments, YPD was exchanged with YPGal one hour before harvesting cells. mRNA was extracted and qRT-PCR was performed using an ABI prism 7800HT system. Primer sequences are listed in the Supplemental Information. Expression of

*COX1, COX2, COX3* was normalized to the expression of the reference genes *ATG27* and *TAF10* as by the method of (Pfaffl, 2001).

Enzyme activity assays

Pyruvate kinase activity was determined as described by (Bergmeyer et al., 1974). Briefly, a reaction mixture containing 24 mM $KH_2PO_4/K_2HPO_4$ (pH 7.0), 150 µM NADH, 1 mM fructose 1,6 bisphosphate, 2.4 mM ADP, 25 U lactate dehydrogenase (Sigma-Aldrich), 10 mM $MgSO_4$, and 4 µg centrifugation-cleared whole-cell extract was supplemented with 800 µM PEP. $OD_{340}$ was used to detect NADH oxidation in 6- to 10-s intervals using an spectrophotometer (Amersham US 2000). TPI activity was determined as previously described (Ralser et al., 2006). $K_m$ and $K_i$ were determined by saturation curves with gly3p and PEP, respectively, in yeast extracts (BY4741), transgenic yeast expressing human TPI (MR101) (Ralser et al., 2006), or purified rabbit muscle TPI (Sigma-Aldrich).

## Supplemental References


Bergmeyer, H.U., Gawehn, K., and Grassl, M. (1974). Methods of Enzymatic Analysis, 2nd Edition, Academic press, NY *1*, 509-510.

Mumberg, D., Muller, R., and Funk, M. (1995). Yeast vectors for the controlled expression of heterologous proteins in different genetic backgrounds. Gene *156*, 119-122.

Pfaffl, M.W. (2001). A new mathematical model for relative quantification in real-time RT-PCR. Nucleic Acids Res *29*, e45.

Wamelink, M.M., Gruning, N.M., Jansen, E.E., Bluemlein, K., Lehrach, H., Jakobs, C., and Ralser, M. (2010). The difference between rare and exceptionally rare: molecular characterization of ribose 5-phosphate isomerase deficiency. J MolMed *88*, 931-939.

***Contributions to Manuscript 2***

Major focus of this thesis was placed on the project published in Manuscript 2. Experimental design, writing of the manuscript and performance of all experiments other than the ones listed below were tasks of this thesis.

Mark Rinnerthaler contributed to this manuscript by scientific discussion, measuring of oxygen consumption in yeast cultures (Fig. 2D and Fig. 2S), by staining of superoxide and subsequent fluorescence measurements (Fig. 3A and Fig. 6B) and by transforming yeast cells with GFP-tagged yeast aconitase and documenting fluorescence of these cells (Fig. 6D).

Katharina Bluemlein established the analytical methods for PYK1 and PYK2 as well as PEP identification and quantification by mass spectrometrical methods (Fig. 1A and 4A).

Michael Muelleder performed the densitometrical picture analysis of data displayed in Fig. 3B, C, 4D and 6A.

Mirjam MC Wamelink took part by quantification of metabolites shown in Fig. 5B.

Hans Lehrach, Cornelis Jakobs and Michael Breitenbach gave support in scientific discussions and allocation of experimental equipment.

Markus Ralser took part experimentally by cloning of TPI mutation alleles and generation of yeast strains expressing those alleles (used to generate the data displayed in Fig. 4C). He contributed equally to writing of the manuscript.

**Manuscript 3**

# No evidence for a shift in pyruvate kinase PKM1 to PKM2 expression during tumorigenesis

Oncotarget. 2011 May;2(5):393-400.

Katharina Bluemlein[1], Nana-Maria Grüning[1], René G. Feichtinger[2], Hans Lehrach[1], Barbara Kofler[2] and Markus Ralser[1,3]

[1] Max Planck Institute for Molecular Genetics, Berlin, Germany

[2] Research Program for Receptorbiochemistry and Tumormetabolism, Department of Pediatrics, Paracelsus Medical University, Salzburg, Austria

[3] Cambridge Systems Biology Centre and Department of Biochemistry, University of Cambridge, Cambridge, United Kingdom

# No evidence for a shift in pyruvate kinase PKM1 to PKM2 expression during tumorigenesis

**Katharina Bluemlein[1], Nana-Maria Grüning[1], René G. Feichtinger [2], Hans Lehrach[1], Barbara Kofler[2] and Markus Ralser[1,3]**

[1] Max Planck Institute for Molecular Genetics, Berlin, Germany

[2] Research Program for Receptorbiochemistry and Tumormetabolism, Department of Pediatrics, Paracelsus Medical University, Salzburg, Austria

[3] Cambridge Systems Biology Centre and Department of Biochemistry, University of Cambridge, Cambridge, United Kingdom

***Correspondence to***: *Markus Ralser, email: mr559@cam.ac.uk*

***Keywords***: *pyruvate kinase, proteomics, cancer metabolism, alternative splicing, Warburg effect*

***Received:*** *May 18, 2011,* ***Accepted:*** *May 22, 2011,* ***Published:*** *May 22, 2011*



## ABSTRACT:

**The Warburg effect describes the circumstance that tumor cells preferentially use glycolysis rather than oxidative phosphorylation for energy production. It has been reported that this metabolic reconfiguration originates from a switch in the expression of alternative splice forms (PKM1 and PKM2) of the glycolytic enzyme pyruvate kinase (PK), which is also important for malignant transformation. However, analytical evidence for this assumption was still lacking. Using mass spectrometry, we performed an absolute quantification of PKM1 and PKM2 splice isoforms in 25 human malignant cancers, 6 benign oncocytomas, tissue matched controls, and several cell lines. PKM2 was the prominent isoform in all analyzed cancer samples and cell lines. However, this PKM2 dominance was not a result of a change in isoform expression, since PKM2 was also the predominant PKM isoform in matched control tissues. In unaffected kidney, lung, liver, and thyroid, PKM2 accounted for a minimum of 93% of total PKM, for 80% - 96% of PKM in colon, and 55% - 61% of PKM in bladder. Similar results were obtained for a panel of tumor and non-transformed cell lines, where PKM2 was the predominant form. Thus, our results reveal that an exchange in PKM1 to PKM2 isoform expression during cancer formation is not occurring, nor do these results support conclusions that PKM2 is specific for proliferating, and PKM1 for non-proliferating tissue.**

## INTRODUCTION

Malignant cell growth entails numerous metabolic changes. The so called 'Warburg' effect describes the decrease in respiration during tumor development, whereas glucose uptake and aerobic glycolysis, as well as lactate production increases [1-3]. The reason why cells undergo the Warburg effect are not entirely understood, but it is broadly assumed that the switching-off of the respiratory metabolism increases metabolic intermediates that are required for the synthesis of biological macromolecules [1, 2, 4]. This assumption is supported by the fact that stroma type cells that deliver metabolites utilized by the tumor for energy production also undergo this metabolic transition [5, 6]. Furthermore, as glycolytic fermentation circumvents oxidative phosphorylation in the respiratory chain, it avoids the release of superoxide from complex I and III, which could prevent oxidative stress [7]

Although important signaling cascades of cellular metabolism such as STAT3 and HIF-1α have been implicated in the regulation of the Warburg effect [8, 9], the mechanisms how it is initiated remain elusive. It has been reported that an exchange in the expression of PKM1 to PKM2, two alternative splice isoforms of the glycolytic enzyme pyruvate kinase (PK) [10, 11], is causative for the Warburg effect during tumorigenesis [10]. These two isoforms differ in a single exon, which facilitates binding of the glycolytic intermediate fructose 1,6 bisphosphate in PKM2 type PK. PKM1 is constitutively active, whereas PKM2 can switch between an active tetrameric and an

incactive dimeric form [12].

It has been concluded from Western blot analysis of cancer cell lines (A549, H1299, 293T, HeLa, MCF10a) and Western blot/immunostaining of mammary gland tissue from MMTV-NeuNT mice that cancer development switches expression from PKM1 to PKM2 [10]. These conclusions were drawn from the comparison of PKM1/PKM2 expression in cancer cell lines with human muscle [10]. However, as protein expression is highly tissue dependent [9,10], and as earlier biochemical studies had reported that pyruvate kinase PKM2 is present in several healthy tissues [13], we re-investigated PKM1/PKM2 expression in tumors, taking into account tissue-matched controls.

Using an absolute quantification (AQUA) strategy with isotope labeled standards, we performed a comprehensive absolute quantification of PKM1 and PKM2 in several cancer tissue of different origin, benign tumors and cell lines, and their tissue matched controls. We found no evidence for an exchange of PKM1 to PKM2 expression during cancer formation. Cancers maintained the PKM isoform expression according to their tissue of origin.

## RESULTS

### Development of an absolute quantification (AQUA) method to quantify of PKM1 and PKM2 in cell extracts

We decided on an absolute quantification of PKM1 and PKM2 by mass spectrometry, since this technology circumvents the drawbacks that may result from the use of antibodies in semiquantitative westernblotting [14, 15] used in earlier studies [10]. As antibodies differ in affinity, similar band intensities obtained with different antibodies do not indicate similar concentration of their target proteins. In contrast, the AQUA strategy allows absolute quantification of a non-purified protein at physiological concentration [16] by spiking the samples with chemically

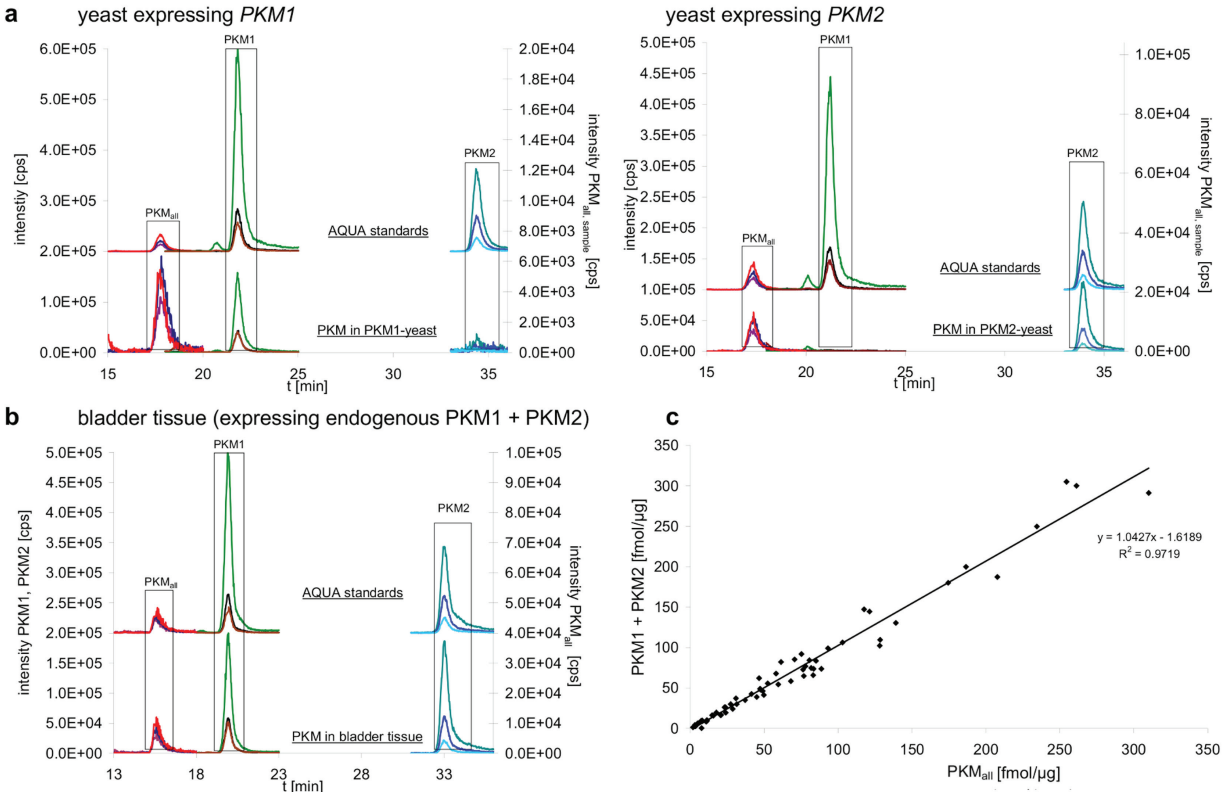


**Figure 1: Absolute quantification of PKM1 and PKM2 splice forms in tissue extracts.**

**a.** Yeast expressing human PKM1 (PKM1-yeast, left panel) and human PKM2 (PKM2-yeast, right panel) were analyzed by nanoflow liquid chromatography/multiple reaction monitoring (LC-MRM) to quantify a PKM1 and a PKM2 specific peptide as well as a peptide which is specific for both isoform ($PKM_{all}$) (lower chromatograms). Matching heavy isotope labeled peptides (AQUA peptides) were included in every sample and used for quantification (upper chromatograms, please note that they are displaced on the Y axis for better illustration). The determined concentrations were 3.3 fmol/µg protein for PKM1, and 19.3 fmol/µg protein for PKM2 in yeast.

**b.** Exemplary chromatogram for a human tissue sample, quantification of PKM1 and PKM2 in bladder tissue by LC-MRM. The analysis was performed as in (a). Absolute and relative values determined in human tissue are given in Table 1.

**c.** Plot of the concentrations obtained for PKM1 plus PKM2 against the concentration of a peptide specific for both isoforms [$PKM_{all}$]. The obtained concentrations show linear correlation ($R^2 > 0.97$)

synthesized, heavy-isotope labeled peptide standards (AQUA peptides) that match the proteolytic peptide of interest in sequence, but are distinguishable from the analyte by mass [14, 15, 17]. To assure accurate PKM quantification, and to detect a potential switch in PKM isoform expression, this analysis was conducted with three PKM specific isotope labeled peptides and on a hybrid ion trap / triple quadrupole mass spectrometer operating in MRM mode. We selected one peptide to be specific for PKM1 ($PKM1_{LFEELVR}$), one peptide for PKM2 ($PKM2_{LAPITSDPTEATAVGAVEASFK}$), and a third peptide specific for both forms ($PKM_{all\ ITLDNAYMEK}$). We tested PKM1 and PKM2 quantification with these peptides on transgenic yeast expressing exclusively either human PKM1 (PKM1-yeast) or human PKM2 (PKM2-yeast). The yeast strains were generated by cloning human PKM1 and PKM2 cDNA into an expression vector and transformation into the yeast strain BY4741. Protein extracts were generated, separated by SDS-PAGE, in-gel digested with trypsin [18], supplemented with the AQUA peptides [15] and analyzed as described previously [19]. The three isotope labeled standards were detected in all samples (Fig 1A, upper chromatograms). In PKM1-yeast, the PKM1 specific and the $PKM_{all}$ peptide were detected but not the PKM2 peptide. In contrast, the analysis of PKM2-yeast detected the PKM2 specific peptide and the $PKM_{all}$ peptide, but not the PKM1 peptide (Fig. 1A, lower chromatograms). Thus, the PKM1 and PKM2 specific peptides were detected and allowed specific discrimination between the PKM isoforms.

## Quantification of PKM1 and PKM2 in human tissue and cancer

To study PKM1 and PKM2 expression before and after cancer development, we analyzed 25 human malignant cancers, 18 tissue-matched controls, 12 cancer cell lines, 4 non-cancer cell lines and 6 benign oncocytomas. In 15 cases (12 malignant cancers, 2 benign tumors, 1 cell line), matched unaffected tissue from the affected individual was available. As described above, the samples were supplemented with the heavy-isotope labeled standards, and the three peptides quantified by multiple reaction monitoring on the QTRAP mass spectrometer. Peptides corresponding to both PKM1 and PKM2 were detected in tissues, cell lines and controls (Fig 1b). To test if the chosen peptides gave consistent results in quantifying PKM1 and PKM2, we plotted the obtained concentration values of PKM1 plus PKM2 versus the quantity obtained for the $PKM_{all}$ peptide which is characteristic for both PKM alternative splice isoforms. The quantities showed with $R^2 = 0.97$ a linear correlation, confirming that the chosen peptides were suitable for

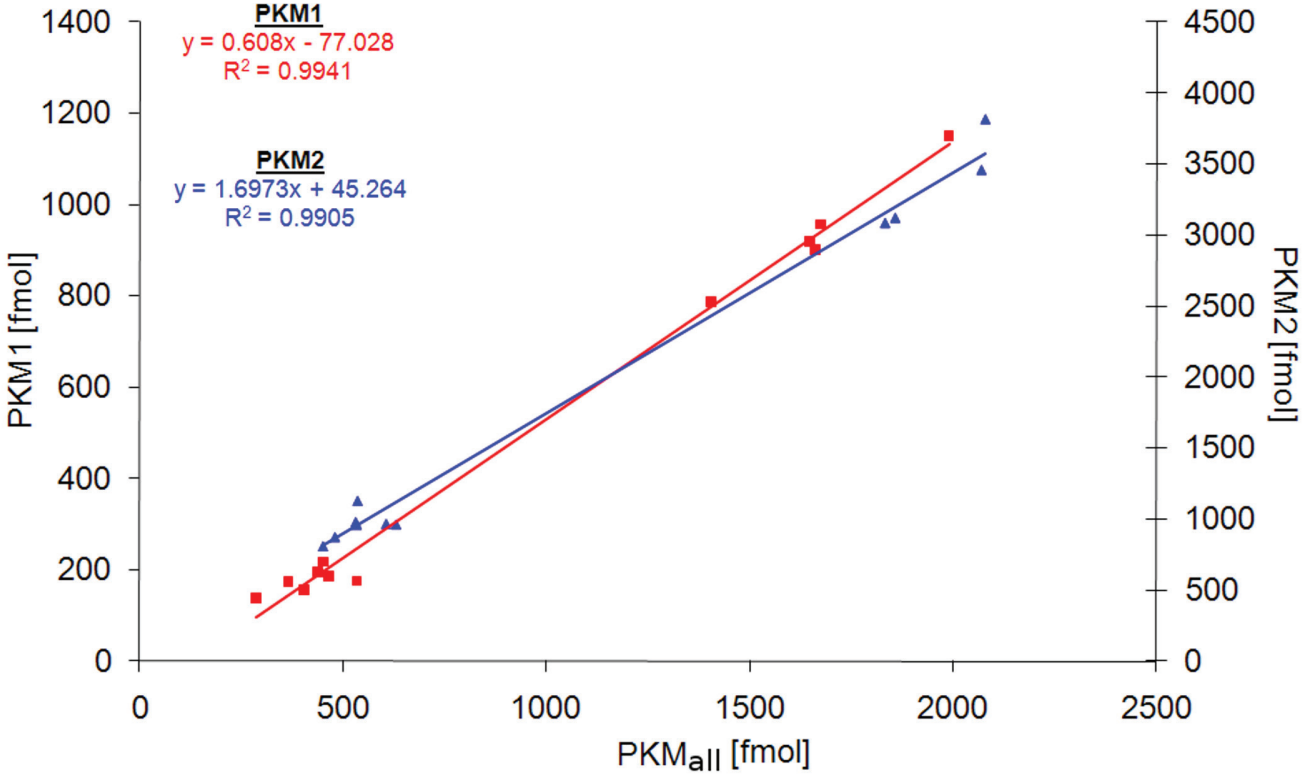


**Figure 2: Accuracy of PKM1 and PKM2 quantification.** Differently concentrated digests of PKM1-yeast (n = 11) and PKM2-yeast (n = 12) were injected, and the peptides PKM1, PKM2, and $PKM_{all}$ quantified as well as their corresponding AQUA standards analyzed by LC-MRM. Shown is a correlation plot of the concentration of the specific peptide (PKM1 or PKM2) and the $PKM_{all}$ peptide, concentrations are given in absolute values (fmol).

**Table 1: Absolute amount of PKM1 and PKM2 as well as relative PKM content in human tumors, control tissues and cell lines.** Concentrations are given in fmol per µg protein.

| Sample | PKM1 [fmol µg$^{-1}$] | PKM2 [fmol µg$^{-1}$] | PKM1 [%] | PKM2 [%] |
|---|---|---|---|---|
| **Malignant tumors** | | | | |
| Renal cell carcinoma 1 (RCC1)[§] | 3.2 | 62.8 | 4.8 | 95.2 |
| Renal cell carcinoma 2 (RCC2)[§] | 1.2 | 39.3 | 3.0 | 97.0 |
| Renal cell carcinoma 3 (RCC3)[§] | 3.1 | 139.4 | 2.2 | 97.8 |
| Renal cell carcinoma 4 (RCC4)[§] | 2.2 | 125.5 | 1.7 | 98.3 |
| Bladder carcinoma 1 (BC1) | 5.5 | 181.9 | 2.9 | 97.1 |
| Bladder carcinoma 2 | 4.4 | 116.0 | 3.7 | 96.3 |
| Bladder carcinoma 3 | 4.6 | 286.7 | 1.6 | 98.4 |
| Bladder carcinoma 4 | 3.5 | 55.1 | 6.0 | 94.0 |
| Hepatocellular carcinoma 1 (HCC1) | 0.6 | 5.8 | 9.4 | 90.6 |
| Hepatocellular carcinoma 2 (HCC2) | n.d. | 10.3 | | 100 |
| Hepatocellular carcinoma 3 (HCC3) | 0.5 | 45.2 | 1.1 | 98.9 |
| Colorectal carcinoma 1 (CRC1) | 1.4 | 129.1 | 1.1 | 98.9 |
| Colorectal carcinoma 2 (CRC2) | 1.0 | 110.2 | 0.9 | 99.1 |
| Colorectal carcinoma 3 | 14.7 | 323.4 | 4.3 | 95.7 |
| Lung carcinoma 1 (LC1) | 3.1 | 80.5 | 3.7 | 96.3 |
| Lung carcinoma 2 (LC2) | 3.5 | 95.8 | 3.5 | 96.5 |
| Lung carcinoma 3 | 0.8 | 47.0 | 1.7 | 98.3 |
| Lung carcinoma 4 | 0.9 | 59.9 | 1.5 | 98.5 |
| Lung carcinoma 5 | 1.3 | 49.8 | 2.5 | 97.5 |
| Follicular thyroid adenoma 1 | 0.5 | 14.6 | 3.3 | 96.7 |
| Follicular thyroid adenoma 2 | 0.7 | 32.5 | 2.1 | 97.9 |
| Follicular thyroid adenoma 3 | 0.6 | 29.4 | 2.0 | 98.0 |
| Follicular thyroid adenoma 4 | 2.3 | 43.9 | 5.0 | 95.0 |
| Follicular thyroid adenoma 5 | 0.9 | 37.0 | 2.4 | 97.6 |
| Papillary thyroid carcinoma 1 | 2.2 | 69.8 | 3.1 | 96.9 |
| **Benign tumors** | | | | |
| Renal oncocytoma 1[#] | 1.4 | 128.1 | 1.1 | 98.9 |
| Renal oncocytoma 2[#] | 1.2 | 83.6 | 1.4 | 98.6 |
| Renal oncocytoma 3 | 0.9 | 57.9 | 1.5 | 98.5 |
| Thyroid oncocytoma 1 (TO1) | 3.8 | 60.1 | 5.9 | 94.1 |
| Thyroid oncocytoma 2 (TO2) | 0.3 | 14.8 | 2.0 | 98.0 |
| Thyroid oncocytoma 3 | 1.1 | 31.9 | 3.3 | 96.7 |
| **Control tissues** | | | | |
| Kidney 1 (RCC1)[§] | 0.8 | 27.6 | 2.8 | 97.2 |
| Kidney 2 (RCC2)[§] | 0.8 | 24.8 | 3.1 | 96.9 |
| Kidney 3 (RCC3)[§] | 0.8 | 32.6 | 2.4 | 97.6 |
| Kidney 4 (RCC4)[§] | 0.7 | 33.8 | 2.0 | 98.0 |
| Bladder 1 (BC1) | 17.2 | 20.8 | 45.3 | 54.7 |
| Bladder 2 | 30.3 | 46.7 | 39.4 | 60.6 |
| Liver 1 (HCC1) | n.d. | 5.2 | | 100 |
| Liver 2 (HCC2) | n.d. | 15.2 | | 100 |
| Liver 3 (HCC3) | n.d. | 14.4 | | 100 |
| Colon 1 (CRC1) | 4.9 | 65.9 | 6.9 | 93.1 |
| Colon 2 (CRC2) | 2.8 | 70.1 | 3.8 | 96.2 |
| Colon 3 | 9.7 | 38.3 | 20.2 | 79.8 |
| Lung 1 (LC1) | 1.3 | 23.9 | 5.2 | 94.8 |
| Lung 2 (LC2) | 0.8 | 15.2 | 5.0 | 95.0 |
| Thyroid 1 (TO1) | 0.8 | 11.7 | 6.4 | 93.6 |
| Thyroid 2 (TO2) | 0.8 | 11.9 | 6.3 | 93.7 |
| Thyroid 3 | 0.5 | 9.7 | 4.9 | 95.1 |
| Thyroid 4 | 1.4 | 22.3 | 5.9 | 94.1 |

| | | | | |
|---|---|---|---|---|
| **cancer cell lines** | | | | |
| 60138 A1 [Tumor associated fibroblasts, breast] (60161 B1) | 21.0 | 88.7 | 19.1 | 80.9 |
| 87442 A1 [breast cancer associated fibroblasts] | 17.4 | 47.6 | 26.8 | 73.2 |
| A459-1 [lung carcinoma] | 3.1 | 302.0 | 1.0 | 99.0 |
| A459-3 [lung carcinoma] | 3.2 | 297.1 | 1.1 | 98.9 |
| HCT [Human colon tumor] | 3.1 | 16.4 | 15.9 | 84.1 |
| HEK-1 [transf., embryonic kidney] | 2.3 | 79.9 | 2.8 | 97.2 |
| HEK-2 [transf., embryonic kidney] | 2.1 | 83.2 | 2.5 | 97.5 |
| HEK-3 [transf., embryonic kidney] | 2.6 | 59.6 | 4.2 | 95.8 |
| HeLa-1 [cervix adenocarcinoma] | 2.4 | 144.9 | 1.6 | 98.4 |
| HeLa-2 [cervix adenocarcinoma] | 2.4 | 142.1 | 1.7 | 98.3 |
| HEP-1 [hepatocellular carcinoma] | 8.1 | 241.8 | 3.2 | 96.8 |
| HEP-2 [hepatocellular carcinoma] | 6.5 | 193.4 | 3.3 | 96.7 |
| MCF 7 [breast epithelial adenocarcinoma] | 1.3 | 66.7 | 1.9 | 98.1 |
| MDA MB-415 [Breast epithelial adenocarcinoma] | 0.6 | 83.8 | 0.7 | 99.3 |
| SPH 77-1 [small cell lung cancer] | 0.5 | 3.8 | 11.6 | 88.4 |
| SPH 77-2 [small cell lung cancer] | n.d. | 0.5 | | 100 |
| **other & control cell lines** | | | | |
| 60161 B1 [breastcancer adjacent fibroblast] (60138 A1) | 32.7 | 147.5 | 18.1 | 81.9 |
| 37098 B1 [breastcancer adjacent fibroblast] | 10.6 | 30.8 | 25.6 | 74.4 |
| MCF 10A [Breast epithelial cell line] | 1.0 | 72.9 | 1.4 | 98.6 |
| MCF 12A [Breast epithelial cell line] | 2.1 | 89.9 | 2.3 | 97.7 |

The abbreviations given in brackets for the control tissues refer to the matched tumor tissues. §The renal cell carcinomas and control tissues have been analyzed in a previous study [25], Renal oncocytoma 1 was case 6, Renal oncocytoma 2 was case 14 in [26].

PKM quantification (Fig 1c). In addition, we tested the reproducibility of PKM1 and PKM2 quantification by performing multiple injections for PKM1 and PKM2 yeast samples at different concentration. Linear regression was demonstrated by a $R^2$ of 0.994 for PKM1 and 0.990 for PKM2 (Fig 2), and thereby representing reliability of the quantification experiments.

### PKM2 dominates in cancer and tissue-matched controls

We found that PKM2 was the predominant PKM isoform in all human cancer cell lines (Table 1), which is in agreement with the earlier results obtained by Western blotting [10]. MCF10a, HeLa, A459 and a HEK-cell line (HEK293) were included in both studies, the AQUA analysis revealed that PKM2 accounted for 98.6% (MCF10a), 98.4% (Hela), 98.9-99.0 % (A459) and 95.8%-97.5% (HEK293) of total PKM. Thus mass spectrometry gave similar results as Western blotting, but the LC-MRM technology was more sensitive as PKM1 was clearly detectable in all samples, even at the lower femtomol range.

PKM1 and PKM2 quantification in further cell lines and malignant cancer samples confirmed the conclusion of PKM2 being the prominent PKM in all analyzed malignant cancer types: PKM2 accounted for a minimum of 94% of total PKM in all 22 malignant cancers, and other cell lines (Table 1). However, we found that PKM2 was also the dominant isoform in matched control tissue and slowly proliferating tumors. PKM1 and PKM2 were quantified in 18 healthy human tissues, and four non-cancer derived cell lines. In healthy kidney, lung, liver, and thyroid tissue, PKM2 accounted for a minimum of 93% of total PKM, for 79.8%-96.2% of PKM in colon, and 54.7%-60.6% of PKM in bladder. A similar picture was seen also in the oncocytoma samples. In these slow growing tumors, PKM2 accounted for 94.1-98.9% of total PKM. In table 1, the matching control/cancer tissue of the same individual is indicated in brackets. A switch in the expression from PKM1 to PKM2 during cancer development was not observed in any case. Only in a single case (bladder carcinoma) the control tissue had a much lower relative amount of PKM2 (54.7%) then the cancer sample (97.1% PKM2), but the change in the percentage resulted predominantly from an up regulation of the PKM2 isoform from 20.8 fmol in the bladder control to 181.9 fmol in the cancer, and not from a switch in alternative splicing.

In general, total PKM was expressed at a higher level in the cancer as in the control tissue. For instance, the average renal cell carcinoma tissue had 94.2 fmol PKM/µg protein, control kidney 30.5 fmol. This corresponds to a three-fold upgregulation in the absolute values. However, PKM1 and PKM2 were equally affected (an increase of 3.1 fold for PKM1 and 3.1 fold for PKM2).

## DISCUSSION

This study addresses a common misinterpretation of the finding that pyruvate kinase PKM2 is expressed in

cancer cells. Pyruvate kinase is the terminal enzyme in glycolysis. It converts phophoenol-pyruvate to pyruvate, a reaction which yields one molecule of ATP, therefore it accounts for glycolytic energy production. The PK product pyruvate is then converted to lactate which is excreted, or enters the mitochondrial citrate cycle. Humans possess four isoforms of pyruvate kinase, an L and R form, present in liver and red blood cells, and the M1 and M2 form, which were originally identified in muscle [11, 13]. Furthermore, based on the data generated with cell lines, a switch of PKM1 to PKM2 during development of cancer was postulated [10]. The results presented here, which base on a quantitative analytical platform that allowed the investigation of multiple samples and tissue-matched controls, challenges these conclusions. Quantitative analysis of PKM1 and PKM2 expression in different cancers and matched control tissue showed that a switch in the expression between these alternative splice isoforms is not associated with tumor development. According to these results PKM2 is not specific for rapidly proliferating tissue, nor tumors. However, the results agree that total PKM is up-regulated in cancer, which matches the observation of a high glycolytic activity of cancer cells.

Our findings prompt for a re-examination of the conclusion drawn in earlier studies [10, 20], and subsequent investigations that are based on these reports. The absolute values, presented here, revealed that the total (PKM1+PKM2) concentration varies highly between tissues, for example lung tissue contained 12.5 - 16.0 fmol PKM/µg protein, whereas in unaffected colon tissue 70.8 -72.9 fmol PKM/µg protein were found. This underlines the requirement of tissue matched controls for analyzing a change in the expression of PKM isoforms. Our results show that the nature of the tissue is the prime determinant of the expressed PKM isoform. For instance, fibroblasts maintained a higher relative PKM1 as other cell lines, irrespective if they were transformed or not (Table 1). This fact might also explain the higher PKM1 content in healthy bladder tissue, as muscle dominates unaffected bladder tissue, and PKM1 was the prominent PKM isoform in muscle [10].

In light of these results it has to be considered that the high concentrated PKM2, although possessing a lower catalytic activity as PKM1 [21], is responsible for most PKM activity in most healthy and cancer tissue. Thus, its exchange by a PKM1 isoform at its endogeneous level would cause a reduction in total PK activity, whereas the observed up-regulation an increase in PK activity. Following this way of thinking, tumors of PKM expressing tissues can possess higher pyruvate kinase activities as their matched controls.

Although the new results require that the current model of glycolysis regulation in cancer has to be re-examined, they do not exclude the possibility that a change in PK activity due to posttranslational modifications of PKM2 is involved in regulating respiratory metabolism. PKM2 can change from its dimeric into a tetrameric form [12], and electrophoretic shift variants point to different post-translationally modified versions of PKM2 [22]. The results are consistent with other investigations which demonstrate that phosphorylation can tune PKM2 activity in cancer [23]. Thus dynamic tuning of PKM2 activity, but not an exchange of PKM1 to PKM2 isoform expression, might be responsible for the tumor cell's Warburg effect.

## METHODS

### Plasmid generation

Plasmids encoding pyruvate kinase PKM1 and PKM2 were generated by amplifying PKM1 from human fetal brain cDNA and PKM2 from cDNA of a pool of twenty adult tissues (Invitrogen) by PCR with primers 5'-GAGAATTCATGTCGAAGCCCCATAGTG -3' and 5'-GAGTCGACTCACGGCACAGGAACAAC -3'. PCR products were ligated into centromeric yeast plasmids containing the *TEF1* promoter (p413TEF) [24]. The plasmids were verified by restriction digest and re-sequencing.

### Sample preparation and analytical method

Human tissue were processed as described earlier [25]. In brief, frozen tissues were cut into 5 µm thick sections with a cryomicrotome at – 20°C. 50 – 100 mg tissue were transferred in 10 – 20-fold volume of SEKT buffer (250 mM saccharose; 2 mM EGTA, 40 mM KCl; 20 mM TRIS; pH 7.4). The samples were homogenized with Potter-S-Homogenisator on ice and centrifuged 10 min at 600g. The supernatant was aliquoted and stored at -70°C

Protein samples from yeast carrying p413TEF-*PKM1* or p413TEF-*PKM2* and human cancer and control tissues were separated on a 10% SDS-PAGE gel and the region corresponding to the mass range 50-70 kDa was excised. Those gel pieces were then subjected to an in-gel tryptic digest, adapted from Kaiser et al. [18]. The AQUA peptide mixture (20 µl) containing all three labeled peptides was spiked to the samples after the digest. The LC-MRM analysis was performed on a nanoLC (Eksigent, Ultra 2D) coupled online to a hybrid triple quadrupole/ion trap mass spectrometer (AB/SCIEX, QTRAP5500) as described earlier [19]. In brief, as mobile phase 0.1% formic acid in water (A) and 0.1% formic acid in acetonitrile (B) were used. After trapping the analytes and standards on a trap column (ReproSil pur, C18-AQ, 5 µm, 0.15 x 10 mm), they were eluted onto a RP-analytical column (Agilent, Zorbax SB300-C18; 3.5 µm, 0.75 x 150 mm). Separation was achieved by applying a linear gradient starting at 15% B and going up to 30% B within 30 min. The

acetonitrile content was then increased to 95% within the next 10 min and kept at that level for 15 min before returning to the starting conditions. The tryptic peptide for PKM1 (LFEELVR) and its isotope labeled analogue (LFEE[LC13N15]VR) were monitored on the MRM transitions resulting from 2y4; 2y5 and 2y6 fragmentation. The tryptic peptide LAPITSDPTEATAVGAVEASFK, specific for PKM2, and its isotope labeled analogues (LAPITSDPTEATAVGAVEAS[FC13N15]K) were monitored on the MRM transitions attributed to 3y8; 3y9 and 3y10 fragment ions. The tryptic peptide ITLDNAYMEK, obtained from both PKM isoforms, and the corresponding isotope labeled peptide (IT[LC13N15] DNAYMEK) were detected on MRM transitions deriving from 2y6, 2y7 and 2y8 fragmentation. Using the peak area of the $PKM_{all}$ peptide in the yeast sample as reference, we calculated a correction factor of 2.1 for the peak areas measured for the PKM1 specific peptide, and 0.6 for PKM2 peptide. Every sample injection was followed by an acetonitrile injection to exclude sample carry over. The identity of the quantified peptides was confirmed by collecting of MS/MS spectra on the QTRAP operating in iontrap mode.

## ETHICS

Tissue samples were kindly provided by the Biobank of the Medical University Graz, the Institute of Pathology and the Department of Urology, Paracelsus Medical University Salzburg. All tissues were frozen and stored in liquid nitrogen within 20 minutes after surgery. Tumor cell content and cellular composition of samples were evaluated using hematoxylin-eosin-stained frozen sections. All analyzed cancer samples had a tumor cell content of over 80%. Matching normal tissue was available for samples given in Table 1. The study was performed according to the Austrian Gene Technology Act. Experiments were performed in accordance with the Helsinki declaration of 1975 (revised 1983) and the guidelines of the Salzburg State Ethics Research Committee being no clinical drug trial or epidemiological investigation. All patients have signed an informed consent concerning the surgical removal and therapy of the tumors. Furthermore, the study did not extend to examination of individual case records. The anonymity of the patients has been ensured.

## ACKNOWLEDGEMENTS

We thank Diego J Walther and Bodo Lange and their laboratories for providing cell lines We also would like to thank B. Lukaszewska-McGreal for sample preparation. All tissue samples were kindly provided by the Biobank Graz, the Institute of Pathology and the Department of Urology Salzburg, Austria. MR is a Wellcome Trust Research Career development and Wellcome Beit price fellow, and acknowledges funding from ERC Starting Grant StG-260809 (MetabolicRegulators).

## REFERENCES

1. Ferreira LM. Cancer metabolism: the Warburg effect today. Experimental and molecular pathology. 2010; 89:372-380.
2. Hsu PP, Sabatini DM. Cancer cell metabolism: Warburg and beyond. Cell. 2008; 134:703-707.
3. Warburg O. Origin of Cancer Cells. Science. 1956; 123:309-314.
4. Wolf A, Agnihotri S, Guha A. Targeting metabolic remodeling in glioblastoma multiforme. Oncotarget. 2010; 1:552-562.
5. Bonuccelli G, Whitaker-Menezes D, Castello-Cros R, Pavlides S, Pestell RG, Fatatis A, Witkiewicz AK, Heiden MG, Migneco G, Chiavarina B, Frank PG, Capozza F, Flomenberg N, Martinez-Outschoorn UE, Sotgia F, Lisanti MP. The reverse Warburg effect: glycolysis inhibitors prevent the tumor promoting effects of caveolin-1 deficient cancer associated fibroblasts. Cell cycle 2010; 9:1960-1971.
6. Pavlides S, Tsirigos A, Vera I, Flomenberg N, Frank PG, Casimiro MC, Wang C, Pestell RG, Martinez-Outschoorn UE, Howell A, Sotgia F, Lisanti MP. Transcriptional evidence for the "Reverse Warburg Effect" in human breast cancer tumor stroma and metastasis: similarities with oxidative stress, inflammation, Alzheimer's disease, and "Neuron-Glia Metabolic Coupling". Aging. 2010; 2:185-199.
7. Cadenas E, Davies KJ. Mitochondrial free radical generation, oxidative stress, and aging. Free radical biology & medicine. 2000; 29:222-230.
8. Darnell JE, Jr. STAT3, HIF-1, glucose addiction and Warburg effect. Aging. 2010; 2:890-891.
9. Demaria M, Giorgi C, Lebiedzinska M, Esposito G, D'Angeli L, Bartoli A, Gough DJ, Turkson J, Levy DE, Watson CJ, Wieckowski MR, Provero P, Pinton P, Poli V. A STAT3-mediated metabolic switch is involved in tumour transformation and STAT3 addiction. Aging. 2010; 2:823-842.
10. Christofk HR, Vander Heiden MG, Harris MH, Ramanathan A, Gerszten RE, Wei R, Fleming MD, Schreiber SL, Cantley LC. The M2 splice isoform of pyruvate kinase is important for cancer metabolism and tumour growth. Nature. 2008; 452:230-233.
11. Mazurek S, Boschek CB, Hugo F, Eigenbrodt E. Pyruvate kinase type M2 and its role in tumor growth and spreading. Semin Cancer Biol. 2005; 15:300-308.
12. Spoden GA, Rostek U, Lechner S, Mitterberger M, Mazurek S, Zwerschke W. Pyruvate kinase isoenzyme M2 is a glycolytic sensor differentially regulating cell proliferation, cell size and apoptotic cell death dependent on glucose supply. 2009; 315:2765-2774
13. Imamura K, Tanaka T. Multimolecular forms of

pyruvate kinase from rat and other mammalian tissues. I. Electrophoretic studies. J Biochem. 1972; 71:1043-1051.

14. Gerber SA, Rush J, Stemman O, Kirschner MW, Gygi SP. Absolute quantification of proteins and phosphoproteins from cell lysates by tandem MS. Proc Natl Acad Sci U S A. 2003; 100:6940-6945.
15. Kettenbach AN, Rush J, Gerber SA. Absolute quantification of protein and post-translational modification abundance with stable isotope-labeled synthetic peptides. Nature protocols. 2011; 6:175-186.
16. Kirkpatrick DS, Gerber SA, Gygi SP. The absolute quantification strategy: a general procedure for the quantification of proteins and post-translational modifications. Methods 2005; 35:265-273.
17. Gallien S, Duriez E, Domon B. Selected reaction monitoring applied to proteomics. J Mass Spectrom. 2011; 46:298-312.
18. Kaiser P, Meierhofer D, Wang X, Huang L. Tandem affinity purification combined with mass spectrometry to identify components of protein complexes. Methods in molecular biology 2008; 439:309-326.
19. Bluemlein K, Ralser M. Monitoring protein expression in whole-cell extracts by targeted label- and standard-free LC-MS/MS. Nature Protocols. 2011; 6: 859–869.
20. Christofk HR, Vander Heiden MG, Wu N, Asara JM, Cantley LC. Pyruvate kinase M2 is a phosphotyrosine-binding protein. Nature. 2008; 452:181-186.
21. Vander Heiden MG, Locasale JW, Swanson KD, Sharfi H, Heffron GJ, Amador-Noguez D, Christofk HR, Wagner G, Rabinowitz JD, Asara JM, Cantley LC. Evidence for an alternative glycolytic pathway in rapidly proliferating cells. Science 2010; 329:1492-1499.
22. Guminska M, Ignacak J, Kedryna T, Stachurska MB. Tumor-specific pyruvate kinase isoenzyme M2 involved in biochemical strategy of energy generation in neoplastic cells. Acta Biochim Pol. 1997; 44:711-724.
23. Hitosugi T, Kang S, Vander Heiden MG, Chung TW, Elf S, Lythgoe K, Dong S, Lonial S, Wang X, Chen GZ, Xie J, Gu TL, Polakiewicz RD, Roesel JL, Boggon TJ, Khuri FR et al. Tyrosine phosphorylation inhibits PKM2 to promote the Warburg effect and tumor growth. Sci Signal. 2009; 2:ra73.
24. Mumberg D, Muller R, Funk M. Yeast vectors for the controlled expression of heterologous proteins in different genetic backgrounds. Gene. 1995; 156:119-122.
25. Meierhofer D, Mayr JA, Foetschl U, Berger A, Fink K, Schmeller N, Hacker GW, Hauser-Kronberger C, Kofler B, Sperl W. Decrease of mitochondrial DNA content and energy metabolism in renal cell carcinoma. Carcinogenesis. 2004; 25:1005-1010.
26. Mayr JA, Meierhofer D, Zimmermann F, Feichtinger R, Kogler C, Ratschek M, Schmeller N, Sperl W, Kofler B. Loss of complex I due to mitochondrial DNA mutations in renal oncocytoma. Clin Cancer Res. 2008; 14:2270-2275.

***Contributions to Manuscript 3***

Part of this thesis was cloning of the human PKM isoforms (PKM1 and PKM2) and the generation of a yeast model which expresses these human PKM isoforms to gain a base for establishing the analytical method for PKM quantification. Furthermore, active contribution to sample organization and handling was part of this thesis.

Katharina Bluemlein designed the AQUA peptides used in this study, established the analytical method for PKM1 and PKM2 identification and quantification, analyzed the data, and was involved in writing of the manuscript.

René G. Feichtinger was responsible for tumor sample and cell extract preparation.

Hans Lehrach gave support in scientific discussion and by supplying experimental equipment.

Barbara Kofler contributed by allocation of tumor material and was involved in writing of the manuscript.

Markus Ralser had the initial idea of this project and wrote the majority of the manuscript.

**Manuscript 4**

(pages 65-81 in print version)

# The Pentose Phosphate Pathway Is a Metabolic Redox Sensor and Regulates Transcription During the Antioxidant Response

Antje Krüger[1], Nana-Maria Grüning[1], Miriam MC Wamelink[2], Martin Kerick[1], Alexander Kirpy[1], Dimitri Parkhomchuk[1], Katharina Bluemlein[1], Michal-Ruth Schweiger[1], Aleksey Soldatov[1], Hans Lehrach[1], Cornelis Jakobs[2] and Markus Ralser[1, 3]

[1] Max Planck Institute for Molecular Genetics, Berlin, Germany
[2] Metabolic Unit, Department of Clinical Chemistry, VU Medical Center, Amsterdam, The Netherlands
[3] Department of Biochemistry, Cambridge Systems Biology Centre, University of Cambridge, Cambridge, United Kingdom

Antioxidants & Redox Signaling. 2011 Jul 15;15(2):311-24.

journal homepage: http://www.liebertpub.com/products/product.aspx?pid=4

DOI link for original publication: http://dx.doi.org/10.1089/ars.2010.3797

***Contributions to Manuscript 4***

The contribution of this thesis to Manuscript 4 comprised performing of the oxidant tolerance tests shown in Fig. 1D, to prepare yeast extracts for metabolite quantifications (Fig. 2) and to perform the experimental steps that were necessary to gain the results displayed in Supplementary Fig. 1: cloning of yeast *tkl1* and *rpe1*, generation of yeast double mutant strains, plasmid shuffle and spotting tests to proof synthetic lethality.

Antje Krüger performed mRNA extraction and cDNA synthesis that were required for generating sequencing data shown in Fig. 3. Furthermore, she performed qRT-PCR experiments (Fig. 4A and B), the preparation of yeast extracts for data shown in Fig. 4C, yeast stress tests (Fig. S2) and measurements of the NADPH/$NADP^+$ ratio displayed in Fig. S3. Furthermore she took part in experimental design and writing of the manuscript.

Mirjam MC Wamelink contributed by measuring PPP metabolites (Fig. 2).

Martin Kerick was responsible for the bioinformatic analysis of next-generation sequencing data shown in Fig. 3.

Alexander Kirpy and Dimitri Parkhomchuk contributed to this manuscript by generating transcriptome profiles that were bases for the data shown in Fig. 3.

Katharina Bluemlein established the analytical method for protein quantification displayed in Fig. 4C.

Michal-Ruth Schweiger, Aleksey Soldatov, Hans Lehrach and Cornelis Jakobs were involved in scientific discussion.

Markus Ralser had the initial idea and conceptualized the project. He generated the yeast deletion strains that were used to generate the data shown in Fig. 1B, C and D, Fig. 2, Fig. 3 and Fig. 4. Furthermore, he performed the oxidant tolerance test in Fig. 1B and C and was involved in bioinformatic analysis of sequencing data. He wrote the majority of the manuscript.

**Manuscript 5**

(pages 83-92 in print version)

# The difference between rare and exceptionally rare: molecular characterisation of ribose 5-phosphate isomerase deficiency

Mirjam MC Wamelink[1], Nana-Maria Grüning[2], Erwin EW Jansen[1], Katharina Bluemlein[2], Hans Lehrach[2], Cornelis Jakobs[1] and Markus Ralser[2]

[1] Metabolic Unit, Department of Clinical Chemistry, VU Medical Center, Amsterdam, The Netherlands

[2] Max Planck Institute for Molecular Genetics, Berlin, Germany

Journal of Molecular Medicine (Berl). 2010 Sep;88(9):931-9.
journal homepage: http://www.springerlink.com/content/0946-2716

DOI link for original publication: http://dx.doi.org/10.1007/s00109-010-0634-1

***Contributions to Manuscript 5***

Part of this thesis was to evaluate RNA expression in human cell lines and yeast cells by qRT-PCRs. This included culturing of yeast cells, RNA extraction and cDNA synthesis from human and yeast cells. Furthermore, the preparation of protein extracts and the performance of western blot experiments shown in Fig. 1A and 2B were also contributed to the manuscript during this thesis. The physiological examination of RPI expression and mutation in photometrical measurements of yeast growth curves was part of this thesis, too.

Mirjam MC Wamelink performed quantification of PPP metabolites and polyols and data analysis (Fig. 3A and B), and established an enzyme-coupled enzyme activity assay to measure RPI activity in human and yeast cell extracts (Fig. 1D and 2C). She was also involved in writing of the manuscript.

Erwin EW Jansen was involved in PPP metabolite and polyol measurements (Fig. 3A and B).

Katharina Bluemlein developed the analytical method to measure the relative RPI protein concentration in cell extracts (Fig. 1B).

Hans Lehrach and Cornelis Jakobs were involved in scientific discussion.

Markus Ralser generated the transgenic yeast strains and spotting test shown in Fig. 2A. These yeast strains were also used to generate the data shown in Fig. 2D. He conceptualized the project and wrote the manuscript.

## Discussion

The metabolic network adjusts itself in response to environmental stimuli and perturbations. As we summarized in our review Grüning *et al.* 2010, the robustness of the metabolic network largely results from its modular architecture. Metabolic modules, or subsets of enzymatic reactions within those, form individual functional units. Although metabolic modules are highly interconnected, perturbations can be balanced inside specific modules without disrupting the entire cellular metabolic flux and, thereby, make modularity a major premise for cellular self-organization and functional adaptation. Metabolic imbalances caused by alterations in nutrient supply, for example, can be overcome by activity adjustments of certain metabolic modules, such as glycolysis or the PPP. Consequences range from fine-tuning of metabolic enzymes to global transcriptional changes. Understanding the mechanisms of metabolic self-adaptation and their roles in the cellular regulome also means understanding fundamental organizational principles of life.

***Activity Tuning of the Glycolytic Enzyme PYK Coordinates Energy- and Redox-Metabolism*** (Grüning *et al.* 2011)

The Warburg effect describes a metabolic transition from oxidative to fermentative metabolism in the presence of sufficient oxygen, thus also called aerobic glycolysis, and is characteristic for proliferating cells and therefore also for tumor cells [156-158]. Even though elucidating the metabolism of tumor cells has long been a capital goal in cancer research, the molecular mechanisms responsible for the Warburg effect are not yet fully understood. A main focus was placed on the glycolytic enzyme pyruvate kinase (PYK) as its activity seems to play an important role in the regulation of aerobic glycolysis. In order to reveal regulatory mechanisms that are triggered by PYK and involved in the coordination of energy metabolism, we designed a model of yeast strains exhibiting different overall PYK activities. The yeast *S. cerevisiae* possesses two PYK isoforms that are differentially expressed from distinct genes dependent on the available carbon source. PYK1 is predominantly expressed, whereas PYK2 expression is glucose-repressed and induced on non-fermentable carbon sources such as ethanol. PYK1 is highly active, whereas PYK2 shows a comparably low substrate turn-over [159]. Thus, *S. cerevisiae* possesses two differently active PYK isoforms as it is the case in mammalian cells (PKM1 and PKM2). By deleting both endogenous PYK loci and cloning either isoform onto plasmids harboring either a

strong (*TEF1*) or a weak (*CYC1*) promoter, four strains with gradually decreasing PYK activity could be generated.

By using those strains, we could show that PYK plays a crucial role in the regulation of oxidative metabolism in yeast. When grown on media containing glucose as carbon source, yeast's growth capacity was impaired with decreased PYK activity. Intriguingly, this phenotype was abolished when the strains with varying PYK activity were grown on media containing galactose instead of glucose (Fig. 2A). One has to note that mitochondrial respiration is repressed in dependence of the available carbon source in yeast, and that this effect is much stronger for glucose than for galactose although both are fermentable carbon sources [106, 160, 161]. Thus, growth rescue of strains with low PYK activity on galactose media could result from increased mitochondrial respiration in those strains. For further validation of this assumption we measured oxygen consumption in liquid cultures by using a Clark electrode (Fig. 2D). Indeed, oxygen consumption was increased when PYK activity was low. Therefore, growth phenotypes and elevated oxygen consumption pointed to an inverse correlation of PYK activity and mitochondrial respiration rate.

However, we had to exclude the possibility that the observed elevation in oxygen consumption was result of an increased activity of oxygen consuming enzymes other than those being part of the respiratory chain (e.g. oxidoreductases). By streaking the cells on the mutagen ethidium bromide, we disrupted mitochondrial DNA, and thereby destroyed functional mitochondrial respiration (generation of $\rho^0$ strains) [162]. Depletion of mitochondrial respiration was confirmed by the absence of yeast growth on media containing the non-fermentable carbon source ethanol, which has to be metabolized *via* mitochondrial respiration in order to gain ATP. Disruption of mitochondrial DNA led to the abolishment of the galactose rescue of strains with low PYK activity, and thus underlined the importance of mitochondrial respiration for yeast growth under low PYK activity (Fig. 2B).

In addition to the oxygen measurements, and the analysis of growth phenotypes we performed quantitative real-time PCR (qRT-PCRs) experiments to confirm the PYK-activity dependent regulation of mitochondrial respiration. When wild-type cells were shifted from glucose to galactose media, and thus glucose repression of mitochondrial respiration was released, genes of the respiratory chain (*COX1*, *COX2*, *COX3*) and TCAC (*CIT1*) were regulated (up regulated: *COX1*, *CIT1*, down regulated: *COX2*, *COX3*). The same pattern of mRNA expression could be observed in cells with

low PYK activity compared to cells with high PYK activity, although these cultures were solemnly grown in glucose media and not shifted to galactose containing media (Fig. 2C). This demonstrated direct influence of PYK activity on the regulation of genes involved in mitochondrial respiration. In summary, these experiments enabled us to conclude that a change from *PYK1* to *PYK2* or low expression of either isoform shifted yeast cells toward higher respiration.

Respiratory metabolism has a higher ATP yield than fermentation, but at the same time, the mitochondrial electron transport chain is also major source for ROS in cells metabolizing oxygen. The cell possesses diverse defense mechanisms against ROS in order to maintain the delicate redox-balance and protect its macromolecules from oxidative damage. Indeed, by staining for superoxide, we showed that an increase in respiration does not necessarily lead to increased intracellular ROS levels. When wild-type cells were grown on galactose they were released from glucose repression and respiration was activated. Noteworthy, they could balance their ROS level compared to cells grown on glucose media (Fig. 3A, upper panel). However, we expected increased sensitivity to oxidative stress in strains with low PYK activity and therefore elevated mitochondrial respiration levels due to higher ROS leakage from the electron transport chain. Surprisingly, the intracellular superoxide and hydrogen peroxide levels were balanced in the four yeast strains with varying PYK activity (Fig. 3A, lower panel). We therefore tested for increased antioxidative capacity by spotting the strains with varying PYK activity onto media containing different external oxidants (diamide, $H_2O_2$, CHP, TBH, menadione, juglone, Fig. 3B). Intriguingly, although strains with low PYK activity respire at higher rates, their tolerance to oxidative stress was increased. Varying grades of resistance to the tested oxidizing chemicals could be observed for the different strains. Different oxidizing stressors cause diverse responses in yeast because of (i) the type of free radical released, (ii) the different oxidant's redox (Nernst) potential, (iii) their primary targets and last but not least (iv) due to the varying grades of evolutionary adaptation [163]. Additionally, it was reported that the glycolytic enzyme GAPDH, located upstream of PYK, is inactivated to a different extent by different oxidants [18, 96]; an effect which might also modulate oxidant-resistance of strains with reduced PYK activity. Growth advantages of yeast strains with low PYK activity under oxidative stress could also be confirmed in photometrical determination of cellular growth, and by measuring cell survival after exposure to a high oxidant dose (Fig. 3C, D). It is also notable that the PYK mutant strains exhibited tolerance to a remarkable

broad spectrum of oxidizing chemicals. In an earlier study, only a small fraction of yeast mutants was resistant to a comparable number of oxidants [163]. This fact points to a general mechanism in the anti-oxidative machinery of the cell that is triggered by low PYK activity.

To elucidate the molecular underpinnings of the phenomenon of increased resistance to oxidative stress in yeast cells with low PYK activity, we performed experiments in order to reveal possible metabolic rearrangements. Hydrophilic interaction liquid chromatography/multiple reaction monitoring (HILIC/MRM) measurements showed strongly increased levels of the PYK substrate phosphoenol pyruvate (PEP) when PYK activity was low (Fig. 4A). Before, there were hints that PEP might interact with another glycolytic enzyme than only with PYK. It influenced an enzyme-coupled enzyme assay of phosphofructokinase by inhibition of triosephosphate isomerase (TPI) in *Escherichia coli* [164]. We also knew from former studies that yeast expressing TPI at a lower activity than the corresponding wild-type shows not only increased resistance to oxidative stress, but also elevated levels of PPP metabolites [18, 145]. As mentioned before, the PPP plays an essential role in the oxidative stress response machinery of the cell. Importantly, it provides reducing equivalents in form of NADPH, which is essential to maintain the cellular redox equilibrium and required by cellular antioxidant mechanisms to neutralize ROS. Indeed, in enzyme activity assays, we could show that PEP inhibits TPI activity at physiological PEP concentrations which were reached when PYK activity was low (Fig. 4B). And furthermore, we could show that PPP intermediates rise in PYK activity dependent manner by liquid chromatography/multiple reaction monitoring measurements. The strain with the lowest activity contained highest PPP metabolite levels in cells grown on media containing glucose as well as for cells grown on media containing galactose (Fig. 5B).

Additionally, we searched for a TPI allele with different PEP sensitivity in order to gain a tool for studying the physiological effects of the TPI-PEP inhibition. In humans, mutations in the TPI gene, located at chromosome 12p13, cause a rare metabolic syndrome called TPI-deficiency. Most patients that were diagnosed for TPI-deficiency are homozygous or compound heterozygous for the $TPI_{Glu104Asp}$ allele. This mutation causes dimerization defects of the enzyme and alters its stability [165]. Additionally, enzyme activity screens in erythrocyte extracts of different population cohorts revealed various missense mutations that were responsible for TPI activity reduction, but did not lead to manifestation of the disease in heterozygous individuals –

even when TPI activity was decreased to about 50% compared to unaffected individuals [144-147]. Testing the TPI alleles found in those screens and expressed in yeast in enzyme-coupled enzyme assays, the $TPI_{Ile170Val}$ allele was shown to be deficient for PEP inhibition (Fig. 4C). This TPI allele has reduced catalytic activity itself and leads to elevated PPP levels and oxidant tolerance when expressed in yeast [18]. Simultaneous reduction in PYK activity, and expression of this TPI isoform, did not lead to a further increase in oxidant tolerance (Fig. 4D). Thereby, TPI inactivation was proven to be essential for the PYK activated metabolic shift into the PPP. In course of these experiments, we could reveal a metabolic feedback loop that is triggered by lowered PYK activity and leads to subsequent PEP accumulation, TPI inhibition and carbohydrate flux redirection into the PPP.

The functional oxidative branch of the PPP (OPPP) is required for an increase in tolerance to oxidative stress upon GAPDH or TPI inactivation [31, 48-52]. Thus, we hypothesized that PYK initiated TPI inhibition with subsequent redirection of the carbohydrate flux into the PPP is a protective mechanism to prevent oxidative damage. For experimental verification of this assumption, we generated strains deleted for the first and rate-limiting enzyme of the OPPP, glucose 6-phosphate dehydrogenase (Zwf1p). As the OPPP is composed of irreversible reactions, deletion of this gene separates this part of the PPP from glycolysis. In fact, yeast strains deficient for the OPPP exhibited increased sensitivity to the oxidative stress causing agent diamide in spotting tests (Fig. 6A), and increased levels of superoxide and hydrogen peroxide under low PYK activity and thus elevated respiration (Fig. 6B). It is a well-known fact that ROS damage cellular macromolecules by oxidization. Here, this was proven in cells with high respiration due to low PYK activity and deleted for Zwf1p compared to cells with intact PPP. In those cells protein carbonylation – an irreversible damage of proteins caused by high ROS levels – was strongly increased (Fig. 6C).

Due to close proximity, mitochondrial macromolecules are especially under threat of elevated superoxide leakage from the electron transport chain [12, 166]. The mitochondrial matrix enzyme aconitase, which is part of the TCAC, carries an iron-sulfur-cluster in its substrate binding pocket and is thus redox prone [166-168]. Experiments with GFP-tagged yeast aconitase revealed changes in staining pattern due to high ROS levels and OPPP deficiency (Fig. 6D). Fluorescence of unaffected yeast aconitase shows a tubular shape of the mitochondrial matrix space (in cells with high PYK activity and wild-type for OPPP), whereas an elevated ROS level induces

fragmentation of the tubular staining pattern and formation of smaller roundish vesicle-like structures (in cells with low PYK activity and deleted for OPPP). This indicates ROS induced damage of yeast aconitase and, therefore, presumably impairment of TCAC function. In summary, we could conclude that a functional OPPP is essential to balance ROS levels in respiring yeast, and thereby increases resistance to oxidative stress and protect cells from oxidative damage when PYK activity is low. Thus, we discovered that pyruvate kinase triggers a metabolic feedback loop that synchronizes energy with redox metabolism in respiring cells.

One could argue that dynamic activation of the PPP occurs also when the glycolytic enzyme GAPDH, upstream of PYK, is inactivated due to externally applied toxic oxidant doses [18, 85], which would question the relevance of additionally blocking TPI upstream of GAPDH. ROS leakage from the respiratory chain, however, does not inhibit glycolysis and GAPDH activity was shown to be stable to continuous oxidant exposure [169, 170]. Additionally, we showed in this manuscript that the superoxide level is balanced in respiring cells (Fig. 3A), and therefore concluded that they do not possess a redox-state which would lead to GAPDH inactivation, and require another shunt for blocking glycolysis. Indeed, decreased TPI activity facilitates a redirection of the carbohydrate flux from upper glycolysis into the PPP, but carbohydrates can still be metabolized through lower glycolysis (they can enter at the site of glyceraldehydes 3-phosphate, introduction Fig. 1), and thus both pathways remain active. Inactivation of GAPDH, for example, might lead to decreased flux of lower glycolysis and decreased NADH production, and therefore different metabolic consequences. Furthermore, the PEP-TPI feedback loop might be biologically relevant, because reduced catalytic turn-over of PYK alone may not be sufficient to accumulate upstream metabolites. Vander Heiden and colleagues [171] published data that revealed mammalian phosphoglycerate mutase (PGM) to be a PEP interaction partner that turns PEP into pyruvate, and thus bypasses the PYK reaction. Blocking TPI that is located further upstream, however, facilitates metabolite accumulation in upper glycolysis and the PPP. Although we cannot exclude that PEP also functions as modulator on other glycolytic enzymes, the feedback loop *via* TPI was shown to be sufficient to balance elevated ROS levels through increased respiration.

It should be considered that there may be differences in the PYK mediated regulation of mitochondrial respiration between yeast and mammalian cells. In contrast to the yeast model, are results derived from mammalian cells that show increased

oxidative phosphorylation and decreased excretion of lactate when PKM has high activity [122]. Thus, there are contradicting results presented in the current literature that yet hinder to determine a definite link between PKM2 activity and tumor metabolism. Due to that, the underlying mechanisms that stimulate OXPHOS in dependence of PYK still have to be elucidated. We exclude a direct role of the PPP since deletion of PPP enzymes did not augment oxygen consumption under low PYK activity (Suppl. Fig. 2). Thus, none of the deleted PPP enzymes, nor the metabolites they generate, may function as transducer to activate respiration. Possible links between reduced PYK activity and elevated OXPHOS could be changes in the NADPH/$NADP^+$ ratio or reporter metabolites that are affected in concentration upon PYK activity changes other than those belonging to the PPP (e.g. metabolites of upper glycolysis).

Furthermore, our experiments showed that the sensing of energy shortage falls short of completely explaining a possible mechanism concerning the regulation of respiration in yeast (Fig. 2). Cells growing in galactose media show higher oxygen consumption, and therefore probably increased ATP production through mitochondrial respiration, compared to cells growing in glucose media. Thus, a further increase in oxygen consumption due to low PYK activity in galactose-grown cells is presumably not attributable to energy sensing pathways (e.g. TOR/AMPK).

Nevertheless, although the link between PYK activity and regulation of mitochondrial respiration still has to be found, we speculate that the PYK protein abundance also plays a major role in the regulation of metabolic rearrangements rather than only its overall activity – in yeast as well as in human tissues. In Bluemlein *et al*. 2011 we demonstrated elevated total PKM (PKM2 and PKM1) expression levels in cancer cell lines and tissues, when comparing PKM1 and PKM2 expression levels to healthy control cells and tissues. This matches our recent and yet unpublished results concerning the concentrations of diverse amino acids in cancer and healthy human tissues as well as in the four different yeast strains expressing the here described PYK plasmids. These data show dependence of the amino acid concentrations (e.g. glutamic acid) on the total PYK expression level rather than on the overall activity in yeast and in human cells. In accordance with our yeast model, it was shown by Luo and coworkers [172] that fermentative gene expression is activated by PKM2 independently of its activity.

In further support to the hypothesis that yeast and mammalian metabolisms respond in a similar way to changes in PYK activity and expression is evidence that the

PYK mediated feedback loop, described by us, is evolutionarily conserved. Firstly, metabolite content upstream of PYK rises in mammalian cells that exhibit the Warburg effect [171] and when PYK is low in *B. subtilis* [173]. Furthermore, we demonstrated that TPI inhibition by PEP was even more efficient for the rabbit and human enzyme species than for the yeast one. This is in accordance with previous observations, where transgenic yeast that expressed human TPI was more resistant to oxidative stress than yeast expressing the yeast paralogue [18].

As mentioned above, most patients that were diagnosed for TPI deficiency carry the $TPI_{Glu104Asp}$ allele which leads to TPI dimerization defects [165]. However, the pathogenesis of the $TPI_{Ile170Val}$ allele is yet unknown. Since impaired redox metabolism has been reported as symptom for TPI deficiency [174], the discovery that the $TPI_{Ile170Val}$ allele is insensitive for PEP feedback inhibition provides a new starting-point for further research on TPI deficiency pathomechanisms in humans.

Additionally, as in yeast, depletion of the Zwf1 paralogue (G6PD) decreases oxidant tolerance and NADPH generation in mammalian cells [175, 176]. It is also assumed that the Warburg effect also facilitates synthesis of macromolecules (nucleic acids, amino acids, lipids) from metabolic intermediates that are required for cellular growth and division [103, 171, 177]. The here described metabolic feedback loop could allow synthesis of these macromolecules because numerous metabolic intermediates derive from the upper part of glycolysis and the PPP, and gives a base for further studies concerning the molecular consequences that might be connected to this metabolic reconfiguration.

### *There is No Switch in Pyruvate Kinase Isoforms during Tumor Development*

(Bluemlein *et al.* 2011)

It has been postulated by Christofk *et al.* 2008 [119] that rapidly proliferating and tumor cells exclusively express the PKM2 isoform and that a switch from PKM1 to PKM2 is necessary for the shift from oxidative phosphorylation toward fermentation and tumor development. This conclusion was drawn from immuno staining of mammary gland tissue before and after tumor development from MMTV-NeuNT mice, and western blot/immuno staining experiments with human cancer cell lines of different origin (A549 and H1299 derive from lung carcinomas, 293T is a transformed embryonic kidney cell line, the HeLa cell line derives from a cervical carcinoma and MCF10a is an immortalized epithelial breast cell line) compared to unaffected mouse

muscle lysate [119]. A single band for PKM1 was obtained from mouse muscle lysate, and a band for PKM2, exclusively, from all shown cancer cell lines. It should, however, be considered that semiquantitative blotting and the use of antibodies comprise drawbacks that might lead to misinterpretations. Antibodies differ in affinity to their target proteins. Thus, similar bands derived from different antibodies do not necessarily indicate similar concentrations of the stained target proteins. Additionally, protein expression strongly depends on the type of tissue [119, 178], and earlier studies reported that PKM2 is also expressed in several healthy tissues [116]. Because of the methodic drawbacks of western blot/immuno staining and the choice of a non-tissue matched control by Christofk *et al.* 2008 [119], PKM1 and PKM2 expression needed to be re-investigated in malignant tissues and cell lines and corresponding healthy controls.

We decided for absolute quantification (AQUA) by mass spectrometry with isotope labeled standards to circumvent the possible drawbacks of the use of antibodies in semiquantitive western blotting [179, 180]. The AQUA strategy involves the spiking of chemically synthesized heavy-isotope labeled peptides (AQUA peptides) to the samples and thereby facilitates absolute quantification of non-purified proteins at physiological concentrations [181]. AQUA peptides are individually designed standards that match the proteolytic peptides of interest in sequence but differ in mass to the analytes [179, 180, 182]. We chose three different AQUA peptides: one peptide specific for PKM1, one for PKM2 and one peptide specific for both isoforms. Measurements were performed on a hybrid ion trap/triple quadrupole mass spectrometer operating in multiple reaction monitoring (MRM) mode. Transgenic yeast deleted for endogenous yeast PYK paralogues and expressing exclusively either human PKM1 or PKM2 was used to verify the sustainability of the chosen protein specific tryptic peptides. The peptide specific for both PKM1 and 2 could be detected in yeast expressing either PKM isoform, whereas the PKM1 and PKM2 specific peptides could be detected only in the corresponding yeast strain - specific discrimination between the different isoforms was therefore granted (Fig. 1A). To investigate PKM1 and PKM2 expression in healthy and carcinogenic human tissue and cell lines we analyzed 25 malignant cancers, 18 tissue-matched controls, 12 cancer cell lines, 4 non-cancer cell lines and 6 benign oncocytomas. In 15 cases (12 malignant cancers, 2 benign tumors and 1 cell line) affected samples and unaffected matched controls were available from the same individual.

PKM2 was the predominant PKM isoform in all analyzed cancer cell lines, which also included cell lines examined by Christofk *et al.* 2008 [119] (MCF10a, HeLa, A549 and a HEK cell line HEK293). Our data were in agreement with those obtained in western blots by Christofk *et al*. 2008 [119] as far as that PKM2 was the major isoform as its expression varied between 95.8% and 99.0% of total PKM. However, the LC-MRM technology proved to be more sensitive than western blot/immuno staining. Although present in the lower femtomol range, we could also clearly detect PKM1 in the analyzed cell lines (table 1). Furthermore, PKM2 accounted for a minimum of 94% of total PKM in all malignant cancers and further cell lines included in this study. Thus, transformed cells did not exclusively express PKM2 as up to 6% of total PKM accounted for PKM1.

Remarkably, PKM2 turned out to be also the predominant isoform in matched control tissues, cell lines and slowly proliferating tumors (oncocytomas). In healthy kidney, lung, liver and thyroid tissue PKM2 accounted for at least 93% of total PKM, for 79.8%-96.2% of PKM in colon and for 54.7%-60.6% of PKM in bladder. Also, the slowly proliferating oncocytomas contained 94.1%-98.9% PKM2 of total PKM. Hence, it can be concluded that there is no switch in PKM isoform expression during tumorigenesis or in rapidly proliferating cells as suggested by Christofk *et al*. 2008 [119]. Bladder was the only analyzed healthy tissue that showed a lower relative PKM2 expression level (54.7% PKM2 of total PKM) than the corresponding malignant sample (97.1% PKM2 of total PKM). However, the difference resulted mainly from PKM2 up-regulation in the tumor tissue (20.8 fmol in the healthy control and 181.9 fmol in the cancer) rather than from a switch in isoforms. Bladder tissue might inherently express PKM1 as the major spliceform as it consists of smooth muscle. It had been reported before that PKM1 is the dominating PKM isoform in muscle tissue [116].

In general, total PKM (PKM1+PKM2) expression was increased in malignant tissues and cancer cell lines compared to the corresponding unaffected controls. We detected a three-fold up-regulation in transformed samples, but PKM1 and PKM2 were equally affected (an increase of 3.1 fold of PKM1 and of 3.1 fold of PKM2). The total PKM amount strongly varied between different tissues (e.g. 16.0-25.2 fmol/µg protein in healthy lung tissue and 70.8-72.9 fmol/µg protein in unaffected colon tissue). This underlines the importance of tissue-matched controls in the comparison of PKM1 and PKM2 expression levels between cancer and healthy cells, and proofs that Christofk *et al*. 2008 [119] did not use the appropriate controls in their western blot experiments.

Nevertheless, an up-regulation of overall PKM matches the reported high glycolytic activity of tumor cells [119]. Although of lower specific activity compared to PKM1 [171], PKM2 is probably responsible for most of the overall PKM activity as it is expressed at higher level. Thus, an exchange of PKM2 to PKM1 at its endogenous level would mean an overall PKM activity reduction; whereas the observed PKM up-regulation would result in an increase of total PKM activity. Along this line of thought, it would be conceivable that some tumors possess higher PKM activity than their untransformed counterparts.

Quantitative analysis of PKM1 and PKM2 in different transformed samples and unaffected controls demonstrated that tumor development is not associated with a switch in PKM spliceforms. Thus, PKM2 is not specific for rapidly proliferating or tumor cells. We conclude that the main determinant for PKM2 and PKM1 expression levels is the type of tissue, rather than the state of proliferation. Therefore, our data challenge the postulation of a switch in PKM isoforms during tumor development stated by Christofk *et al.* 2008 [119], and suggest reassessing of experimental results and conclusions based on this assumption.

The new results presented by Bluemlein *et al.* 2011 show that the current model of glycolysis regulation during tumorigenesis has to be revisited, but it does not exclude that PKM activity regulation may rely on posttranslational modifications. The PKM2 enzyme species inherits pre-conditions for tuning of its activity. Upon allosteric binding of FBP, PKM2 can change from a low-active dimeric to a higher-active tetrameric state. Furthermore, different variants in the electrophoretic shift of PKM2 point to posttranslational modified versions of the enzyme [183], and phosphorylation was shown to tune PKM2 activity in cancer [122]. In summary, dynamic tuning of PKM activity as well as the overall PKM expression level seem to be more important for the adjustment of metabolic cellular demands during proliferation than an exchange of PKM isoforms.

***Dynamic PPP Activation is Essential for Accurate Timing of the Cellular Anti-Oxidative Stress Response*** (Krüger et al. 2011)

Dynamic metabolic rearrangements are fundamental mechanisms in cellular self-adaptation to changing conditions and environmental perturbations, such as oxidative stress [18, 92]. Responses to an imbalance in the cellular redox-state can be split into two categories: i) acute reactions, which maintain the cell's survival under

sudden oxidative stress situations, and ii) balancing processes, which continuously keep naturally occurring levels of oxidants in the physiological range [19]. Although many biochemical details of anti-oxidative defense and repair mechanisms are well understood, there is sparse knowledge about the transducers and cellular redox-sensors which monitor the redox-state, and induce and control defense and balancer systems. Changing conditions often affect the metabolic network at first [2]. The fact that the metabolome is closely interconnected with the transcriptome and proteome [2, 184] suggests that redox-sensors might have evolved around metabolic reactions or pathways that underly variations in turn-over upon oxidative stress situations.

The PPP is a major target for regulation under oxidative conditions. Earlier studies showed an up-regulation of this pathway on the transcript, protein, enzyme-activity and metabolic levels when cells were exposed to an oxidant [18, 85, 90, 95]. Contact with oxidants (e.g. $H_2O_2$) leads to inactivation of at least one glycolytic enzyme, GAPDH, and to a redirection of the glycolytic flux into the PPP and thereby to an increase in the concentration of PPP metabolites [18]. The speed at which an elevation in PPP metabolite content occurs (within seconds) is of unique importance in the cellular oxidant-defense reaction as it grants the cell's survival in an acute oxidative stress situation [92]. This is due to irreversible enzymatic reactions of the OPPP, which reduce two molecules $NADP^+$ to NADPH for every metabolized glucose molecule. Thus, the elevated release of NADPH, by the above described immediate metabolic transition, provides anti-oxidative defense mechanisms with adequate amounts of their redox cofactor NADPH [22, 23]. In contrast, the reversible reactions of the NOPPP operate independently of the cofactors NAD(H) or NADP(H), and an active participation of the NOPPP in cellular antioxidative response mechanisms had not been reported until recently. However, LC-MRM measurements revealed that metabolites of the NOPPP accumulate under oxidative stress [18, 92], and that distortion of several NOPPP reactions impairs the cell's tolerance to oxidants [163, 185]. Thus, we questioned whether the PPP's role in the cellular reaction to oxidants goes beyond providing NADPH.

In order to investigate this hypothesis, we generated a yeast strain deleted for the first rate-limiting enzyme of the OPPP (Zwf1p) and for the NOPPP enzyme transaldolase 1 (Tal1p). Therefore, this double mutant strain (*Δzwf1Δtal1*) was incapable of $NADP^+$ reduction through the OPPP, and had impaired flux through the NOPPP. It

had been reported before that deletion of Zwf1 causes hypersensitivity to various oxidants in different organisms, including yeast [175, 185]. Those results could be confirmed by our studies which showed that the two single mutants exhibited sensitivity toward $H_2O_2$ (*Δzwf1* and *Δtal1*, Fig. 1b). Remarkably, the double mutant (*Δzwf1Δtal1*) exhibited an even more pronounced sensitivity to $H_2O_2$ than the single mutants. Furthermore, we increased influx to the NOPPP by transgenic expression of sedoheptulokinase (SHPK). SHPK is a mammalian enzyme and, therefore, normally not present in yeast. It converts the non-PPP sugar sedoheptulose into the PPP-metabolite sedoheptulose 7-phosphate, and thus increases NOPPP metabolite load. This SHPK-expressing yeast showed a higher resistance to $H_2O_2$ than wild-type cells (Fig. 1C). Thus, the decreased tolerance toward $H_2O_2$ in a yeast strain with disturbed NOPPP which cannot utilize the PPP for $NADP^+$ reduction and the increased tolerance toward $H_2O_2$ achieved by an influx to the NOPPP, indicate that the NOPPP, beside the OPPP, might also play an important role in the anti-oxidative machinery of the cell.

To investigate the influence of different oxidants on the phenotype and also to address the question whether deletions of OPPP and NOPPP enzymes cause divergent or similar redox phenotypes, we spotted various yeast strains deleted for enzymes of the OPPP and NOPPP onto media containing different oxidants. Indeed, each PPP deletion mutant exhibited a specific phenotype to the oxidants applied. For example, *Δtal1* cells were sensitive to $H_2O_2$, but resistant to diamide; whereas *Δsol4* cells were resistant to $H_2O_2$ and cumene hydroperoxide (CHP), and sensitive to diamide. These phenotypes were observable irrespectively whether the enzyme was deleted from the OPPP or NOPPP. In summary, these results gave strong reason to postulate a NADP(H)-independent role of the PPP in the cellular response to oxidants.

In yeast, PPP metabolites elevate in content within seconds [92], whereas the first transcriptional changes can be observed not until ~2-3 min after exposure to an oxidizing stressor. All gene expression changes which follow show a strict time-course in occurrence characteristic for stress induced mRNAs [6]. Since fast rising of PPP intermediates precedes transcriptional adaptation, we questioned whether PPP activation is connected to the induction and timing of the transcriptional control machinery during the oxidative-stress response. As shown in previous studies, deletion of endogenous *TPI1* and expression of the mutant $TPI_{Ile170Val}$ allele causes a TPI activity reduction to ~30% of the wild-type activity level, and thus a constitutive redirection of the glycolytic

flux into the PPP [186]. It was demonstrated that the $TPI_{Ile170Val}$ expressing strain contains elevated PPP intermediate levels, an increased NADPH/$NADP^+$ ratio and shows increased resistance to oxidants [18, 145]. In order to elucidate transcriptional changes that entail the metabolic shift (glycolysis/PPP), we compared the transcriptome profiles of $H_2O_2$ treated wild-type cells with $TPI_{Ile170Val}$ expressing cells. Therefore, we isolated mRNA, transcribed these into cDNA and generated global mRNA expression profiles by quantitative shotgun sequencing on a Genome Analyzer II (Illumina). By massive parallel sequencing, the RNA-Seq expression profiles provide information about the whole set of transcripts expressed in a cell in a qualitative and quantitative way [187]. Remarkably, we could detect a ~40% overlap of regulated target genes in the cells with constitutive PPP activation ($TPI_{Ile170Val}$ expressing strain) and $H_2O_2$ treated wild-type strain.

Exposure to $H_2O_2$ causes an oxidizing environment, whereupon constitutive activation of the PPP the NADPH/$NADP^+$ ratio is shifted towards reducing molecules. This raises the question whether an overlap of transcriptional changes could be attributable to redox balancing processes. Indeed, 60 of 140 transcripts were regulated according to the redox-state – in the wild-type strain they were down-regulated upon $H_2O_2$ treatment and up-regulated in the $TPI_{Ile170Val}$ expressing strain or *vice versa*. However, the larger fraction (80 of 140 transcripts) was changed in the same direction and therefore in line with the metabolic transition. Examination of these transcripts in oxidant-untreated PPP deletion strains (Δ*tal1*, Δ*tkl1*, Δ*zwf1*) demonstrated their dependence on regulation of the PPP. Comparison of the $TPI_{Ile170Val}/H_2O_2$ and PPP deletion mutant transcriptome profiles revealed a substantial overlap of target transcripts; e.g., 92% of transcripts that correlate with the metabolic shift were affected in at least two PPP deletion mutant strains. Gene ontology (GO) comparison of the transcripts regulated upon the metabolic shift unveiled components involved or dependent on energy metabolism to be enriched. Two predominant GO categories comprised genes related to chromatin assembly and disassembly (e.g. transcripts *HHT1* and *HHO1*) and genes that are part of the cellular respiratory chain (e.g. transcript *COX1*). Smaller gene subsets pointed to involvement of the PPP in regulation of protein biogenesis. Interestingly, analyzing of GO terms which correlated with the redox-state revealed also factors of protein biosynthesis to be enriched. However, transcripts that responded to the metabolic shift included factors of early processes like assembly and

biosynthesis of ribosomes, whereas transcripts correlating with the redox-state related to successive mechanisms like translation (Fig. 3d).

The induction of initial components of protein biosynthesis, which are followed by processes of other regulatory origin, indicates a role of the PPP in the coordination of early events in the stress response. To pursue this hypothesis, qRT-PCR experiments and targeted proteomics by MRM measurements were performed for wild-type, *Δtal1*, *Δtkl1* and *Δzwf1* cells in time courses after $H_2O_2$ treatment. PPP deletion mutants exhibited delayed and disturbed time-courses in the expression of chromatin components, enzymatic subunits of the respiratory chain and transcripts related to ribosome biogenesis and translation. Therefore, PPP integrity and activation upon an oxidative burst is required for correct timing and regulation of the transcriptional stress response.

Currently, the best understood redox-sensors that modulate the cellular transcriptional program upon an oxidative burst are redox sensitive transcription factors. Those transcription factors (e.g., the AP-1-like transcription factor *YAP1* [188]) contain regulatory cysteines whose thiol-groups can be oxidized - either directly or indirectly *via* transfer of redox-equivalents by an interaction partner such as glutathione peroxidase 3 (Gpx3). Transcriptionfactor oxidation induces transcription of anti-oxidant enzymes [188-190]. However, this system does not explain transcriptional changes upon PPP activation in strains that did not experience an oxidative stress situation (e.g. $TPI_{Ile170Val}$ expressing strain). In wild-type cells transcriptional changes occurred early after the oxidative treatment (~2 min). This matches the time-course of the metabolic shift whose amplitude can be observed ~1 min after the oxidative burst [92]. However, transcriptional changes in PPP deficient mutants reached its amplitudes much later (~15 min). Thus, the metabolic transition probably fulfills a functional role in the early response and other mechanisms follow in the time-course of the response to oxidative perturbations. In accord with this assumption are regulated genes whose promoters contain binding sites for redox sensitive transcription factors. The metabolic transition and the activation of oxidative-responsive transcription factors presumably work with different kinetics, but complement and overlap.

Possibly, one or various PPP intermediates act as reporter metabolites and bind to stress-responsive mediators which regulate transcription. So-called reporter metabolites are small molecules whose concentration changes are entailed by

transcriptional changes. Their existence has been reported for glycolysis, but reporter metabolites are not yet known for the PPP [2]. Perhaps, PPP enzymes or metabolites modulate the binding affinity of transcription factors. A strong correlation between transcription factor binding affinity and timing of transcriptional events has been reported before [98].

Posttranslational modifications or protein-protein interactions of PPP enzymes with components of signaling cascades are other possibilities that might be initiated by a PPP enzyme. An example for an interaction of a metabolic enzyme with a regulatory protein has been reported for GAPDH. Under high glycolytic flux, the level of the GAPDH substrate glyceraldehyde 3-phosphate rises. This causes release of the GTPase Rheb from GAPDH. Then, Rheb acts as activator for the mTOR complex 1 which takes part in signaling cascades, e.g., those involved in cell growth and proliferation [191].

Main transcriptional targets of the metabolic shift (glycolysis/PPP) were processes involved or directly connected to energy metabolism, such as ribosome biogenesis, subunits of the respiratory chain and chromatin components. Regulation of those factors could have impact on stress signaling. Chromatin rearrangements are important parts of the cellular response to energy shortage. Histone modifications are under direct influence of central carbohydrate metabolism [192]. As reported before, the NADH concentration has a strong impact on histone modifications such as catalyzed by HDACs [30]. Thus, chromatin structure reacts to and changes under metabolic variations and stress [193]. For instance, heat stress causes domain-wide displacements of histones which facilitates transcription of heat shock genes independent of the yeast nucleosome remodeling complex Swi/Snf [194]. Such processes might also play roles under oxidative stress. Hence, the PPP plays a crucial role in transmitting information of oxidative threat to the transcriptional adaptation program of the cell and, thus, takes a central position in the cellular regulome.

***A Rare Combination of Mutations in the PPP Enzyme RPI Causes Severe Physiological Disorders in a Single Diagnosed Patient*** (Wamelink *et al.* 2010)

Pathways of central carbohydrate metabolism, such as the PPP, take pivotal positions in the metabolic network. Thus, dysfunctions of enzymes of these pathways can lead to disturbance of the whole metabolic network and cellular homeostasis. In humans, inheritable defects of metabolic enzymes can cause severe physiological disorders. Although mutations in the mammalian genome occur non-directed and at a

frequency of ~$10^{-6}$ per locus and gamete [141], numerous deficiencies of carbohydrates metabolizing enzymes are diagnosed far less frequently or never [140] – pointing to lethality of homozygous classic null alleles. Frameshift mutations, which often lead to total loss of protein expression or activity, can occur all along the coding sequence [142]. However, point mutations of specific bases, which modulate or partially retain an enzyme's expression or activity, occur far less frequently.

There are three PPP enzymopathies reported that are associated with clinical symptoms. With more than ~400 million diagnosed cases worldwide, Glucose 6-phosphate dehydrogenase (G6PD)-deficiency is the most common human enzymopathy [139]. Transaldolase deficiency has been reported to be present in few unrelated families of Turkish, Arabian, Pakistani, and Polish origin [195, 196]. However, the third PPP enzymopathy, ribose 5-phospahte isomerase (RPI)-deficiency, appears to be exceptionally rare. Since description of RPI-deficiency in 1999 [150] and 2004 [151], only a single patient, born in 1984, was diagnosed to suffer from that disease.

Via magnetic resonance imaging, the patient was diagnosed for brain white matter disease (leukoencephalopathy) with peripheral neuropathy, resulting in epilepsy, progressive deterioration in vision, speech clarity, seizure control and intellectual abilities. When he was fourteen, a neuropsychological test (Snijders-Oomen non-verbal intelligence test [197]) disclosed a developmental age of 2.6-4.8 years. Hope for improvement of the patient's condition was lost by that time [150].

RPI is an enzyme of the NOPPP that interconverts ribulose 5-phosphate and ribose 5-phosphate. The patient was diagnosed for altered levels of the PPP metabolites ribulose 5-phosphate/xylulose 5-phosphate and ribose 5-phosphate. Also, elevated levels of the polyols D-arabitol, xylitol and ribitol were detected in brain and body fluids [150, 151], and could function as RPI-deficiency biomarkers.

Sequencing of the RPI gene cDNA revealed two heterozygous mutations. One allele carries a frameshift mutation resulting in premature translation termination at codon 180 (c.540delG), and the other allele carries a missense mutation (c.182-C > T) that leads to the exchange of an alanine for a valine residue at position 61 [151]. However, classic total loss of enzyme activity, which could also occur due to frameshift mutations everywhere in the RPI coding sequence, would lead to more than only one diagnosed case of RPI deficiency. Extensive laboratory work-up of the basic molecular defect seemed necessary in order to give certainty about the cause for the patient's suffering. Additionally, elucidating the anomaly that makes RPI-deficiency occur less

frequently than the natural mutation frequency would predict was interesting from the scientific point of view. In Wamelink *et al.* 2010, we describe a detailed analysis of the molecular etiology of RPI-deficiency.

We started with the examination of two patient derived cell lines – lymphoblasts and fibroblasts – with focus on basic features resulting from the RPI mutations: mRNA expression, protein concentration and enzyme activity. Western Blot experiments revealed a reduced enzyme amount in patient lympho- and fibroblasts compared to healthy controls (Fig. 1A). The truncated version of the enzyme, encoded by the frameshift allele, was not detectable. Presumably, it is not expressed or rapidly degraded. The western blot experiments were confirmed by MRM measurements on a QTRAP5500 (AB/Sciex) mass spectrometer, and demonstrated a decrease of RPI protein content to ~30% of wild-type level in patient lymphoblasts (Fig. 1B). Furthermore, qRT-PCR experiments demonstrated a strongly reduced RPI mRNA expression level in patient cells. Interestingly, there was a large difference in RPI mRNA expression levels between both patient derived cell lines. Patient lymphoblasts contained ~40% of RPI mRNA compared to healthy control cells; patient fibroblasts contained even only ~1% (Fig. 1C). Due to the frameshift mutation on one allele, a 50% RPI mRNA expression reduction would be expected. However, an even lower mRNA content pointed to a decline in RPI expression compared to wild-type also from the second allele. Consistent with these results were data derived from subsequent enzyme-coupled enzyme activity assays. Patient lymphoblasts possessed ~30% residual RPI activity compared to healthy control cells, whereas in patient fibroblasts, RPI activity was below the assay's detection limit (Fig. 1D). It was still possible that RPI enzyme amount and activity varied between different fibroblast cell lines. Nevertheless, this assumption could be ruled out by control enzyme activity assays that demonstrated similar RPI activities in four different unaffected fibroblast cell lines. In summary, these results confirmed that the patient does not suffer from a total lack of RPI activity. Expression of a certain amount of functional $RPI_{Ala61Val}$ enzyme is strongly cell type dependent. Different RPI expression levels in different cell types could be an explanation for the severe neuronal defects of the RPI patient. Perhaps, the CNS consists of a higher percentage of cells expressing RPI at a lower level than other organs. Due to the lack of biopsy material, this issue could not be analyzed in experiment.

From the cell culture system, we could not distinguish whether reduced overall RPI activity was due to the lower expression level of the enzyme or the Ala61Val missense allele. For this reason, a transgenic yeast model was generated and used for a comparison of the physiological effects of low-level RPI expression and the amino acid exchange. Deletion of the endogenous yeast RPI orthologue *RKI* is lethal. However, transformation of centromeric plasmids expressing either human wild-type RPI or human $RPI_{Ala61Val}$ rescues yeast growth. This was proven in plasmid shuffle experiments in order to validate the suitability of the yeast model for studying RPI deficiency (Fig. 2A).

The $RPI_{Ala61Val}$ expressing *Δrki* strain exhibited RPI activity which was reduced to ~30% of wild-type level (Fig. 2C). Thus, the amino acid exchange Ala61Val led to reduced specific RPI activity and was comparable to the overall RPI activity detected in patient lymphoblasts. To examine the metabolic consequences of varying RPI expression levels, the human RPI wild-type gene was cloned into centromeric plasmids either harboring a strong (*GPD1*) or a weak (*CYC1*) promoter. When RPI was expressed under control of the weak *CYC1* promoter, its overall activity was ~18% compared to RPI activity detected in cells expressing RPI under control of the *GPD1* promotor (Fig. 2C). In order to examine the impact of the Ala61Val mutation and low-level RPI expression on yeast's physiology, their growth in liquid cultures was monitored spectroscopically. As long as human $RPI_{Ala61Val}$ was expressed at high level, residual activity was sufficient to allow growth similar to yeast expressing human wild-type RPI. However, expression of human wild-type RPI placed under control of a weak promoter led to much slower growth (Fig. 2D). These results demonstrated that the $RPI_{Ala61Val}$ allele complements for the loss of yeast Rki1p to an extent that enabled normal growth, and that low expression of human wild-type RPI did not fully compensate for the loss of the essential yeast enzyme. Thus we conclude that the extremely low RPI activity in patient fibroblasts is largely attributable to the expression defect of the RPI allele.

In summary, we could show that the $RPI_{Ala61Val}$ allele has two defects. The Ala61Val point mutation results in reduction of RPI specific activity, and also causes cell type dependent mRNA expression deficits. The mechanism that is causative for the mRNA expression defect has to be investigated in future studies. The C → T exchange is located in the first codon of exon three, and thus close to the spliceacceptor site. Therefore, the mutation could affect the maturation of RPI mRNA. Alternatively, the

amino acid residue exchange could destroy or generate a binding site for a yet unknown transcription regulator.

As mentioned above, the RPI patient shows a clear metabolic pattern. Nevertheless, secondary effects besides the RPI defect leading to the metabolic phenotype could not be excluded due to the fact that no comparable cases have been diagnosed up to date. The yeast model allowed metabolite measurements by LC-MRM which could confirm the metabolic profile typical for RPI deficiency. Measurements of PPP metabolites and polyols in the described transgenic yeast strains demonstrated that the changes in metabolite concentrations also occur in the yeast model and are therefore indeed attributable to reduced RPI activity (Fig. 3A and B). Confirmation of polyols as suitable biomarkers for RPI-deficiency could facilitate diagnosis of further cases in the future. The strain expressing wild-type RPI at low level displayed an even stronger metabolic phenotype than the strain expressing $RPI_{Ala61Val}$, and therefore underlined again the importance of a normal RPI expression level for integrity of the cell's metabolism.

In conclusion, we could demonstrate low-level expression of RPI in combination with an enzyme activity reducing missense mutation as RPI deficiency etiology, and that the extent of RPI activity reduction is cell type dependent. As there are no homozygous RPI patients, and since Rki1 knock-out is lethal for yeast, we speculate that total loss of RPI enzyme activity is not accordable with life in humans. Rather the compound heterozygous combination of mutated RPI alleles is reason for the extremely rare incidence of the disease.

## Summary

The metabolic network responds rapidly to changing conditions in order to self-adapt and ensure cellular survival. Metabolic modules such as pathways of carbohydrate metabolism can gain activity when required by varying demands. In Grüning *et al*. 2011 we demonstrated a metabolic feedback loop that synchronizes energy- and redox-metabolism in respiring yeast cells. The activity of the glycolytic enzyme PYK plays a crucial role in the regulation of mitochondrial respiration and simultaneous PPP activation. Coordinated activation of both processes protects yeast cells from oxidative damage by ROS produced through the respiratory chain. However, the question for the connecting mechanism between low PYK activity and elevated mitochondrial respiration is still unanswered. Also, elucidating the sources that fuel mitochondria when PYK activity is low will be subject of continuative projects. In cancer cells, an isoform switch of pyruvate kinase (PKM1 and PKM2) was stated to be causative for increased fermentation and lowered respiration - the tumor-typical Warburg effect. In Bluemlein *et al*. 2011 we could refute this postulation. The comprehensive LC-MRM dataset did not confirm an exchange in PKM isoforms, but an upregulation of PKM1 and PKM2 in human malignant cells. These data point to importance of the total PKM expression level for cancer cell metabolism. Future studies have to elucidate the mechanisms that require PKM upregulation in proliferating cells, and therefore provide an advantage for growing cells. Metabolic rearrangements such as caused by varying PYK activities or oxidative stress lead to wide-ranging effects on the whole cellular reaction network. In Krüger *et al*. 2011, regulatory importance of PPP activation in timing of the transcriptional oxidative-stress program could be proven. Therefore, the PPP does not only provide the cell with NADPH as immediate reaction to counter-act the oxidative stress situation, fast changes in PPP metabolite levels also function as mediator for the stress signal to regulatory components of the transcriptional machinery which follow in time. The sensors that are stimulated by changes in line with PPP activation are still to be found. Disruptions in central pathways of the metabolic network can lead to severe physiological dysfunctions in humans. Deficiency of the PPP enzyme RPI was reported as the rarest inheritable human disease to date. In Wamelink *et al*. 2010 we revealed the molecular RPI-deficiency pathogenesis, to our knowledge, with a single diagnosed patient, the rarest disease on earth. A combination of two mutations that cause cell-type dependent reduced RPI expression levels and decreased

specific RPI activity lead to the manifestation of RPI-deficiency symptoms. Finally, investigating metabolic transitions gives insight into fundamental biological organizational principles that mostly affect not only the metabolome, but also other hierarchical layers such as the transcriptome and proteome. Regarding the cell as complex reaction network, that dynamically reacts to changing conditions, has always to be considered in tackling biological questions.

## Zusammenfassung

Das metabolische Netzwerk reagiert schnell auf sich ändernde Bedingungen, um sich an die neuen Umstände anzupassen und so das Überleben der Zelle zu ermöglichen. Metabolische Module, wie Stoffwechselwege des zentralen Kohlenhydratstoffwechsels, können an Aktivität gewinnen, wenn dies durch die sich ändernden Bedingungen erforderlich ist. In dem Manuskript Grüning *et al.* 2011 zeigen wir einen metabolischen feedback-loop in atmenden Hefezellen, der den Energie- mit dem Redox-Stoffwechsel koordiniert. Das glykolytische Enzym Pyruvatkinase (PYK) spielt eine entscheidende Rolle in der Regulierung der mitochondrialen Atmung und der zeitgleichen Aktivierung des Pentosephosphat Weges (PPP). Durch die mitochondriale Atmungskette kommt es zu einer erhöhten Produktion freier Sauerstoffradikale (ROS). Die koordiniert Aktivierung von Zellatmung und PPP schütz Hefezellen jedoch vor Schäden, die durch ROS verursacht werden können. Allerdings konnte bislang nicht geklärt werden, wie ein Wechsel in der PYK Aktivität die mitochondriale Atmung reguliert. Außerdem wird die Frage nach den Nährstoffen, die eine erhöhte mitochondriale Atmung bei geringer PYK Aktivität ermöglichen, Gegenstand zukünftiger Arbeit sein. In Krebszellen wurde ein Wechsel von Pyruvatkinase Isoformen (PKM1 und PKM2) als ursächlich für den Tumor-typischen Warburg Effekt, eine Reduzierung der Zellatmung und Erhöhung der Fermentation, erklärt. In dem Manuskript Bluemlein *et al*. 2011 konnten wir diese Behauptung widerlegen. Ein umfassender Datensatz, der mittels LC-MRM erstellt wurde, konnte keinen Austausch beider Isoformen während der Tumorigenese bestätigen. Vielmehr kommt es, im Vergleich zu gesunden Kontrollen, zu einer Hochregulierung beider Isoformen in Tumorzellen. Diese Daten verweisen auf eine entscheidende Rolle des PKM Expressionslevels im Krebsstoffwechsel. In zukünftigen Studien soll geklärt werden, welche zellulären Mechanismen eine PKM Hochregulierung erfordern und dadurch Krebszellen einen Proliferationsvorteil verschaffen. Metabolische Verschiebungen, wie sie z.B. durch eine Veränderung der PYK Aktivität oder oxidativen Stress verursacht werden, haben weitreichende Konsequenzen für das gesamte zelluläre Reaktionsnetzwerk. In Krüger *et al.* 2011 konnten wir die regulatorische Bedeutung der PPP Aktivität für das anti-oxidative transkriptionelle Stressprogramm der Zelle beweisen. Es konnte gezeigt werden, dass der PPP nicht nur NADPH bereitstellt, um sofort auf die oxidative Stresssituation zu reagieren - die schnellen Änderungen der PPP-Metabolitkonzentrationen fungieren auch

als Signale für regulatorische Komponenten der Transkriptionsmaschinerie, welche für die längerfristige Anpassung an oxidativen Stress benötigt wird. Die Sensoren, die durch eine erhöhte PPP Aktivität aktiviert werden, bleiben Fokus zukünftiger Forschung. Störungen des zentralen Kohlenhydratstoffwechsels können zu schweren physiologischen Beeinträchtigungen im Menschen führen. Die Defizienz des PPP Enzyms RPI gilt bislang, mit einem diagnostizierten Patienten, als die seltenste Erbkrankheit. In Wamelink *et al.* 2010 konnten wir die Ätiologie dieser Krankheit entschlüsseln. Die Manifestierung der RPI-Defizienz Symptome basiert auf der Kombination zweier Mutationen, die zu einer Zelltyp-spezifischen Reduzierung des Expressionslevels und zu einer Reduzierung der spezifischen Enzymaktivität führen. Abschließend lässt sich sagen, dass die Untersuchung metabolischer Verschiebungen Einblicke in fundamentale biologische organisatorische Prinzipien bietet. Diese Verschiebungen betreffen dabei nicht nur das Metabolom, sondern ebenfalls andere hierarchische Ebenen der Zelle wie das Transkriptom oder Proteom. Bei der Untersuchung biologischer Fragestellungen sollte daher die Zelle stets als komplexes Reaktionsnetzwerk, welches sich dynamisch an ändernde Bedingungen anpasst, betrachtet werden.

# Bibliography


1. **Caetano-Anollés, G., et al.,** ***The origin and evolution of modern metabolism.*** **The International Journal of Biochemistry & Cell Biology, 2009. 41(2): p. 285-297.**

2. **Gruning, N.M., H. Lehrach, and M. Ralser,** ***Regulatory crosstalk of the metabolic network.*** **Trends Biochem Sci, 2010. 35(4): p. 220-7.**

3. **Wilson, D.F., M. Erecinska, and P.L. Dutton,** ***Thermodynamic relationships in mitochondrial oxidative phosphorylation.*** **Annu Rev Biophys Bioeng, 1974. 3(0): p. 203-30.**

4. **Soh, K.C. and V. Hatzimanikatis,** ***Network thermodynamics in the post-genomic era.*** **Curr Opin Microbiol, 2010. 13(3): p. 350-7.**

5. **Berg, J.M., J.L. Tymoczko, and L. Stryer,** ***Stryer Biochemie*****. 6 ed. 2007, München: Elsevier GmbH.**

6. **Chechik, G., et al.,** ***Activity motifs reveal principles of timing in transcriptional control of the yeast metabolic network.*** **Nat Biotechnol, 2008. 26(11): p. 1251-9.**

7. **Romano, A.H. and T. Conway,** ***Evolution of carbohydrate metabolic pathways.*** **Res Microbiol, 1996. 147(6-7): p. 448-55.**

8. **Ng, T.K., A. Ben-Bassat, and J.G. Zeikus,** ***Ethanol Production by Thermophilic Bacteria: Fermentation of Cellulosic Substrates by Cocultures of Clostridium thermocellum and Clostridium thermohydrosulfuricum.*** **Appl Environ Microbiol, 1981. 41(6): p. 1337-43.**

9. **Mitchell, P. and J. Moyle,** ***Chemiosmotic hypothesis of oxidative phosphorylation.*** **Nature, 1967. 213(5072): p. 137-9.**

10. **Luttik, M.A., et al.,** ***The Saccharomyces cerevisiae NDE1 and NDE2 genes encode separate mitochondrial NADH dehydrogenases catalyzing the oxidation of cytosolic NADH.*** **J Biol Chem, 1998. 273(38): p. 24529-34.**

11. **Dimroth, P., G. Kaim, and U. Matthey,** ***Crucial role of the membrane potential for ATP synthesis by F(1)F(o) ATP synthases.*** **J Exp Biol, 2000. 203(Pt 1): p. 51-9.**

12. **Cadenas, E. and K.J. Davies,** ***Mitochondrial free radical generation, oxidative stress, and aging.*** **Free Radic Biol Med, 2000. 29(3-4): p. 222-30.**

13. **Muller, F., *The nature and mechanism of superoxide production by the electron transport chain: Its relevance to aging.* AGE, 2000. 23(4): p. 227-253.**

14. **Herrero, E., et al., *Redox control and oxidative stress in yeast cells.* Biochim Biophys Acta, 2008. 1780(11): p. 1217-35.**

15. **Devasagayam, T.P., et al., *Free radicals and antioxidants in human health: current status and future prospects.* J Assoc Physicians India, 2004. 52: p. 794-804.**

16. **Hensley, K., et al., *Reactive oxygen species, cell signaling, and cell injury.* Free Radic Biol Med, 2000. 28(10): p. 1456-62.**

17. **Gutteridge, J. and B. Halliwell, *Free Radicals in Biology and Medicine*. 1989, Oxford: Clarendon Press.**

18. **Ralser, M., et al., *Dynamic rerouting of the carbohydrate flux is key to counteracting oxidative stress.* J Biol, 2007. 6(4): p. 10.**

19. **Moradas-Ferreira, P., et al., *The molecular defences against reactive oxygen species in yeast.* Mol Microbiol, 1996. 19(4): p. 651-8.**

20. **Wood, Z.A., et al., *Structure, mechanism and regulation of peroxiredoxins.* Trends Biochem Sci, 2003. 28(1): p. 32-40.**

21. **Drakulic, T., et al., *Involvement of oxidative stress response genes in redox homeostasis, the level of reactive oxygen species, and ageing in Saccharomyces cerevisiae.* FEMS Yeast Res, 2005. 5(12): p. 1215-28.**

22. **Ying, W., *NAD+/NADH and NADP+/NADPH in cellular functions and cell death: regulation and biological consequences.* Antioxid Redox Signal, 2008. 10(2): p. 179-206.**

23. **Pollak, N., C. Dolle, and M. Ziegler, *The power to reduce: pyridine nucleotides--small molecules with a multitude of functions.* Biochem J, 2007. 402(2): p. 205-18.**

24. **Koch-Nolte, F., et al., *ADP-ribosylation of membrane proteins: unveiling the secrets of a crucial regulatory mechanism in mammalian cells.* Ann Med, 2006. 38(3): p. 188-99.**

25. **Karras, G.I., et al., *The macro domain is an ADP-ribose binding module.* EMBO J, 2005. 24(11): p. 1911-20.**

**26. Ladurner, A.G., *Inactivating chromosomes: a macro domain that minimizes transcription.* Mol Cell, 2003. 12(1): p. 1-3.**

**27. Ziegler, M., *New functions of a long-known molecule. Emerging roles of NAD in cellular signaling.* Eur J Biochem, 2000. 267(6): p. 1550-64.**

**28. Oei, S.L., et al., *Regulation of RNA polymerase II-dependent transcription by poly(ADP-ribosyl)ation of transcription factors.* J Biol Chem, 1998. 273(48): p. 31644-7.**

**29. Braunstein, M., et al., *Transcriptional silencing in yeast is associated with reduced nucleosome acetylation.* Genes Dev, 1993. 7(4): p. 592-604.**

**30. McGuinness, D., et al., *Sirtuins, bioageing, and cancer.* J Aging Res, 2011. 2011: p. 235754.**

**31. Agledal, L., M. Niere, and M. Ziegler, *The phosphate makes a difference: cellular functions of NADP.* Redox Rep, 2010. 15(1): p. 2-10.**

**32. Zahedi Avval, F. and A. Holmgren, *Molecular Mechanisms of Thioredoxin and Glutaredoxin as Hydrogen Donors for Mammalian S Phase Ribonucleotide Reductase.* J Biol Chem, 2009. 284(13): p. 8233–8240.**

**33. Hayes, J.D., J.U. Flanagan, and I.R. Jowsey, *Glutathione transferases.* Annu Rev Pharmacol Toxicol, 2005. 45: p. 51-88.**

**34. Nauseef, W.M., *Biological roles for the NOX family NADPH oxidases.* J Biol Chem, 2008. 283(25): p. 16961-5.**

**35. Shi, F., et al., *Molecular properties, functions, and potential applications of NAD kinases.* Acta Biochim Biophys Sin (Shanghai), 2009. 41(5): p. 352-61.**

**36. McKenna, M.C., et al., *Neuronal and astrocytic shuttle mechanisms for cytosolic-mitochondrial transfer of reducing equivalents: current evidence and pharmacological tools.* Biochem Pharmacol, 2006. 71(4): p. 399-407.**

**37. Todisco, S., et al., *Identification of the mitochondrial NAD+ transporter in Saccharomyces cerevisiae.* J Biol Chem, 2006. 281(3): p. 1524-31.**

**38. Outten, C.E. and V.C. Culotta, *A novel NADH kinase is the mitochondrial source of NADPH in Saccharomyces cerevisiae.* EMBO J, 2003. 22(9): p. 2015-24.**

**39.** **Strand, M.K., et al.,** ***POS5 gene of Saccharomyces cerevisiae encodes a mitochondrial NADH kinase required for stability of mitochondrial DNA.*** **Eukaryot Cell, 2003. 2(4): p. 809-20.**

**40.** **Kawai, S., et al.,** ***Molecular cloning and identification of UTR1 of a yeast Saccharomyces cerevisiae as a gene encoding an NAD kinase.*** **FEMS Microbiol Lett, 2001. 200(2): p. 181-4.**

**41.** **Shi, F., et al.,** ***Identification of ATP-NADH kinase isozymes and their contribution to supply of NADP(H) in Saccharomyces cerevisiae.*** **FEBS J, 2005. 272(13): p. 3337-49.**

**42.** **Bieganowski, P., et al.,** ***Synthetic lethal and biochemical analyses of NAD and NADH kinases in Saccharomyces cerevisiae establish separation of cellular functions.*** **J Biol Chem, 2006. 281(32): p. 22439-45.**

**43.** **Lerner, F., et al.,** ***Structural and functional characterization of human NAD kinase.*** **Biochem Biophys Res Commun, 2001. 288(1): p. 69-74.**

**44.** **Castegna, A., et al.,** ***Identification and functional characterization of a novel mitochondrial carrier for citrate and oxoglutarate in Saccharomyces cerevisiae.*** **J Biol Chem, 2010. 285(23): p. 17359-70.**

**45.** **Grabowska, D. and A. Chelstowska,** ***The ALD6 gene product is indispensable for providing NADPH in yeast cells lacking glucose-6-phosphate dehydrogenase activity.*** **J Biol Chem, 2003. 278(16): p. 13984-8.**

**46.** **Maeng, O., et al.,** ***Cytosolic NADP(+)-dependent isocitrate dehydrogenase protects macrophages from LPS-induced nitric oxide and reactive oxygen species.*** **Biochem Biophys Res Commun, 2004. 317(2): p. 558-64.**

**47.** **Longo, L., et al.,** ***Maternally transmitted severe glucose 6-phosphate dehydrogenase deficiency is an embryonic lethal.*** **EMBO J, 2002. 21(16): p. 4229-39.**

**48.** **Pandolfi, P.P., et al.,** ***Targeted disruption of the housekeeping gene encoding glucose 6-phosphate dehydrogenase (G6PD): G6PD is dispensable for pentose synthesis but essential for defense against oxidative stress.*** **EMBO J, 1995. 14(21): p. 5209-15.**

**49.** **Kruger, A., et al.,** ***The pentose phosphate pathway is a metabolic redox sensor and regulates transcription during the antioxidant response.*** **Antioxid Redox Signal, 2011. 15(2): p. 311-24.**

**50.** **Ursini, M.V., et al.,** ***Enhanced expression of glucose-6-phosphate dehydrogenase in human cells sustaining oxidative stress.*** **Biochem J, 1997. 323 ( Pt 3): p. 801-6.**

**51.** **Salvemini, F., et al.,** ***Enhanced glutathione levels and oxidoresistance mediated by increased glucose-6-phosphate dehydrogenase expression.*** **J Biol Chem, 1999. 274(5): p. 2750-7.**

**52.** **Frank, J.E.,** ***Diagnosis and management of G6PD deficiency.*** **Am Fam Physician, 2005. 72(7): p. 1277-82.**

**53.** **Daran-Lapujade, P., et al.,** ***The fluxes through glycolytic enzymes in Saccharomyces cerevisiae are predominantly regulated at posttranscriptional levels.*** **Proc Natl Acad Sci U S A, 2007. 104(40): p. 15753-8.**

**54.** **Krishna, S., et al.,** ***Structure and function of negative feedback loops at the interface of genetic and metabolic networks.*** **Nucleic Acids Res, 2006. 34(8): p. 2455-62.**

**55.** **Boiteux, A., A. Goldbeter, and B. Hess,** ***Control of oscillating glycolysis of yeast by stochastic, periodic, and steady source of substrate: a model and experimental study.*** **Proc Natl Acad Sci U S A, 1975. 72(10): p. 3829-33.**

**56.** **Betz, A. and B. Chance,** ***Phase Relationship of Glycolytic Intermediates in Yeast Cells with Oscillatory Metabolic Control.*** **Arch Biochem Biophys, 1965. 109: p. 585-94.**

**57.** **Duysens, L.N. and J. Amesz,** ***Fluorescence spectrophotometry of reduced phosphopyridine nucleotide in intact cells in the near-ultraviolet and visible region.*** **Biochim Biophys Acta, 1957. 24(1): p. 19-26.**

**58.** **Ghosh, A. and B. Chance,** ***Oscillations of glycolytic intermediates in yeast cells.*** **Biochem Biophys Res Commun, 1964. 16(2): p. 174-81.**

**59.** **Das, J. and H.G. Busse,** ***Analysis of the dynamics of relaxation type oscillation in glycolysis of yeast extracts.*** **Biophys J, 1991. 60(2): p. 369-79.**

**60.** **Richard, P.,** ***The rhythm of yeast.*** **FEMS Microbiol Rev, 2003. 27(4): p. 547-57.**

**61.** **Chance, B., et al.,** ***Cyclic and Oscillatory Responses of Metabolic Pathways Involving Chemical Feedback and Their Computer Representations.*** **Ann N Y Acad Sci, 1964. 115: p. 1010-24.**

**62.** **Chance, B., B. Schoener, and S. Elsaesser,** ***Control of the Waveform of Oscillations of the Reduced Pyridine Nucleotide Level in a Cell-Free Extract.*** **Proc Natl Acad Sci U S A, 1964. 52: p. 337-41.**

**63.** **Termonia, Y. and J. Ross,** ***Oscillations and control features in glycolysis: numerical analysis of a comprehensive model.*** **Proc Natl Acad Sci U S A, 1981. 78(5): p. 2952-6.**

**64.** **Hess, B. and A. Boiteux,** ***Mechanism of glycolytic oscillation in yeast. I. Aerobic and anaerobic growth conditions for obtaining glycolytic oscillation.*** **Hoppe Seylers Z Physiol Chem, 1968. 349(11): p. 1567-74.**

**65.** **Sel'kov, E.E.,** ***Stabilization of energy charge, generation of oscillations and multiple steady states in energy metabolism as a result of purely stoichiometric regulation.*** **Eur J Biochem, 1975. 59(1): p. 151-7.**

**66.** **Bier, M., B.M. Bakker, and H.V. Westerhoff,** ***How yeast cells synchronize their glycolytic oscillations: a perturbation analytic treatment.*** **Biophys J, 2000. 78(3): p. 1087-93.**

**67.** **Goldbeter, A. and R. Lefever,** ***Dissipative structures for an allosteric model. Application to glycolytic oscillations.*** **Biophys J, 1972. 12(10): p. 1302-15.**

**68.** **Reijenga, K.A., et al.,** ***Control of glycolytic dynamics by hexose transport in Saccharomyces cerevisiae.*** **Biophys J, 2001. 80(2): p. 626-34.**

**69.** **Reijenga, K.A., et al.,** ***Control analysis for autonomously oscillating biochemical networks.*** **Biophys J, 2002. 82(1 Pt 1): p. 99-108.**

**70.** **Markus, M., D. Kuschmitz, and B. Hess,** ***Chaotic dynamics in yeast glycolysis under periodic substrate input flux.*** **FEBS Lett, 1984. 172(2): p. 235-8.**

**71.** **Goldbeter, A.,** ***Biochemical Oscillations and Cellular Rhythms.*** **1996, Cambridge: Cambridge University Press.**

**72.** **Tu, B.P., et al.,** ***Logic of the yeast metabolic cycle: temporal compartmentalization of cellular processes.*** **Science, 2005. 310(5751): p. 1152-8.**

**73.** **Tu, B.P., et al.,** ***Cyclic changes in metabolic state during the life of a yeast cell.*** **Proc Natl Acad Sci U S A, 2007. 104(43): p. 16886-91.**

**74.** **Wolf, J., et al.,** ***Mathematical analysis of a mechanism for autonomous metabolic oscillations in continuous culture of Saccharomyces cerevisiae.*** **FEBS Lett, 2001. 499(3): p. 230-4.**

**75.** **Mair, T., et al.,** ***Control of glycolytic oscillations by temperature.*** **Biophys J, 2005. 88(1): p. 639-46.**

**76.** **De la Fuente, I.M.,** ***Diversity of temporal self-organized behaviors in a biochemical system.*** **Biosystems, 1999. 50(2): p. 83-97.**

**77.** **Murray, D.B.,** ***On the Temporal Self-Organisation of Saccharomyces cerevisiae.*** **Current Genomics, 2004. 5(8): p. 665-671.**

**78.** **Svatos, A.,** ***Single-cell metabolomics comes of age: new developments in mass spectrometry profiling and imaging.*** **Anal Chem, 2011. 83(13): p. 5037-44.**

**79.** **Sherman, F.,** ***Getting started with yeast.*** **Methods Enzymol, 2002. 350: p. 3-41.**

**80.** **Wolf, J., et al.,** ***Transduction of intracellular and intercellular dynamics in yeast glycolytic oscillations.*** **Biophys J, 2000. 78(3): p. 1145-53.**

**81.** **Westerhoff, H.V., et al.,** ***Elusive control.*** **J Bioenerg Biomembr, 1995. 27(5): p. 491-7.**

**82.** **Westerhoff, H.V., et al.,** ***Thermodynamics of the control of metabolism.*** **Cell Biophys, 1987. 11: p. 239-67.**

**83.** **Ravichandran, V., et al.,** ***S-thiolation of glyceraldehyde-3-phosphate dehydrogenase induced by the phagocytosis-associated respiratory burst in blood monocytes.*** **J Biol Chem, 1994. 269(40): p. 25010-5.**

**84.** **Newman, S.F., et al.,** ***An increase in S-glutathionylated proteins in the Alzheimer's disease inferior parietal lobule, a proteomics approach.*** **J Neurosci Res, 2007. 85(7): p. 1506-14.**

**85.** **Shenton, D. and C.M. Grant,** ***Protein S-thiolation targets glycolysis and protein synthesis in response to oxidative stress in the yeast Saccharomyces cerevisiae.*** **Biochem J, 2003. 374(Pt 2): p. 513-9.**

**86.** **Colussi, C., et al.,** ***H2O2-induced block of glycolysis as an active ADP-ribosylation reaction protecting cells from apoptosis.*** **Faseb J, 2000. 14(14): p. 2266-76.**

**87.** **Chuang, D.M., C. Hough, and V.V. Senatorov,** ***Glyceraldehyde-3-phosphate dehydrogenase, apoptosis, and neurodegenerative diseases.*** **Annu Rev Pharmacol Toxicol, 2005. 45: p. 269-90.**

**88.** **Dastoor, Z. and J.L. Dreyer,** ***Potential role of nuclear translocation of glyceraldehyde-3-phosphate dehydrogenase in apoptosis and oxidative stress.*** **J Cell Sci, 2001. 114(Pt 9): p. 1643-53.**

**89.** **Le Goffe, C., et al.,** ***Metabolic control of resistance of human epithelial cells to H2O2 and NO stresses.*** **Biochem J, 2002. 364(Pt 2): p. 349-59.**

**90.** **Janero, D.R., D. Hreniuk, and H.M. Sharif, *Hydroperoxide-induced oxidative stress impairs heart muscle cell carbohydrate metabolism.* Am J Physiol, 1994. 266(1 Pt 1): p. C179-88.**

**91.** **Nogae, I. and M. Johnston, *Isolation and characterization of the ZWF1 gene of Saccharomyces cerevisiae, encoding glucose-6-phosphate dehydrogenase.* Gene, 1990. 96(2): p. 161-9.**

**92.** **Ralser, M., et al., *Metabolic reconfiguration precedes transcriptional regulation in the antioxidant response.* Nat Biotechnol, 2009. 27(7): p. 604-5.**

**93.** **Tu, B.P. and J.S. Weissman, *The FAD- and O(2)-dependent reaction cycle of Ero1-mediated oxidative protein folding in the endoplasmic reticulum.* Mol Cell, 2002. 10(5): p. 983-94.**

**94.** **Rajasekaran, N.S., et al., *Human alpha B-crystallin mutation causes oxido-reductive stress and protein aggregation cardiomyopathy in mice.* Cell, 2007. 130(3): p. 427-39.**

**95.** **Godon, C., et al., *The H2O2 stimulon in Saccharomyces cerevisiae.* J Biol Chem, 1998. 273(35): p. 22480-9.**

**96.** **Grant, C.M., K.A. Quinn, and I.W. Dawes, *Differential protein S-thiolation of glyceraldehyde-3-phosphate dehydrogenase isoenzymes influences sensitivity to oxidative stress.* Mol Cell Biol, 1999. 19(4): p. 2650-6.**

**97.** **Ito, Y., et al., *Oxidative stress increases glyceraldehyde-3-phosphate dehydrogenase mRNA levels in isolated rabbit aorta.* Am J Physiol, 1996. 270(1 Pt 2): p. H81-7.**

**98.** **Chechik, G. and D. Koller, *Timing of gene expression responses to environmental changes.* J Comput Biol, 2009. 16(2): p. 279-90.**

**99.** **Landriscina, M., et al., *Adaptation to oxidative stress, chemoresistance, and cell survival.* Antioxid Redox Signal, 2009. 11(11): p. 2701-16.**

**100.** **Demple, B. and C.F. Amabile-Cuevas, *Redox redux: the control of oxidative stress responses.* Cell, 1991. 67(5): p. 837-9.**

**101.** **Warburg, O., *Über den Stoffwechsel der Carcinomzelle.* Naturwissenschaften, 1924. 12(50): p. 1131-1137.**

**102.** **Ferreira, L.M., *Cancer metabolism: the Warburg effect today.* Exp Mol Pathol. 89(3): p. 372-80.**

**103. Hsu, P.P. and D.M. Sabatini, *Cancer cell metabolism: Warburg and beyond.* Cell, 2008. 134(5): p. 703-7.**

**104. Warburg, O., *On the origin of cancer cells.* Science, 1956. 123(3191): p. 309-14.**

**105. Mazurek, S., *Pyruvate kinase type M2: a key regulator of the metabolic budget system in tumor cells.* Int J Biochem Cell Biol. 43(7): p. 969-80.**

**106. Ruckenstuhl, C., et al., *The Warburg effect suppresses oxidative stress induced apoptosis in a yeast model for cancer.* PLoS One, 2009. 4(2): p. e4592.**

**107. Colombo, S.L., et al., *Anaphase-promoting complex/cyclosome-Cdh1 coordinates glycolysis and glutaminolysis with transition to S phase in human T lymphocytes.* Proc Natl Acad Sci U S A. 107(44): p. 18868-73.**

**108. Prigione, A., et al., *The senescence-related mitochondrial/oxidative stress pathway is repressed in human induced pluripotent stem cells.* Stem Cells. 28(4): p. 721-33.**

**109. Wolf, A., S. Agnihotri, and A. Guha, *Targeting metabolic remodeling in glioblastoma multiforme.* Oncotarget. 1(7): p. 552-62.**

**110. Bonuccelli, G., et al., *The reverse Warburg effect: glycolysis inhibitors prevent the tumor promoting effects of caveolin-1 deficient cancer associated fibroblasts.* Cell Cycle. 9(10): p. 1960-71.**

**111. Pavlides, S., et al., *Transcriptional evidence for the "Reverse Warburg Effect" in human breast cancer tumor stroma and metastasis: similarities with oxidative stress, inflammation, Alzheimer's disease, and "Neuron-Glia Metabolic Coupling".* Aging (Albany NY). 2(4): p. 185-99.**

**112. Darnell, J.E., Jr., *STAT3, HIF-1, glucose addiction and Warburg effect.* Aging (Albany NY). 2(12): p. 890-1.**

**113. Demaria, M., et al., *A STAT3-mediated metabolic switch is involved in tumour transformation and STAT3 addiction.* Aging (Albany NY). 2(11): p. 823-42.**

**114. Mazurek, S., et al., *Pyruvate kinase type M2: a crossroad in the tumor metabolome.* Br J Nutr, 2002. 87 Suppl 1: p. S23-9.**

**115. Mazurek, S., et al., *Pyruvate kinase type M2 and its role in tumor growth and spreading.* Semin Cancer Biol, 2005. 15(4): p. 300-8.**

**116. Imamura, K. and T. Tanaka, *Multimolecular forms of pyruvate kinase from rat and other mammalian tissues. I. Electrophoretic studies.* J Biochem, 1972. 71(6): p. 1043-51.**

**117. Reinacher, M. and E. Eigenbrodt, *Immunohistological demonstration of the same type of pyruvate kinase isoenzyme (M2-Pk) in tumors of chicken and rat.* Virchows Arch B Cell Pathol Incl Mol Pathol, 1981. 37(1): p. 79-88.**

**118. Yamada, K. and T. Noguchi, *Regulation of pyruvate kinase M gene expression.* Biochem Biophys Res Commun, 1999. 256(2): p. 257-62.**

**119. Christofk, H.R., et al., *The M2 splice isoform of pyruvate kinase is important for cancer metabolism and tumour growth.* Nature, 2008. 452(7184): p. 230-3.**

**120. Spoden, G.A., et al., *Pyruvate kinase isoenzyme M2 is a glycolytic sensor differentially regulating cell proliferation, cell size and apoptotic cell death dependent on glucose supply.* Exp Cell Res, 2009. 315(16): p. 2765-74.**

**121. Christofk, H.R., et al., *Pyruvate kinase M2 is a phosphotyrosine-binding protein.* Nature, 2008. 452(7184): p. 181-6.**

**122. Hitosugi, T., et al., *Tyrosine phosphorylation inhibits PKM2 to promote the Warburg effect and tumor growth.* Sci Signal, 2009. 2(97): p. ra73.**

**123. Luo, W., et al., *Pyruvate kinase M2 is a PHD3-stimulated coactivator for hypoxia-inducible factor 1.* Cell. 145(5): p. 732-44.**

**124. Cakir, T., et al., *Integration of metabolome data with metabolic networks reveals reporter reactions.* Mol Syst Biol, 2006. 2: p. 50.**

**125. Patil, K.R. and J. Nielsen, *Uncovering transcriptional regulation of metabolism by using metabolic network topology.* Proc Natl Acad Sci U S A, 2005. 102(8): p. 2685-9.**

**126. Fujita, Y., *Carbon catabolite control of the metabolic network in Bacillus subtilis.* Biosci Biotechnol Biochem, 2009. 73(2): p. 245-59.**

**127. Steinberg, G.R. and B.E. Kemp, *AMPK in Health and Disease.* Physiol Rev, 2009. 89(3): p. 1025-78.**

**128. Wullschleger, S., R. Loewith, and M.N. Hall, *TOR signaling in growth and metabolism.* Cell, 2006. 124(3): p. 471-84.**

**129. Theobald, U., et al.,** ***In vivo analysis of glucose-induced fast changes in yeast adenine nucleotide pool applying a rapid sampling technique.*** **Anal Biochem, 1993. 214(1): p. 31-7.**

**130. Kresnowati, M.T., et al.,** ***When transcriptome meets metabolome: fast cellular responses of yeast to sudden relief of glucose limitation.*** **Mol Syst Biol, 2006. 2: p. 49.**

**131. Guetsova, M.L., K. Lecoq, and B. Daignan-Fornier,** ***The isolation and characterization of Saccharomyces cerevisiae mutants that constitutively express purine biosynthetic genes.*** **Genetics, 1997. 147(2): p. 383-97.**

**132. Pinson, B., et al.,** ***Metabolic intermediates selectively stimulate transcription factor interaction and modulate phosphate and purine pathways.*** **Genes Dev, 2009. 23(12): p. 1399-407.**

**133. Dang, L., et al.,** ***Cancer-associated IDH1 mutations produce 2-hydroxyglutarate.*** **Nature, 2009. 462(7274): p. 739-44.**

**134. Climent, F., et al.,** ***Red cell glycolytic enzyme disorders caused by mutations: an update.*** **Cardiovasc Hematol Disord Drug Targets, 2009. 9(2): p. 95-106.**

**135. Etiemble, J., et al.,** ***Erythrocytic pyruvate kinase deficiency and hemolytic anemia inherited as a dominant trait.*** **Am J Hematol, 1984. 17(3): p. 251-60.**

**136. Martinov, M.V., et al.,** ***Deficiencies of glycolytic enzymes as a possible cause of hemolytic anemia.*** **Biochimica et Biophysica Acta (BBA) - General Subjects, 2000. 1474(1): p. 75-87.**

**137. Schneider, A.S., et al.,** ***Hereditary Hemolytic Anemia with Triosephosphate Isomerase Deficiency.*** **N Engl J Med, 1965. 272: p. 229-35.**

**138. Waller, H.D. and H.C. Benöhr,** ***Enzymdefekte in Glykolyse und Nukleotidstoffwechsel roter Blutzellen bei nichtsphärocytären hämolytischen Anämien.*** **Journal of Molecular Medicine, 1976. 54(17): p. 803-821.**

**139. Cappellini, M.D. and G. Fiorelli,** ***Glucose-6-phosphate dehydrogenase deficiency.*** **Lancet, 2008. 371(9606): p. 64-74.**

**140. Glass, H.C., A. Feigenbaum, and J.T. Clarke,** ***A study on the nature of genetic metabolic practice at a major paediatric referral centre.*** **J Inherit Metab Dis, 2006. 29(1): p. 175-8.**

**141. Schlager, G. and M.M. Dickie,** ***Natural mutation rates in the house mouse. Estimates for five specific loci and dominant mutations.*** **Mutat Res, 1971. 11(1): p. 89-96.**

**142. Wamelink, M.M., et al.,** ***The difference between rare and exceptionally rare: molecular characterization of ribose 5-phosphate isomerase deficiency.*** **J Mol Med (Berl). 88(9): p. 931-9.**

**143. Ralser, M., et al.,** ***Sequencing and genotypic analysis of the triosephosphate isomerase (TPI1) locus in a large sample of long-lived Germans.*** **BMC Genet, 2008. 9: p. 38.**

**144. Schneider, A.S.,** ***Triosephosphate isomerase deficiency: historical perspectives and molecular aspects.*** **Baillieres Best Pract Res Clin Haematol, 2000. 13(1): p. 119-40.**

**145. Ralser, M., et al.,** ***Triose phosphate isomerase deficiency is caused by altered dimerization--not catalytic inactivity--of the mutant enzymes.*** **PLoS One, 2006. 1: p. e30.**

**146. Orosz, F., J. Olah, and J. Ovadi,** ***Triosephosphate isomerase deficiency: new insights into an enigmatic disease.*** **Biochim Biophys Acta, 2009. 1792(12): p. 1168-74.**

**147. Schneider, A. and M. Cohen-Solal,** ***Hematologically important mutations: triosephosphate isomerase.*** **Blood Cells Mol Dis, 1996. 22(1): p. 82-4.**

**148. Huck, J.H., et al.,** ***Profiling of pentose phosphate pathway intermediates in blood spots by tandem mass spectrometry: application to transaldolase deficiency.*** **Clin Chem, 2003. 49(8): p. 1375-80.**

**149. Wamelink, M.M., et al.,** ***Quantification of sugar phosphate intermediates of the pentose phosphate pathway by LC-MS/MS: application to two new inherited defects of metabolism.*** **J Chromatogr B Analyt Technol Biomed Life Sci, 2005. 823(1): p. 18-25.**

**150. van der Knaap, M.S., et al.,** ***Leukoencephalopathy associated with a disturbance in the metabolism of polyols.*** **Ann Neurol, 1999. 46(6): p. 925-8.**

**151. Huck, J.H., et al.,** ***Ribose-5-phosphate isomerase deficiency: new inborn error in the pentose phosphate pathway associated with a slowly progressive leukoencephalopathy.*** **Am J Hum Genet, 2004. 74(4): p. 745-51.**

**152. Kuepfer, L., U. Sauer, and L.M. Blank,** ***Metabolic functions of duplicate genes in Saccharomyces cerevisiae.*** **Genome Res, 2005. 15(10): p. 1421-30.**

**153. Hillenmeyer, M.E., et al.,** ***The chemical genomic portrait of yeast: uncovering a phenotype for all genes.*** **Science, 2008. 320(5874): p. 362-5.**

**154. Blank, L.M., L. Kuepfer, and U. Sauer, *Large-scale 13C-flux analysis reveals mechanistic principles of metabolic network robustness to null mutations in yeast.* Genome Biol, 2005. 6(6): p. R49.**

**155. Ishii, N., et al., *Multiple high-throughput analyses monitor the response of E. coli to perturbations.* Science, 2007. 316(5824): p. 593-7.**

**156. Kondoh, H., *Cellular life span and the Warburg effect.* Exp Cell Res, 2008. 314(9): p. 1923-8.**

**157. Pedersen, P.L., *Tumor mitochondria and the bioenergetics of cancer cells.* Prog Exp Tumor Res, 1978. 22: p. 190-274.**

**158. Warburg, O., *On respiratory impairment in cancer cells.* Science, 1956. 124(3215): p. 269-70.**

**159. Boles, E., et al., *Characterization of a glucose-repressed pyruvate kinase (Pyk2p) in Saccharomyces cerevisiae that is catalytically insensitive to fructose-1,6-bisphosphate.* J Bacteriol, 1997. 179(9): p. 2987-93.**

**160. Jayaraman, J., et al., *Biochemical correlates of respiratory deficiency. VII. Glucose repression.* Arch Biochem Biophys, 1966. 116(1): p. 224-51.**

**161. Carlson, M., *Glucose repression in yeast.* Curr Opin Microbiol, 1999. 2(2): p. 202-7.**

**162. Goldring, E.S., L.I. Grossman, and J. Marmur, *Petite mutation in yeast. II. Isolation of mutants containing mitochondrial deoxyribonucleic acid of reduced size.* J Bacteriol, 1971. 107(1): p. 377-81.**

**163. Thorpe, G.W., et al., *Cells have distinct mechanisms to maintain protection against different reactive oxygen species: oxidative-stress-response genes.* Proc Natl Acad Sci U S A, 2004. 101(17): p. 6564-9.**

**164. Fenton, A.W. and G.D. Reinhart, *Disentangling the web of allosteric communication in a homotetramer: heterotropic inhibition in phosphofructokinase from Escherichia coli.* Biochemistry, 2009. 48(51): p. 12323-8.**

**165. Rodriguez-Almazan, C., et al., *Structural basis of human triosephosphate isomerase deficiency: mutation E104D is related to alterations of a conserved water network at the dimer interface.* J Biol Chem, 2008. 283(34): p. 23254-63.**

**166. Klinger, H., et al., *Quantitation of (a)symmetric inheritance of functional and of oxidatively damaged mitochondrial aconitase in the cell division of old yeast mother cells.* Exp Gerontol, 2010. 45(7-8): p. 533-42.**

**167. Gardner, P.R., D.D. Nguyen, and C.W. White,** ***Aconitase is a sensitive and critical target of oxygen poisoning in cultured mammalian cells and in rat lungs.*** **Proc Natl Acad Sci U S A, 1994. 91(25): p. 12248-52.**

**168. Robbins, A.H. and C.D. Stout,** ***Structure of activated aconitase: formation of the [4Fe-4S] cluster in the crystal.*** **Proc Natl Acad Sci U S A, 1989. 86(10): p. 3639-43.**

**169. Cyrne, L., et al.,** ***Glyceraldehyde-3-phosphate dehydrogenase is largely unresponsive to low regulatory levels of hydrogen peroxide in Saccharomyces cerevisiae.*** **BMC Biochem, 2010. 11: p. 49.**

**170. Meredith, S.A. and A.H. Romano,** ***Uptake and phosphorylation of 2-deoxy-D-glucose by wild type and respiration-deficient bakers' yeast.*** **Biochim Biophys Acta, 1977. 497(3): p. 745-59.**

**171. Vander Heiden, M.G., et al.,** ***Evidence for an alternative glycolytic pathway in rapidly proliferating cells.*** **Science, 2010. 329(5998): p. 1492-9.**

**172. Luo, W., et al.,** ***Pyruvate kinase M2 is a PHD3-stimulated coactivator for hypoxia-inducible factor 1.*** **Cell, 2011. 145(5): p. 732-44.**

**173. Emmerling, M., et al.,** ***Metabolic flux responses to pyruvate kinase knockout in Escherichia coli.*** **J Bacteriol, 2002. 184(1): p. 152-64.**

**174. Ahmed, N., et al.,** ***Increased formation of methylglyoxal and protein glycation, oxidation and nitrosation in triosephosphate isomerase deficiency.*** **Biochim Biophys Acta, 2003. 1639(2): p. 121-32.**

**175. Ho, H.Y., et al.,** ***Enhanced oxidative stress and accelerated cellular senescence in glucose-6-phosphate dehydrogenase (G6PD)-deficient human fibroblasts.*** **Free Radic Biol Med, 2000. 29(2): p. 156-69.**

**176. Zhang, Z., et al.,** ***High glucose inhibits glucose-6-phosphate dehydrogenase, leading to increased oxidative stress and beta-cell apoptosis.*** **FASEB J, 2010. 24(5): p. 1497-505.**

**177. Najafov, A. and D.R. Alessi,** ***Uncoupling the Warburg effect from cancer.*** **Proc Natl Acad Sci U S A, 2010. 107(45): p. 19135-6.**

**178. Demaria, M., et al.,** ***A STAT3-mediated metabolic switch is involved in tumour transformation and STAT3 addiction.*** **Aging (Albany NY), 2010. 2(11): p. 823-42.**

**179. Gerber, S.A., et al.,** ***Absolute quantification of proteins and phosphoproteins from cell lysates by tandem MS.*** **Proc Natl Acad Sci U S A, 2003. 100(12): p. 6940-5.**

**180.** **Kettenbach, A.N., J. Rush, and S.A. Gerber,** ***Absolute quantification of protein and post-translational modification abundance with stable isotope-labeled synthetic peptides.*** **Nat Protoc, 2011. 6(2): p. 175-86.**

**181.** **Kirkpatrick, D.S., S.A. Gerber, and S.P. Gygi,** ***The absolute quantification strategy: a general procedure for the quantification of proteins and post-translational modifications.*** **Methods, 2005. 35(3): p. 265-73.**

**182.** **Gallien, S., E. Duriez, and B. Domon,** ***Selected reaction monitoring applied to proteomics.*** **J Mass Spectrom, 2011. 46(3): p. 298-312.**

**183.** **Guminska, M., et al.,** ***Tumor-specific pyruvate kinase isoenzyme M2 involved in biochemical strategy of energy generation in neoplastic cells.*** **Acta Biochim Pol, 1997. 44(4): p. 711-24.**

**184.** **Heinemann, M. and U. Sauer,** ***Systems biology of microbial metabolism.*** **Curr Opin Microbiol, 2010. 13(3): p. 337-43.**

**185.** **Juhnke, H., et al.,** ***Mutants that show increased sensitivity to hydrogen peroxide reveal an important role for the pentose phosphate pathway in protection of yeast against oxidative stress.*** **Mol Gen Genet, 1996. 252(4): p. 456-64.**

**186.** **Ralser, M., U. Zeidler, and H. Lehrach,** ***Interfering with glycolysis causes Sir2-dependent hyper-recombination of Saccharomyces cerevisiae plasmids.*** **PLoS One, 2009. 4(4): p. e5376.**

**187.** **Wang, Z., M. Gerstein, and M. Snyder,** ***RNA-Seq: a revolutionary tool for transcriptomics.*** **Nat Rev Genet, 2009. 10(1): p. 57-63.**

**188.** **Ikner, A. and K. Shiozaki,** ***Yeast signaling pathways in the oxidative stress response.*** **Mutat Res, 2005. 569(1-2): p. 13-27.**

**189.** **Brandes, N., S. Schmitt, and U. Jakob,** ***Thiol-based redox switches in eukaryotic proteins.*** **Antioxid Redox Signal, 2009. 11(5): p. 997-1014.**

**190.** **Veal, E.A., A.M. Day, and B.A. Morgan,** ***Hydrogen peroxide sensing and signaling.*** **Mol Cell, 2007. 26(1): p. 1-14.**

**191.** **Lee, M.N., et al.,** ***Glycolytic flux signals to mTOR through glyceraldehyde-3-phosphate dehydrogenase-mediated regulation of Rheb.*** **Mol Cell Biol, 2009. 29(14): p. 3991-4001.**

**192.** **Wellen, K.E., et al.,** ***ATP-citrate lyase links cellular metabolism to histone acetylation.*** **Science, 2009. 324(5930): p. 1076-80.**

**193. Ladurner, A.G., *Rheostat control of gene expression by metabolites.* Mol Cell, 2006. 24(1): p. 1-11.**

**194. Zhao, J., J. Herrera-Diaz, and D.S. Gross, *Domain-wide displacement of histones by activated heat shock factor occurs independently of Swi/Snf and is not correlated with RNA polymerase II density.* Mol Cell Biol, 2005. 25(20): p. 8985-99.**

**195. Verhoeven, N.M., et al., *Transaldolase deficiency: liver cirrhosis associated with a new inborn error in the pentose phosphate pathway.* Am J Hum Genet, 2001. 68(5): p. 1086-92.**

**196. Wamelink, M.M., E.A. Struys, and C. Jakobs, *The biochemistry, metabolism and inherited defects of the pentose phosphate pathway: a review.* J Inherit Metab Dis, 2008. 31(6): p. 703-17.**

**197. Moore, C., S. O'Keefe, and D. Lawhon, *Concurrent Validity of the Snijders-Oomen Nonverbal Intelligence Test 2 1/7-7 - Revised with the Wechsler Preschool and Primary Scale of Intelligence Revised.* Physiological Reports, 1998. 82: p. 619-625.**

## Abbreviations

| | |
|---|---|
| Acetyl-CoA | acetyl-coenzyme A |
| ADP | adenosine diphosphate |
| AICAR | 5'-phosphoribosyl-5-amino-4-imidazole carboxyamide |
| ALDH | acetaldehyde dehydrogenase |
| AMP | adenosine monophosphate |
| AMPK | adenosine monophosphate kinase |
| AP-1 | activator protein 1 |
| ATP | adenosine triphosphate |
| cADPr | cyclic ADP-ribose |
| CHP | cumene hydroperoxide |
| CIT1 | citrate synthase 1 |
| CNS | central nervous system |
| COX1 | cytochrome *c* oxidase subunit 1 |
| COX2 | cytochrome *c* oxidase subunit 2 |
| COX3 | cytochrome *c* oxidase subunit 3 |
| CYP | cytochrome P450 |
| cyt *c* | cytochrome *c* |
| dNTP | deoxyribonucleotides |
| $e^-$ | electron |
| FAD | oxidized flavin adenine dinucleotide |
| FADH2 | reduced flavin adenine dinucleotide |
| FBP | fructose 1,6-bisphosphate |
| G6PD | glucose 6-phosphate dehydrogenase |
| GAPDH | glyceraldehyde 3-phosphate dehydrogenase |
| GC | gas chromatography |
| GMP | guanosine monophosphate |
| GO | gene ontology |
| GRX | glutaredoxins |
| Gut2 | glycerol 3-phosphate:ubiquinone oxidoreductase |
| $H^+$ | proton |
| $H_2O_2$ | hydrogen peroxide |
| HDAC | histone deacetylase |
| HHO1 | histone H1 |
| HHT1 | histone H3 |
| HIF1α | hypoxia inducible factor 1α |
| $HO^{\cdot}$ | hydroxyl radical |
| IDP | isocitrate dehydrogenase |
| IMP | inosine monophosphate |
| IPS | induced pluripotent stem cells |
| LC | liquid chromatography |
| ME | malic enzyme |
| MRM | multiple reaction monitoring |

| | |
|---|---|
| MS | mass spectrometer |
| mTOR | mammalian target of rapamycin |
| NAADP | nicotinic acid adenine dinucleotide phosphate |
| $NAD^+$ | oxidized nicotinamide adenine dinucleotide |
| NADH | reduced nicotinamide adenine dinucleotide |
| NADK | NAD kinase |
| $NADP^+$ | oxidized nicotinamide adenine dinucleotide phosphate |
| NADPH | reduced nicotinamide adenine dinucleotide phosphate |
| Nde1, Nde2 | external NADH dehydrogenases 1 and 2 |
| Ndi1 | internal NADH dehydrogenase 1 |
| NFκB | nuclear factor κB |
| NMR | nuclear magnetic resonance spectroscopy |
| NNT | nicotinamide nucleotide transhydrogenase |
| NOPPP | non-oxidatve branch of the pentose phosphate pathway |
| NOX | NADPH oxidase |
| $O_2^{\cdot -}$ | superoxide |
| OH· | hydroxyl radical |
| OPPP | oxidative branch of the pentose phosphate pathway |
| OXPHOS | oxidative phosphorylation |
| p53 | protein 53 |
| PEP | phosphoenol pyruvate |
| $P_i$ | phosphate |
| PKA | protein kinase A |
| PKM | pyruvate kinase (mammals), isoforms 1 and 2 |
| PPP | pentose phosphate pathway |
| PRX | peroxiredoxins |
| PYK | pyruvate kinase (yeast), isoforms 1 and 2 |
| Q | ubiquinone |
| qRT-PCR | quantitative real time polymerase chain reaction |
| RBC | red blood cell (erythrocyte) |
| Rheb | Ras homolog enriched in brain |
| ROS | reactive oxygen species |
| SAICAR | succinyl-AICAR |
| Sir2 | silent information regulator 2 |
| STAT3 | signal transducer and activator of transcription 3 |
| TBH | tert-butylhydroperoxide |
| TCAC | tricarbon acid cycle |
| TOR | target of rapamycin |
| TPI | triose phosphate isomerase |
| TRX | thioredoxins |

# ERKLÄRUNG

Hiermit erkläre ich, daß ich diese Arbeit selbst verfaßt und keine anderen als die hier angegebenen Quellen und Hilfsmittel in Anspruch genommen habe.

Ich versichere, daß diese Arbeit in dieser oder ähnlicher Form keiner anderen Prüfungsbehörde vorgelegt wurde.

Berlin, Januar 2012 Nana-Maria Grüning